MISSOURI S&T

CENTER FOR TRANSPORTATION INFRASTRUCTURE AND SAFETY

Development of Hand-Held Thermographic Inspection Technologies

by

Dr. Glenn Washer, Ph.D., P.E.
with Graduate Research Assistants
Richard Fenwick and Naveen Bolleni

NUTC
R198

**A National University Transportation Center
at Missouri University of Science and Technology**

Disclaimer

The contents of this report reflect the views of the author(s), who are responsible for the facts and the accuracy of information presented herein. This document is disseminated under the sponsorship of the Department of Transportation, University Transportation Centers Program and the Center for Transportation Infrastructure and Safety NUTC program at the Missouri University of Science and Technology, in the interest of information exchange. The U.S. Government and Center for Transportation Infrastructure and Safety assumes no liability for the contents or use thereof.

Technical Report Documentation Page

1. Report No.	2. Government Accession No.	3. Recipient's Catalog No.
NUTC R198		

4. Title and Subtitle	5. Report Date
Development of Hand-Held Thermographic Inspection Technologies	August 2009
	6. Performing Organization Code

7. Author/s	8. Performing Organization Report No.
Dr. Glenn Washer, Ph.D., P.E. with Graduate Research Assistants Richard Fenwick and Naveen Bolleni	00014073

9. Performing Organization Name and Address	10. Work Unit No. (TRAIS)
Center for Transportation Infrastructure and Safety/NUTC program Missouri University of Science and Technology 220 Engineering Research Lab Rolla, MO 65409	11. Contract or Grant No. DTRT06-G-0014

12. Sponsoring Organization Name and Address	13. Type of Report and Period Covered
U.S. Department of Transportation Research and Innovative Technology Administration 1200 New Jersey Avenue, SE Washington, DC 20590	Final
	14. Sponsoring Agency Code

15. Supplementary Notes

16. Abstract

Subsurface deterioration in concrete structures presents a significant challenge for inspection and maintenance engineers. Cracking, delaminations and spalling that can occur as a result of corrosion of embedded reinforcing steel can lead to pot holes and even punch-through in concrete decks. For overpass bridges, concrete can separate from the structure and fall into traffic below the bridge, and there have been numerous deadly accidents as a result. Although this deterioration can frequently be detected using hammer sounding and/or chain dragging, these inspection techniques require hands-on access to the surface of the concrete. For both overpass bridges and decks, lane closures are required to gain access to the structure, and the resulting traffic disruptions makes inspections expensive and logistically difficult. The proposed research would explore the use of hand-held infrared cameras for the remote detection of deterioration in concrete. This technology could reduce the need for lane closures and improve the ability of inspection and maintenance personnel to detect and monitor deterioration in its embryonic stages, such that maintenance procedures can be employed before deterioration becomes critical. The technology can also be used to monitor and improve concrete repairs by rapidly identifying the extent of deterioration and locating its boundaries.

17. Key Words	18. Distribution Statement
Field testing, nondestructive evaluation, concrete	No restrictions. This document is available to the public through the National Technical Information Service, Springfield, Virginia 22161.

19. Security Classification (of this report)	20. Security Classification (of this page)	21. No. Of Pages	22. Price
unclassified	unclassified	116	

Form DOT F 1700.7 (8-72)

Development of Hand-held Thermographic Inspection Technologies

Final Report

August 19, 2009

MoDOT Project number RI06-038

NUTC Project number R198

Report Submitted to the
Center for Transportation Infrastructure and Safety
A National University Transportation Center (NUTC)
at
Missouri University of Science and Technology

Principal Investigator: Dr. Glenn Washer, Ph.D., P.E.

Richard Fenwick, Graduate Research Assistant
Naveen Bolleni, Graduate Research Assistant
Department of Civil and Environmental Engineering
University of Missouri – Columbia
E2503 Lafferre Hall
Columbia, MO 65211

Contents

List of Figures

List of Tables

Acknowledgments

This research was funded by the Missouri (MO), New York (NY) State and Texas (TX) Departments of Transportation under Pooled Fund 152, and the National University Transportation Center at Missouri S&T (NUTC). The authors gratefully acknowledge their support. The authors would also like to acknowledge the support of Emery Sapp & Sons, Columbia, MO, for their assistance during construction of the research test site.

The opinions, findings and conclusions expressed in this publication are not necessarily those of the MO, TX, and NY Departments of Transportation or the Federal Highway Administration. This report does not constitute a standard, specification or regulation.

Executive Summary

This study explored the application of hand-held thermographic cameras for the detection of subsurface delaminations in concrete bridges. The goal of the research was to provide maintenance and inspection personnel with an effective tool for detecting and monitoring concrete deterioration without disrupting traffic flow. The objectives of the research included developing guidelines for the use and application of the technology by characterizing the environmental conditions necessary for thermography to be effective. This included evaluating the effects of solar loading, diurnal temperature variations, wind speed and relative humidity. The applicability of the technology to areas of a bridge with and without radiant heating from the sun was studied. A second objective of the research was to investigate the operational constraints to implementation by providing the technology to states to be used in the condition assessment of bridges.

The deterioration of concrete as a result of corrosion of embedded reinforcing steel is a widespread problem for State Departments of Transportation. Corrosion typically initiates at the level of the embedded reinforcing steel, resulting in delaminations in the concrete that are not apparent through visual assessments of the surface of the concrete. As the deterioration progresses, delaminations develop into spalling of the concrete that further exposes the reinforcing steel to the ambient environment, resulting in increased deterioration rates. Additionally, spalling of the concrete reduces the service life of bridge decks and can create hazardous driving conditions. Concrete that spalls from the soffit of overpass bridges can fall into traffic and present a hazard to motorists.

Existing technologies used to assess subsurface deterioration range from simple hammer sounding to advanced technologies such as Ground Penetrating Radar (GPR). Infrared (IR) thermography has been used to detect characteristic thermal signatures associated with

delaminations, primarily in concrete bridge decks. Delaminations are detected by measuring the difference in surface temperature that may exist between a region of sound concrete and a delaminated region of concrete under certain environmental conditions. The primary advantage of thermography over traditional methods such as hammer sounding is that direct, hands-on access to the surface to be assessed is not required, because thermal cameras capture images of a surface from a distance. This reduces the need for traffic closures to gain access to portions of the bridge, and may greatly reduce the cost and time required to perform condition assessment. The primary disadvantage of thermography is that it depends on certain ambient environmental conditions, such as solar loading and ambient temperature changes, to establish the necessary thermal gradients in the concrete to make subsurface defects detectable. Because of the technologies' reliance on environmental conditions, the technology does not have a consistent and reliable performance level, rather the performance level depends on the particular environmental conditions of a given day or night. Therefore, to apply the technology practically, additional guidance is needed on what specific environmental conditions are most likely to result in a high performance level, and which environmental conditions are expected to result in poor performance. The research reported here developed guidance on the appropriate environmental conditions for practical application of the technology in the field.

The experimental portion of the research involved monitoring the behavior of a large concrete test block with implanted targets intended to model the behavior of subsurface defects (delaminations) in a concrete bridge. Targets were strategically placed in the block to model the behavior of delaminations at different depths in the concrete. Monitoring of the block was conducted on portions of the block exposed to direct solar loading to model the behavior of, for example, bridge decks. Monitoring was also conducted on portions of the block in the shade, to model the soffit area of a bridge. Ambient environmental conditions at the test block were monitored including solar loading, ambient temperature changes, wind speed and relative humidity. Data was collected for a period of six months and analyzed to determine

environmental conditions that would make detection of subsurface delaminations most likely during practical bridge inspections. The results of the testing showed that direct, uninterrupted solar loading and low wind speeds (< 8 mph) provided optimum conditions for detection of delaminations in areas exposed to solar loading. For areas not exposed to solar loading, ambient temperature changes of at least 8°C provided adequate conditions for detection for both day and night-time inspections. It was also found that high rates of change of the ambient temperature had a positive effect on the detectability of subsurface targets. Based on the experimental results, inspection periods during which thermographic inspections should be conducted were developed, based on the anticipated depth of the delaminations and the solar exposure conditions. Quantitative guidance on the appropriate environmental conditions for inspection were developed based on the experimental study. The experiences of the participating states using the thermographic cameras in the field is also reported based on some limited testing in the field. The results of the study and guidelines for application of the technology in the field are reported herein.

1 INTRODUCTION

The research reported herein explored the application of infrared (IR) thermography for the detection or deterioration in concrete bridges. The research focused on the potential use of hand-held thermographic cameras for use during routine or special bridge inspections, where areas of interest would include concrete decks, soffit areas of bridges, superstructure members, and exposed substructure components. Experimental testing on the effects of environmental parameters has been conducted and is reported herein.

The deterioration of concrete as a result of corrosion of embedded reinforcing steel is a widespread problem for State Departments of Transportation. Cracking in the concrete that develops at a subsurface level manifests as delaminations(Maser and Roddis 1990). These delaminations develop due to the expansion of the reinforcing steel during corrosion processes, and as such typically occur at the level of the reinforcing steel mat (Huston et al. 2002). The mat is typically located at a depth of 51 to 76 mm (2 to 3 in.) from the surface of the concrete. As deterioration progresses, these subsurface delaminations can mechanically separate from the concrete structure, a condition typically referred to as spalling (Maser and Roddis 1990; Masliwec 1988). The spalling of the concrete further exposes the reinforcing steel to the ambient environment, resulting in increased deterioration rates. Additionally, the concrete that spalls from the soffit of overpass bridges can fall into traffic and present a hazard to motorists. Condition assessment tools that can detect these delaminations before spalling occurs are needed to ensure bridge safety and identify maintenance and repair needs.

Nondestructive evaluation (NDE) methods used to assess subsurface defects in concrete vary in complexity and reliability. These methods range from simple hammer sounding to detect characteristic tones resulting from delaminations, to advanced technologies such as Ground Penetrating Radar (GPR). Infrared (IR) thermography has been used to detect characteristic thermal signatures associated with delaminations, primarily in concrete bridge decks(Maser and

Roddis 1990). Delaminations are detected by measuring the difference in surface temperature that may exist between a region of sound concrete and a delaminated region of concrete under certain environmental conditions(Manning 1980). The method is dependent upon environmental conditions, and can become ineffective if conditions are unfavorable. As a result, IR thermography has certain limitations as an inspection tool. Weather conditions must be suitable to enable detection of subsurface features such as delamination. The “suitable” conditions are not well defined, but generally include sufficient changes in the ambient environment to produce a thermal gradient in the concrete. Solar loading (sunlight) can provide a strong radiant heating source that establishes a thermal gradiant. Subsurface defects such as delaminations disrupt the heat transfer in the concrete, and if a sufficient thermal gradient exists, then a variation in the surface temperature of the concrete in the area above the delamination can be observed. This phenomena depends in part on the depth of the defect being observed, with a deeper defect having less influence on the resulting surface temperature than a shallow defect. Because the ambient environmental conditions cannot be controlled, the effectiveness of the method varies significantly depending on the environmental conditions at the time the inspection is being conducted(Manning 1983). As a result, experiences with this technology in the field have been mixed.

Thermographic imaging has several advantages over other techniques. One of the most significant advantages is its ability to image a large area of concrete from a distance. The soffit of a bridge, for example, can be observed from the ground level, without the need for bridge access vehicles that might be required to hammer-sound the structure. The deck of a bridge can be imaged from the roadside, and other elements of the bridge can be observed without gaining direct, hands-on access. This has the advantage of reducing the requirements for traffic control and costs associated with using special access vehicles. Additionally, the time required to conduct the inspection may be significantly reduced, because large areas are being imaged. With hammer sounding, for example, every area that is to be evaluated must be accessed to

impact the surface with the hammer. This can be a labor-intensive and time-consuming process for large areas of concrete, such as a bridge deck. Another advantage of thermography is that the results are available in real-time and require little or no processing. The thermal contrasts resulting from a defect are observed on the camera screen during the inspection, and additional investigation to confirm results or further explore anomalies in the image can be conducted, if necessary. Finally, modern IR cameras are relatively easy to use, with intuitive menu structures that can be easily learned. As a result, training on how to use the cameras is minimal, such that the tool could be practically implemented within a bridge inspection program.

The primary disadvantage of thermography is that because the effectiveness of the method is dependant on the environmental conditions, the method can be unreliable when applied in the field without careful consideration of the surrounding environmental conditions. A better understanding of environmental influences on the detection of delaminations using thermography is needed to support its use as a condition assessment tool for concrete bridges.

This research is focused on developing knowledge and data to determine appropriate environmental conditions (and limits) for the effective application of thermography to detect subsurface delaminations in concrete. To develop this knowledge, a large concrete test block has been constructed with embedded targets to model the effect of subsurface defects in concrete. The targets have been placed at strategic depths in the concrete to evaluate the effects of depth on the thermal contrast produced, and to model the response of the defects to changing environmental conditions.

1.1 Purpose

This research is conducted to develop guidance on the application of infrared thermography for the inspection of highway bridges. Although IR thermography has been an available tool for the condition assessment of highway bridges, there has been limited use of the technology. This is due in part to the complexity of applying thermography within the context of

bridge inspection. Because of the technology's reliance on environmental conditions for the detection of defects in concrete, the technology does not have a consistent and reliable performance level, rather the performance level depends on the particular environmental conditions of a given day or night. Therefore, to apply the technology practically, additional guidance is needed on what specific environmental conditions are most likely to result in a high performance level, and which environmental conditions are expected to result in poor performance.

There are three specific applications for the technology that were of interest in the study.

1. Deck inspections: Decks are typically exposed to sunlight during the day, which provides a strong driving force for development of thermal contrast. The ability to use a hand-held camera to conduct inspection on a bridge deck could improve the speed of inspection, reduce traffic control requirements, and provide a rapid means of scanning a deck for areas that may require further evaluation such as sounding.
2. Soffit inspections: Although not typically used for the inspection of the soffit area of a bridge, where there is no exposure to sunlight, such an application for the technology could have several distinct advantages. A primary area of interest is to detect delamination in the soffit of a bridge that may break free from the structure and fall into traffic below, presenting a hazard to motorists. It was envisioned that the technology could be applied as a scanning tool to look for areas of potentially severe deterioration, where concrete may be coming loose from the structure and needs to be repaired. Because thermography does not require hands-on access to the surface being inspected, it could be more readily applied than in-depth inspections, and used to identify areas where further evaluation is warrented.

3. Evaluation of carbon fiber composites: There is also an application for the technology for the detection of defects in carbon fiber composite overlays that are used to repair bridges. Although not specifically addressed within the experimental portion of this research, the environmental conditions explored for the detection of subsurface defects in concrete would also apply generally to the inspection of composite materials.

The application of thermography for deck and soffit inspections were not studied directly in the experimental portion of the research reported here. The research focused on controlled testing of the environmental conditions that would typically be experienced in these applications. For the condition assessment of bridge decks, one portion of the study focused on the thermal behavior of concrete surfaces exposed to direct sunlight. This is the more traditional application for thermography, using the heat from the sun to heat the surface of the concrete and provide the needed thermal gradient for detection of delaminations.

To address soffit inspections, where direct sunlight is not available to develop the necessary thermal gradients, another portion of the study focused on the behavior of concrete surfaces in the shade. This is perhaps the most innovative, original and important aspect of the research. Thermography has not traditionally been applied for such areas, because the driving force for thermal gradients provided by the sun is not available. However, changes in the ambient environmental temperatures can provide a driving force for the development of thermal contrast and therefore enable the detection of delaminations. Thermal contrasts would be much smaller than when radiant heating is applied. However, if effective guidelines could be developed to identify optimum conditions for inspections in the soffit area of a bridge, then the potential usefulness of the technology for the condition assessment of bridges would be greatly enhanced. The research reported here shows that the ambient environment can provide the necessary conditions for detecting subsurface delaminations without radiant heating from the

sun, a significant development that may have a broad impact on the level of implementation of thermography as a tool for bridge condition assessment.

1.2 Goals

The goal of the research is to provide maintenance and inspection personnel with an effective tool for detecting and monitoring concrete deterioration without disrupting traffic flow.

1.3 Objectives

The objectives of this research are as follows:

- Develop guidelines for the use of IR thermography for the condition assessment of highway bridges.
    - Characterize the environmental conditions that are necessary for thermography to be effective as a condition assessment tool
    - Evaluate the effects of solar loading, diurnal temperature variation, wind speed and relative humidity on the detectability of subsurface defects in concrete
    - Explore the applicability of thermography for image defects with and without radiant heating from the sun
- Investigate the operational constraints to implementation by providing thermographic cameras and training to participating States.

This report focuses primarily on the research conducted to evaluate the environmental conditions necessary for effective application of thermography. Field testing of the technology by participating states is also described.

1.4 Approach

The detection of subsurface features using IR thermography depends on a thermal gradient being established in the material under inspection. This thermal gradient causes heat to flow through the material, from areas of high temperature to areas of low temperature.

Subsurface features that affect the rate of thermal conduction through the material, such as the air gap created by a delamination, can be detected by their effect on the surface temperature resulting from the disruption of heat flow. The extent to which the surface temperature of the material is effected by disruptions in the heat flow from subsurface features depends in part on the depth from the surface to the feature, with deeper features generally having a smaller effect on surface temperature than near-surface features. For concrete structures, the thermal gradient is established by heat transferred from the surrounding environment into the concrete. The primary environmental factors believed to affect the heat transfer from the environment into the concrete include:

- Solar loading
- Diurnal temperature variations
- Wind speed

To evaluate the effect of these parameters on the ability of IR thermography to detect and image subsurface features (i.e. delaminations), a test block was constructed with embedded targets at different depths from the surface of the block. The depths of the targets were selected to model typical depths where delaminations may occur in a concrete structure. The foam targets were placed at depth of 25 mm (1 in.), 51 mm (2 in), 76 mm (3 in.) and 127 mm (5 in.). The 25 mm (1 in.) depth is intended to model very shallow delaminations, such as a patch or thin overlay. The 51 mm (2 in) and 76 mm (3 in) depth intended to model the range of delaminations stemming from corrosion of the rebar mat, and the 127 mm (5 in.) deep target to evaluate capabilities for detecting very deep targets approaching a limit where thermography would typically be effective for reinforced concrete.

An IR thermographic camera was used to collect images of the surface of the block periodically to monitor the effect of the subsurface targets on the apparent surface temperatures. The environmental parameters were monitored to assess their influence on the

surface temperature of the block, and the magnitude of thermal contrast developed between surface areas above the targets and intact portions of the block.

The behavior of the test block was monitored for approximately six months. This included a period of approximately three months on the south side of the block that was exposed to direct solar loading (November - January, 2008). On this side of the block, the concrete is heated by radiant energy from the sun, and as such the total solar loading, that is, the intensity and duration of the sun, provides the driving force to establish thermal gradients in the concrete. Data was also collected for approximately three months on the north side of the test block, which was not exposed to direct solar loading (May – July, 2008). This side of the test block is analogous to viewing the shaded portion of a bridge, such as the soffit area. Under this condition, thermal gradients in the concrete are established by convective heating and cooling of the block, and therefore depend on the diurnal ambient air temperature variations to establish thermal gradients in the concrete.

In addition to the testing of the concrete test block, suitable field cameras were provided to the three State Departments of Transportion (DOTs) involved in the project, Missouri, New York and Texas. Training modules were developed and delivered to personnel from the participating states, and the camera were operated by the state personnel to evaluate the integration of this technology into real inspection and condition assessment programs within the given states. To provide additional weather-related data to the states, a system was developed that included a fieldable computer and associated web site that could be queried from the field to determine the current environmental condition during an inspection. Due to several technology developments that occurred over the course of the research, the development and use of this system was limited. However, the web site developed under the research has potential for application in the future, based on the guidelines developed through the research.

The data collected from the test block was utilized to develop guidelines for the application of thermography in the field. These guidelines provide guidance on suitable

environmental conditions for the application of thermography for the condition assessment of concrete structures.

Specific details of the equipment, data collection scheme, test block design and other experimental details are described fully in Chapter 3, EXPERIMENTAL DESIGN. The methodologies used to analyze the data and render useful results are described in Chapter 4, ANALYSIS. Results of the analysis are reported in Chapter 5, RESULTS. Results from testing in the field by the participating States is described in Chapter 6. The conclusions reached from the analysis of the results are documented in Chapter 7, CONCLUSIONS. Guidelines for the inspection of concrete bridges using infrared thermography are in Appendix A.

2 BACKGROUND

2.1 Introduction

The basic principle behind thermographic inspection of civil structures is that the flow of heat through the material being inspected is disrupted by the presence of a subsurface defect(Clemena 1978; Manning 1980; Yehia et al. 2007). The disruption in heat flow can manifest as a variation in the surface temperature of the material. An infrared (IR) camera, which measures the intensity of energy emitted from the material in the IR range, can be used to produce an image of the surface temperature of the material. Variations in the uniformity of the surface temperature resulting from the subsurface defect can be observed in the image produced(Arnold 1969). When the temperature of the material is increasing, such as during the daytime when the sun and ambient environment (air temperature) are heating the block, the surface area above a subsurface delamination warms at a faster rate than surface areas where the concrete is intact, as shown schematically in Figure 2.1. During the nighttime, when air temperatures are falling and the material is cooling, the surface area above the delaminations cools at a faster rate than the intact concrete (Figure 2.1). Therefore, during the daytime, delaminations can be detected as “hot spots” on the surface of the material, relative to intact concrete. During the nighttime, those areas appear as “cold spots” relative to the intact concrete. Defects are detected by a qualitative assessment of the thermographic image to determine areas in the image that appear in to have a thermal contrast with areas that are intact (i.e. “hot” spots or “cold” spots.)

The environmental conditions surrounding the test, such as ambient temperature, solar loading, thermal loading and wind, can have an impact on the quality of the thermal images that are produced(Love 1986; Maser and Roddis 1990). These environmental factors are difficult to predict and characterize, and obviously vary over time. The temperature variations that result from subsurface defects can be small, such that there is a need to conduct an inspection with

some knowledge that the environmental conditions are adequate to anticipate that a subsurface defect will produce sufficient thermal contrast to be detected.

This section provides an introduction to the theory behind thermographic inspections with the intention of illuminating some of the challenges faced in developing this technology. The section describes several important characteristics of heat transfer that effect the thermographic inspection of bridges.

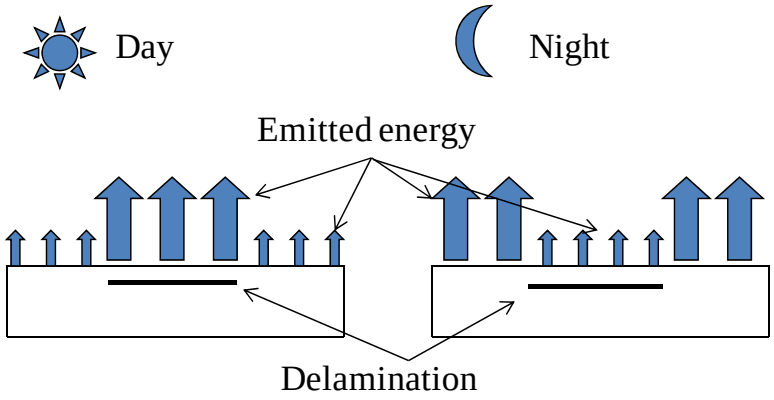

Figure 2.1 : IR energy emitted from a concrete deck under day and nighttime conditions.

2.1.1 IR Theory

The light we see is a very small portion of the electromagnetic spectrum. The electromagnetic spectrum includes radiation ranging from small wavelength x-rays to long wave-length radio waves. The wavelength of infrared radiation is longer than that of radiation in the visible region. The wavelength range from 1 μm to 1000 μm of the electromagnetic spectrum is described as the infrared range. All materials emit radiation in the infrared range when their temperature is above absolute zero (-273ºC). The rate at which this energy is emitted is a function of the temperature of the material and its emissivity. IR cameras can be used to measure the electromagnetic radiation emitted or reflected from the surface of a material. The energy of emitted radiation can be expressed by the Stefan-Boltzmann equation:

$$E = \varepsilon \sigma T^4 \qquad \text{(Equation 2.1)}$$

Where:

E = radiant energy emitted by a surface at all wavelengths,

ε = emissivity of the material,

σ = Stefan – Boltzmann constant (5.67×10^{-8} W/(m^2 – K^4)) and

T = Temperature in degrees Kelvin.

As shown in this equation, the radiant energy emitted from a material in proportional to the fourth power of its temperature, such that small variation in temperature will result in large changes in the radiant energy. The emissivity of a surface is the ratio of its emissive power relative to a black body. A black body absorbs all incident radiation regardless of wavelength and incident direction, such that there is no reflection and all of the radiation leaving the surface is emitted by the surface. As such, a black body is a perfect emitter and provides a useful comparison to provide a relative measure of the rate at which a given surface will emit radiation at a given temperature. In other words, the emissivity of an object is a relative measurement of rate at which the object emits radiation, 1 being a perfect emitter and 0 being no emission at all. In general, concrete has relatively high emissivity, between 0.9 and 1.0. As such, it is a good emitter relative to other materials such as metals.

For the application of IR thermography to civil structures, where a qualitative measure of the contrast in an image is used in an attempt to identify subsurface deterioration, specific emissivity values may not be required. The values of emissivity are valuable if the actual temperature of an object or material is needed, but to identify the contrast in a thermal image it is not needed. However it is important in terms of assessing thermographic images, because different materials will emit radiation at different rates, even though they may be at the same temperature. Therefore, if a thermal image includes different materials, such as paint on the surface of the concrete, the paint may appear at a different temperature than the concrete because its emissivity is different, even though its' temperature may be same. The surface

roughness of a material will also have an effect on emissivity values, with rough surfaces generally having higher emissivity than smooth surfaces. This is an important practical consideration in the application thermography in the field, though it was not studied explicitly in this research.

The rate of heat transfer across a solid in steady – state can be expressed using the Fourier equation:

$$q_x = -kA_x \frac{dT}{dx} \qquad \text{(Equation 2.2)}$$

Where:

A_x = surface area normal to the direction of heat flow (x)

q_x = rate of heat transfer in watts.

k = thermal conductivity watts per meter – degree Celsius $\left(\frac{w}{m°C}\right)$

T = Temperature

The Fourier equation presents the most basic relationship for heat transfer in materials, representing a steady-state in which heat transfer is independent of time. For a realistic case, the situation is typically more complicated by time-varying heat input and different thermal properties (e.g. k values) of materials making up the system being examined. However, the equation is useful in that it indicates the dependence of heat transfer on the thermal gradient. The thermal gradient is the difference in temperature as a function of distance $\left(\frac{dT}{dx}\right)$, for example, if the surface of the concrete is hot and the internal temperature is cold, it is said to have a *thermal gradient*. This thermal gradient will cause heat to flow, and a subsurface delamination that interrupts that heat flow will cause the heat to flow differently in the defective area than in intact areas, which may result in a variation in the surface temperature in that area.

2.1.2 Environmental Factors

For civil structures, several different factors effect the heat transfer in concrete exposed to the ambient environment. The important environmental factors that effect the ability of thermography to detect subsurface defects in concrete include solar loading, ambient temperature changes, and wind speed. Relative humidity has also been suggested in the literature as a factor (Manning 1983). This section briefly describes what each of these environmental parameters is, and why it affects the thermal contrast developed from a subsurface defect in concrete.

A primary driving force for the development of thermal gradients in concrete is radiant heating from the sun. Radiant energy from the sun imparts thermal energy into the surface of the concrete that causes the concrete to heat up (Figure 2.2). The surface heats up at a much higher rate than the core of the concrete, developing a thermal gradient with high temperatures at the surface and cooler temperatures at depths into the concrete. To achieve thermal equilibrium, the heat at the surface of the concrete is transferred (conducted) toward the core of the concrete. The amount of solar loading may be expressed as the radiant energy of the sun measured in Watts/m^2, which is the radiant energy at a given point in time. In this research, the *solar loading area* or amount of solar radiation was developed as a parameter for analysis of the effects of direct sun exposure. The solar loading area was found by determining the area under a solar radiant energy curve.

The temperature of the air surrounding the concrete will also impart a thermal gradient. In the daytime, when temperatures are typically rising over the course of a day, the ambient air temperature is higher than the temperature of the concrete, and as a result heat is transferred into the concrete to move the concrete toward thermal equilibrium with its surroundings. This will establish a thermal gradient in the concrete, as the surface warms faster than the core of the concrete. Obviously, the greater the difference between the ambient air temperature and the concrete, the larger the thermal gradient established. The temperature of the concrete lags in

time relative to changes in the ambient environment, due to its large mass and low thermal conductivity. As a result, if there are large changes in the ambient environmental temperature, there will develop a large difference between the temperature of the air and the temperature of the concrete, therefore a greater thermal gradient. For this reason, the change in the ambient temperature over the course of the day is the parameter that controls the level to which a subsurface target will effect the surface temperature of the block, i.e. be detectable with a thermographic camera. The actual environmental temperature really plays no role at all; the thermal gradient would be the same if the air were maintained at 40°C (104°F) than if it were maintained at 0°C (32°F), if the concrete was in thermal equilibrium with its surroundings. However, if the air temperature were to change from 0 to 40°C (32 to 104°F) over a period of 10 hrs, the concrete could not change that fast, and a thermal gradient results.

The rate of heat transfer between the ambient air temperature and the concrete is controlled by convection (Figure 2.2). The rate of convective heat transfer typically depends on a number of factors, including the ambient air temperature and wind speed. For a large difference in temperature between the concrete and the air, the rate of convective heat transfer can be large. If the wind speed is high, the convective heat transfer will be increased. This is analogous to blowing on a bowl of soup to cool it off. The result of these effects is that the high rate of convective heat transfer can reduce effects of radiant heating from the sun by cooling the surface of the concrete, making it more difficult to detect a subsurface defect in the concrete by reducing the thermal gradient. In other words, the wind blowing on the surface that is warmer than the ambient air due to radiant heating from the sun has the effect of cooling the surface, making the surface temperature closer to the core temperature and reducing the thermal gradient. However, if the air temperature were greater than that of the concrete, then increased convective heat transfer would warm the surface of block, and this would occur more rapidly if wind speeds were high than if wind speeds were low. Therefore, in the absence of radiant energy from the sun, high wind speeds could increase the thermal gradient, and therefore make

subsurface features more readily detected than they otherwise would. Conversely, at night, when air temperatures are cooler than concrete temperature, high wind speeds could increase the negative thermal gradient in the concrete. The effect of wind speed on the detectability of subsurface features in concrete has been studied here for both conditions when radiant energy from the sun is available to heat the concrete block, and for shady conditions without radiant heating of the sun.

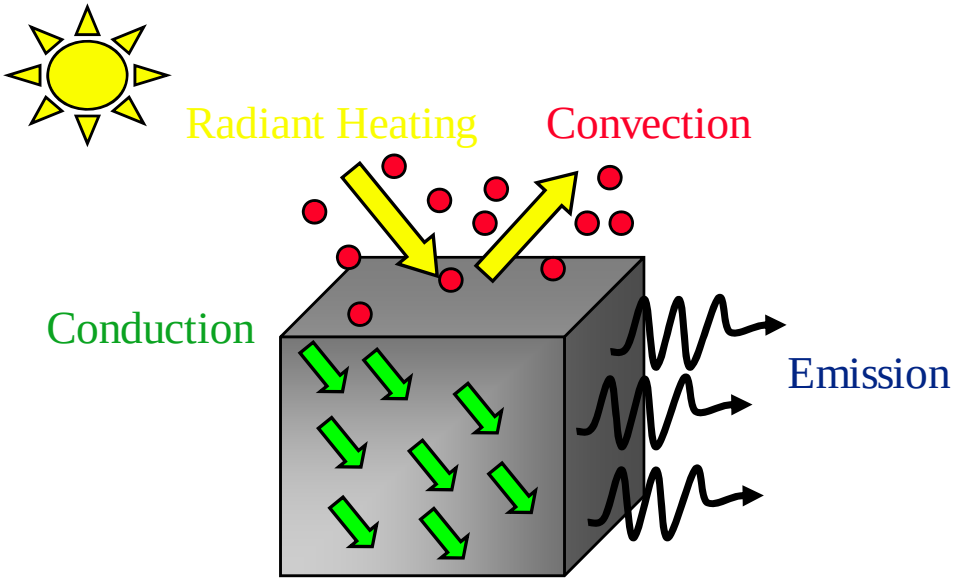

Figure 2.2 : Heat transfer factors for a concrete block in the environment.

The effect of wind speed and the resulting convective heat transfer on the thermal behavior of concrete when radiant heating is not applied are not well defined. For practical application of thermography as a general tool for the condition assessment of bridges, the application of the technology to areas that are not exposed to sunlight (radiant heating from the sun) would be a tremendous advantage. For most bridges, significant areas of the bridge are never exposed to sunlight, such as the entire soffit of the bridge. The condition assessment of these areas of the bridge is needed if thermography is to be utilized for typical bridge inspections, and as such there is a need to determine the condition under which thermographic inspections are most likely to be effective in these areas. To the knowledge of the research

team, previous research to explore that ability of thermography to detect defects in bridges in areas not exposed to direct sunlight has been limited (Clark et al. 2003). However, there has been experience that suggest that the technology can work for the detection of defects in the soffit area of a bridge. The research reported here explores the effect of wind speed on the detectability of subsurface features in concrete for both conditions where radiant heating from the sun is applied, and in regions where there is no radiant heating from the sun (shady areas).

Convective heat transfer properties are also effected by the relative humidity of the ambient air surrounding the concrete(Zhang et al. 2007). Increases in relative humidity increase the convective heat transfer coefficient, increasing the rate of heat transfer. As a result, it would be expected that humid air would transfer heat into the concrete more rapidly than dry air, increasing the thermal gradient and thus having a positive effect on the detectability of subsurface features in the concrete.

2.1.3 Thermography Applications

Thermography has traditionally been applied for the condition assessment of concrete bridge decks(Maser 2008). The development of delaminations and spalling in bridge decks due to corrosion of the reinforcing steel is well known. Because bridge decks are often exposed to direct sunlight, the radiant heating from the sun can provide a high thermal gradient that enables the detection of subsurface delaminations. A number of fieldable systems that utilize thermal cameras mounted on vehicles have been developed and utilized for the condition assessment of decks with some success. There has been for many years an ASTM standard test method that describes the condition assessment of bridge decks using vehicle-mounted cameras (ASTM 2007). This test method was first approved in 1988, and is based on research conducted in Canada and the United States. This research consisted of field testing several bridges with known delaminations, and evaluating the performance of thermography for those specific field conditions. Some data on the environmental conditions necessary for detection of

subsurface delaminations are provided, and these conditions are summarized in Table 2.1. The standard test method notes that based on available data, infrared thermography can detect between 80 and 90% of delaminations found in an exposed concrete bridge deck and 80 to 90% in asphalt covered bridge decks. No data is provided for the detection of delaminations in areas not exposed to direct sunlight, i.e. in the shade or for the deck soffit. In spite of being available since 1988, the standard test method has not seen widespread application for the condition assessment of concrete bridge decks.

Table 2.1 : Environmental conditions for deck inspections according to ASTM D 4788-07.

Time of Year	Direct Sunlight (hrs)	Change in Ambient Temp.	Wind Speed	Detection Limit (Δ_t)	Notes
Summer	3 hrs	None specified	< 30 mph (50 km/hr	0.5° C (1.8°F)	Dry deck for 24 hrs prior to test
Winter	4 hrs	11°C (20°F)	< 15 mph (24km/hr)	0.5° C (1.8°F)	Ambient Temp > 0° C (32°F)
Winter, asphalt covered deck	6 hrs	11°C (20°F)	< 15 mph (24km/hr)	0.5° C (1.8°F)	Ambient Temp > 0° C (32°F)

One limitation of this test method is that there is no consideration of the depth at which the delaminations are anticipated. Exploration of the reported research referenced in the document revealed that testing was conducted on relatively shallow delaminations between 10 mm (0.39 in.) and 24 mm (1.0 in.)(Manning 1980), to a maximum depth of perhaps 44 mm (1.73 in.)(based on concrete cover) (Manning 1983). Given that typical concrete cover in a bridge deck is ~51 mm (2 in.), the delaminations on which the specifications are based may not be representative of typical bridge decks in the United States. This may contribute to the lack of widespread application of the test method; a performance in the field would not match that described in the test method if deeper delaminations are to be detected.

An additional complication is that naturally occurring delaminations have size, shape and texture that vary. A delaminations may vary in depth significantly across its area, may be intermittent, and the degree of contact between the surfaces of the delamination cannot be

predicted. Additionally, delaminations are sometimes saturated with water. Because water has significantly different thermal properties from both air and concrete, the thermal behavior of a delamination that is saturated with water will be significantly different than a dry delamination. This may be partially addressed in the ASTM test method through the requirement for the deck to be dry for 24 hrs prior to the testing, but this is believed to actually refer to the need to have a dry surface. Moisture on the surface of the concrete will preclude the application of thermography for two reasons: First, evaporative drying of the surface will pull heat away from the surface, possibly masking the effect of a subsurface defect. Second, water has a different emissivity than concrete, such that a wet area will appear at a different temperature than the concrete in a thermal image, even if its temperature were the same.

These factors, among others, may contribute to the limited application of the technology since the standard test method was first introduced. In particular, the varying characteristics of naturally occurring delaminations make predicting the thermal contrast that will result for a given set of environmental conditions difficult. The specific effects of the varying nature of delaminations on the thermal contrast developed were not the subject of the research reported here. Rather, this research focused on determining environmental conditions that would make detection of subsurface delaminations most likely, by studying an idealized set of delaminations at various depths in a concrete block. As a result, the magnitude of thermal contrast observed in the test block constructed for this research do not transfer directly to field applications. Rather, it is intended that the environmental condition identified can be transferred to the field to identify suitable conditions that make detection most likely. Consideration of the variation in characteristics of the delaminations to be detected is an important consideration for implementation of the guidelines developed.

3 EXPERIMENTAL DESIGN

This section describes the construction and monitoring methods utilized to evaluate the thermal behavior of a large concrete test block. This test block had embedded targets intended to model the response of delaminations in concrete to changing environmental conditions. The block was constructed at a test site in Columbia, MO.

3.1 Introduction

To evaluate and model the response of concrete with subsurface delaminations, a large test block was constructed. The size of the test block was selected to provide sufficient thermal mass to allow for the behavior of a large concrete structure to be modeled, specifically to ensure that the changes in temperature that occurred in the block were representative of those changes that would occur in a real bridge. To evaluate the actual thermal response of the block to changing environmental conditions, thermocouples were embedded throughout the block such that the thermal gradient at the surface could be determined. Environmental parameters at the test block were monitored by an on-site weather station. To evaluate the thermal response of the subsurface targets, a thermographic camera was used to capture images of the test block periodically. This chapter describes all aspects of the field test site used in the study.

A data acquisition system was developed to collect data from both the on-site weather station and the thermocouples in the test block. This data acquisition system is described herein. Fundamental aspects of data analysis and reduction necessary to enable statistical studies of the effects of environmental parameters are also described.

3.2 Field Research Site

The field research site included the large concrete test block and a environmentally controlled data house used to house data acquisition equipment, including the thermal camera used to monitor the test block. The field research site was located in an open field that is part of

a research farm located 12 miles northwest of Columbia, MO. Key factors for selecting the site included the following:

- A large, clear area of field was available for the construction of the test block. This field provided a large, clear area such that reflections of radiant energy from the sun from objects such as nearby buildings or forest would be minimized. Because there were no nearby structures or trees, there would also not be any shading of the block, which could complicate analysis of results.
- Adequate electrical service was in-place at the site to provide a power for the experimental station developed to monitor the behavior of the block.

The location of the test site is shown in Figure 3.1. The latitude and longitude for the test location is 38º 59' 45.74" North and 92º 28' 18.28" W, respectively.

Figure 3.1 : Location of research test block.

3.2.1 Test Block

To model conditions for subsurface defect detection of concrete structures, a 2.44 m x 2.44 m x 0.91 m (8 ft. x 8 ft. x 3 ft.) thick concrete test block was constructed. The test block

was constructed to model the general construction characteristics for a “typical” highway bridge structure. A reinforced concrete footing was constructed to support the block and distribute the block’s dead weight to prevent settlement. A reinforcing steel cage of #4 rebar placed at approximately 305 mm (12 in.) on-center was constructed and tied into the footing. A Class B2, 27.6 MPa (4000 psi) standard structural concrete mix was used as the concrete material for the block.

The block was oriented such that the large 2.44 m x 2.44 m (8 ft. x 8 ft.) side of the block faced south, where direct sunlight would be applied to the block. The opposite 2.44 m x 2.44 m (8 ft. x 8 ft) faced north, such that it would not be exposed to the sun. In this configuration, the south side of the block provided a model of a bridge deck, south facing facia girder or exposed exterior support. The north side provided a model of shaded surfaces such as the underside/soffit of a bridge deck, the soffit of a box beam or an interior support.

The block was built with 305 x 305 x 13 mm (12 in. x 12in. x 0.5 in.) thick embedded foam board targets at depths of 25, 51, 76 and 127 mm (1, 2, 3, and 5 in.) on the north and south sides, and at 25 and 76 mm (1 and 3 in.) on the east and west sides. The layout of the targets in the test block is shown in Figure 3.2 for the south and west side. The foam targets were fastened to the rebar cage with nylon stand-offs to set the proper depth of the targets in the concrete and to prevent the targets from moving during the concrete pour. The thickness of the foam material was selected to ensure the targets did not deform during the pour. These targets were not intended to model precisely the behavior of a real concrete delamination, but provide a more uniform response that could be used to evaluate the effects of environmental variables and ensure there was no uncertainty in the depth of the targets in the concrete. If the targets became deformed or shifted such that they were no longer parallel to the surface of the block during the pour, the resulting thermal contrast developed could be difficult to interpret. As previously mentioned, because the targets are made of foam, the magnitude of the thermal contrast will typically be much larger than would be expected from a real delamination.

However, the characteristics of the response to varying environmental conditions, in terms of the optimum conditions for detection, relative amplitude of contrast and effect of depth are expected to be similar to that of a delamination.

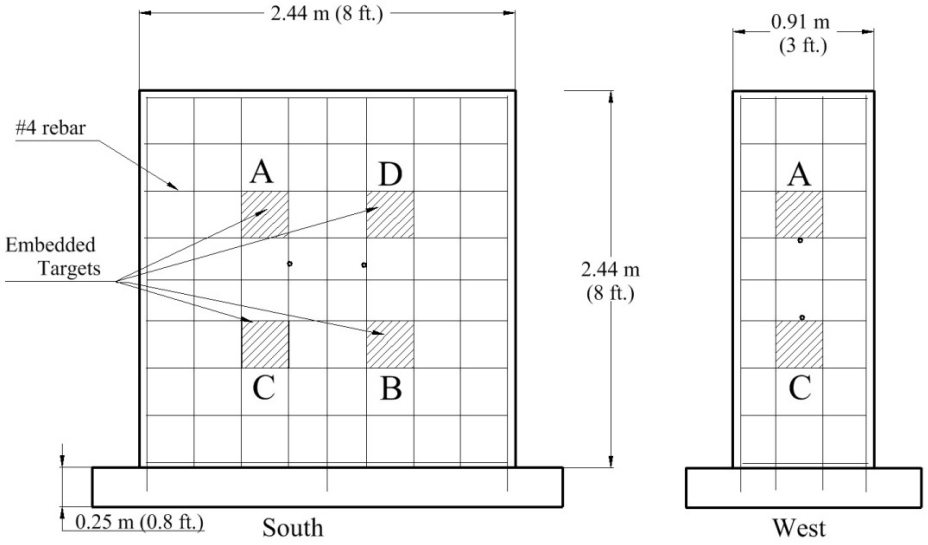

Figure 3.2 : Schematic diagram of the south and west faces of the test block.

Targets on the east and west sides of the test block were not observed as part of the research reported here. A summary of the target depths for each side of the test block is shown in Table 3.1.

Table 3.1 : Target depth in each side of the test block.

Test Block Side	Embedded Target Label and Corresponding Depth			
	A	B	C	D
	25 mm (1 in.)	51 mm (2 in.)	76 mm (3 in.)	127 mm (5 in.)
North	X	X	X	X
East	X		X	
South	X	X	X	X
West	X		X	

A photograph of the test block prior to placing the concrete is shown in Figure 3.3. As can be seen in the figure, plywood forms were placed around the rebar cage after the targets had been affixed to the cage. These forms were placed to maintain a concrete cover above the reinforcing steel of 51 mm (2 in.). The forms were supported by a series of wooden struts, and

held in place with steel ties that traversed the block in the north-south and east-west directions. These steel ties held the forms at a fixed separation during the concrete pour. The ties were cast into the block and ground flush once the concrete was cured.

Figure 3.3 : Photograph of the test block during construction showing the targets mounted on the rebar cage.

Thermocouples (TCs) were cast into the block to provide a means of monitoring the thermal gradients in the test block, and to measure the internal temperature of the block. These TCs were mounted in a 25 mm (1 in.) diameter PVC pipe to contain the TC wires and maintain fixed spacings for the sensors. Sensors were place close together near the surface of the block, where thermal gradients would be expected to be high, and were spaced farther apart in the core of the block, where significant gradients would not be expected. A series of 17 TC sensors were configured in a 0.97 m (38 in.) section of PVC pipe to form the N-S array, which was placed in the block traversing through the thickness in the north-south direction as shown in Figure 3.4. This figure shows the east portion of the block and the alignment of the E-W and N-S arrays. A second N-S array was placed symmetrically about the centerline of the block, but is not shown in the figure. Sensors were placed at a spacing of 25 mm (1 in.) near the surface of

the block and were spaced at 152 mm (6 in.) through the middle portion of the block, as shown in the figure. The E-W array consisted of a 2.49 m (98 in.) section of PVC pipe containing 15 TC sensors. The thermal couple array that traversed the block in the east-west direction (E-W array) has a similar alignment, with sensors placed at 25 mm (1 in.) separation near the east and west surfaces (1, 2, 3 and 5 in. depths), at a depth of 305 mm (12 in) and spaced at 305 mm (12 in.) through the depth of the block. Two arrays were used in each direction in the block to provide redundancy, in case one array failed during the monitoring of the test block. Only one of the arrays in each direction (N – S, E – W) was monitored, and no sensor failures were experienced during the testing.

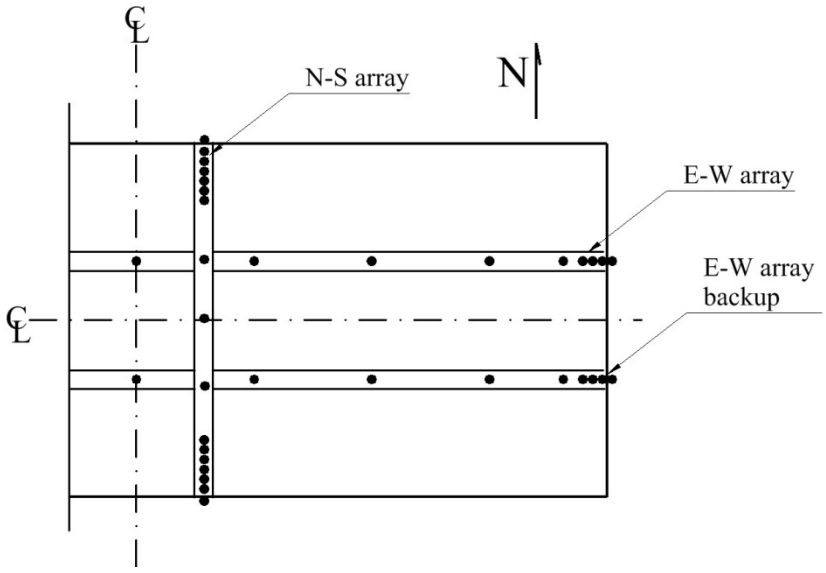

Figure 3.4 : Diagram of thermocouple arrays in test block.

3.2.2 Data House

To store and shelter the data acquisition equipment, camera, and computer, a secure and temperature-controlled data house was built, as shown in Figure 3.5. It was made as a small insulated work station (internally about 0.91 m x 0.91 m x 2.3 m (3 ft. x 3 ft. 7.5 ft.) tall with a roof sloping away from the viewing aperture, and thermostatically controlled air conditioning and heating units were used to ensure consistent temperatures within the data house.

The computer and vital equipment were also powered through surge protection and an Uninterruptible Power Supply (UPS) to account for short power failures and surges in the area. The UPS could run the vital equipment for up to 30 minutes in the case of a short power failure.

Figure 3.5 : Data house and inside layout with thermal imaging camera, standalone PC, and data acquisition (DAQ) equipment.

3.2.3 Thermal Imaging Camera

The camera used on site for the test block was a FLIR ThermaCAM S65, which is a research grade camera. Thermal sensitivity of 0.08°C coupled with a 320 x 240 pixel display provides accurate, high-resolution 14-bit thermal images in real time. The built-in external 102 mm LCD screen displays thermal images captured by the camera system. Table 3.2 shows relevant specifications of the camera.

Table 3.2 : Specifications of the FLIR S65 ThermaCAM

Characteristics	Specifications
Thermal Imaging Performance	
Field of View / min. focus distance	24°×18° / 0.3 m
Spatial Resolution (IFOV)	1.3 mrad
Thermal Sensitivity	0.08°C at 30°C
Image Frequency	50/60 Hz
Focus	Automatic / Manual
Detector type	Focal Plane Array (FPA), Uncooled microbolometer 320×240 pixels
Spectral Range	7.5 to 13 µm
Measurement	
Temperature Range	-40°C to +1500°C
Accuracy	+/-2° C, +/-2% of reading
Measurement Mode	Spot/Manual (up to 10 movable), Isotherm, Line profile

The images captured by the IR camera are displayed in the viewfinder and on the handheld LCD display, and stored on computer. Images were captured according to a pre-defined schedule of 1 image captured every 10 min, 24 hrs a day. The camera required a distance of approximately 6 m (20 ft.) to capture the entire 2.4 m x 2.4 m (8 ft. x 8 ft.) face of the test block with its regular lens. Figure 3.6 shows the FLIR S65 ThermaCAM.

Figure 3.6 : FLIR ThermaCAM S65 infrared research camera.

3.2.4 Weather Station

A WeatherHawk™ weather station was used to measure and store on-site weather conditions at the field research site. The weather station was mounted onsite on top of a 4.3 m (14 ft) extended tripod frame approximately 14 m (30 ft.) from the test block. A cable extending

from the weather station to the data house was required to provide power and data transfer to the data acquisition system.

The weather station had the capacity to measure ambient air temperature, wind speed, wind direction, solar radiation, relative humidity, rainfall, and barometric pressure. Each measurement was displayed in the user's choice of units. Table 3.3 shows the variables which were measured and the units of measure used during data acquisition at the test block.

Table 3.3 : Environmental parameters, sensor type and units for weather station.

Environmental Parameter	Sensor Type	Units
Air Temperature (Ambient)	Thermistor	°C
Barometric Pressure	Piezoresistive transducer	kPa
Solar Radiation	Silicon pyranometer	W/m^2
Rain gauge	Tipping bucket	mm
Wind Speed	Cup anemometer	m/s
Wind Direction	Vane	360° mechanical
Relative Humidity	Precision temperature corrected, bulk polymer	%

3.2.5 Data Acquisition

Data collection at the test block was achieved through three separate programs. The FLIR IR cameras has supporting software that allows for the camera to be controlled and images collected remotely. This software was used to program the camera to capture an image of the test block every 10 minutes, 24 hours a day. The environmental parameters measured by the Weatherhawk™ weather station was also collected with software provided by the manufacturer.

The collection of thermocouple data requires specialized equipment for signal conditioning of the raw data, which then assimilates, converts, displays and stores the necessary information. National Instruments data acquisition equipment was used, and LabVIEW was employed as the hardware/software interface. An environment was created in LabVIEW for this unique application, with the PC and Multi-function data acquisition (DAQ) card

converting and amplifying the refined signal from the signal conditioning card. The field set up is shown in Figure 3.7.

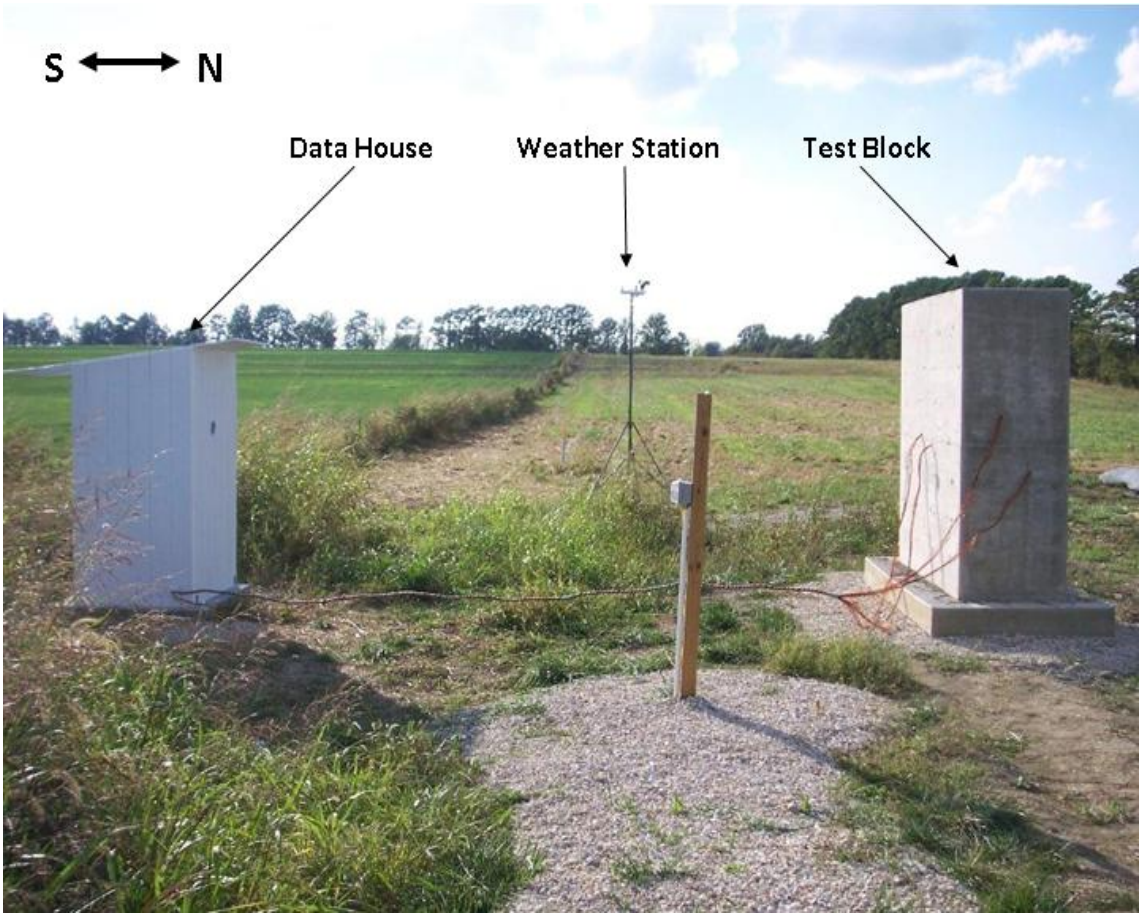

Figure 3.7 : Research site layout complete with data house, weather station, and concrete test block.

3.3 Data Processing

This section describes data processing conducted to configure the data for analysis. This includes details of the data acquisition, and how thermal contrasts were developed from raw thermal images to provide quantitative analysis of the thermal behavior of the test block.

3.3.1 Data Display and Recording

Once the experimental set up was complete, each system had to be configured to display and record the necessary data in sync with one another. The 32 thermocouple temperature readings were stored every minute. The weather station data for all the

environmental variables were sampled and stored every minute. The thermal images were captured and stored on the hard drive every 10 minutes. All data was stored on a standard PC in the data house. Data was periodically collected from the data house PC and transferred to a computer on campus for analysis.

3.3.2 Thermal Image Data to Temperature Data

Thermal images captured by the IR camera represent surface temperatures by a user-selected color scale, with thermal variations in the image represented by different colors. The span of temperatures across which the color scale is applied is user-selected, and as such the colors represent temperatures within the span selected. However, to perform quantitative analysis of the data, it is necessary to utilize the actual temperatures, not the colors. Additionally, because the color represents temperatures only within the span selected, and that span may change from one image to another, it was necessary to process data in the raw images such that effective analysis could be performed.

When viewing an image in an attempt to identify defects, the operator is analyzing the variations in temperature as represented by color variations in the image. For example, the color palette used may represent relatively “hot” areas as white, “cold” areas as black, and temperatures between the “hot” and “cold” as varying across a chosen color pallet. As such, variations in surface temperature caused by a defect are assessed by their color “contrast” when compared with areas that are intact.

To replicate this situation in the research, the thermal “contrast” was calculated that measures the difference in surface temperature between the surface area directly above each target and the surface temperature in the intact acreage area of the block. Figure 3.8 shows a thermal image taken from the south side of the test block to illustrate how this thermal contrast was derived from the thermal images.

When a thermal image is stored, the temperature value measured by the camera at each pixel (320 x 240 pixels per image) is stored. Any spot on the image can be selected and its actual temperature measurement determined, rather than the arbitrary color scale displayed. A location was selected on the surface above the target, such as point A in Figure 3.8 for the 51 mm (2 in.) deep target. A second location was selected to represent the temperature of sound concrete, such as point B in Figure 3.8. The thermal contrast was then determined from the difference in temperature measured at the two locations:

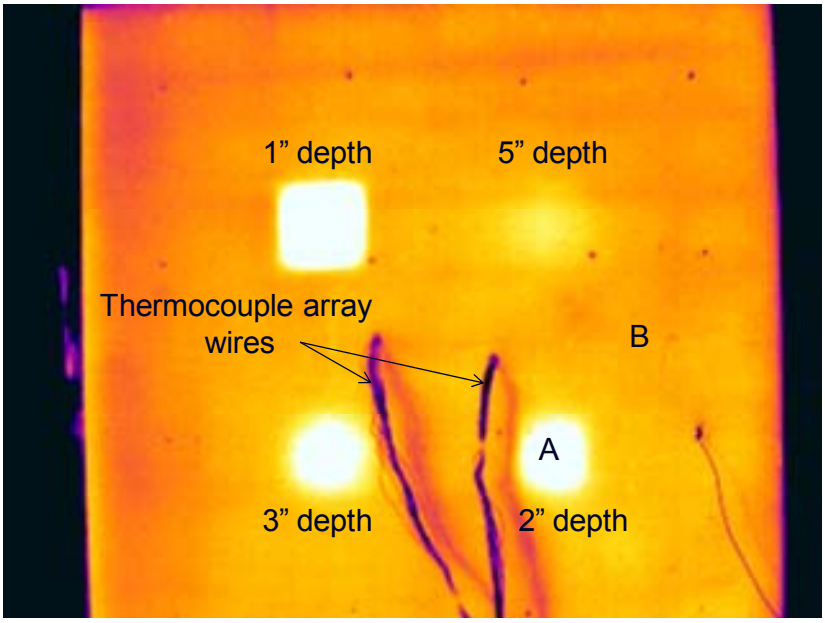

Figure 3.8 : Thermal image of the south side of the test block showing 4 target locations and measurement points for thermal contrast.

$$T_{contrast} = T_A - T_B \qquad \text{(Equation 3.1)}$$

The result is four thermal contrasts (temperature differentials) that represent the temperature difference between a defective region of concrete relative to sound concrete in the same image. This provides a numerical value for the color contrast that can then be used to process data more effectively than simply comparing multiple images.

The camera was configured to capture a thermal image every 10 minutes. These images were then processed using consistent locations for determining the thermal contrast at each target. The process is shown schematically in Figure 3.9. The same locations were

selected for analysis in every image, as shown in the figure. This provided a thermal contrast value for each target location as a function of time, such that the thermal behavior could be assessed and compared with environmental variables that vary with time.

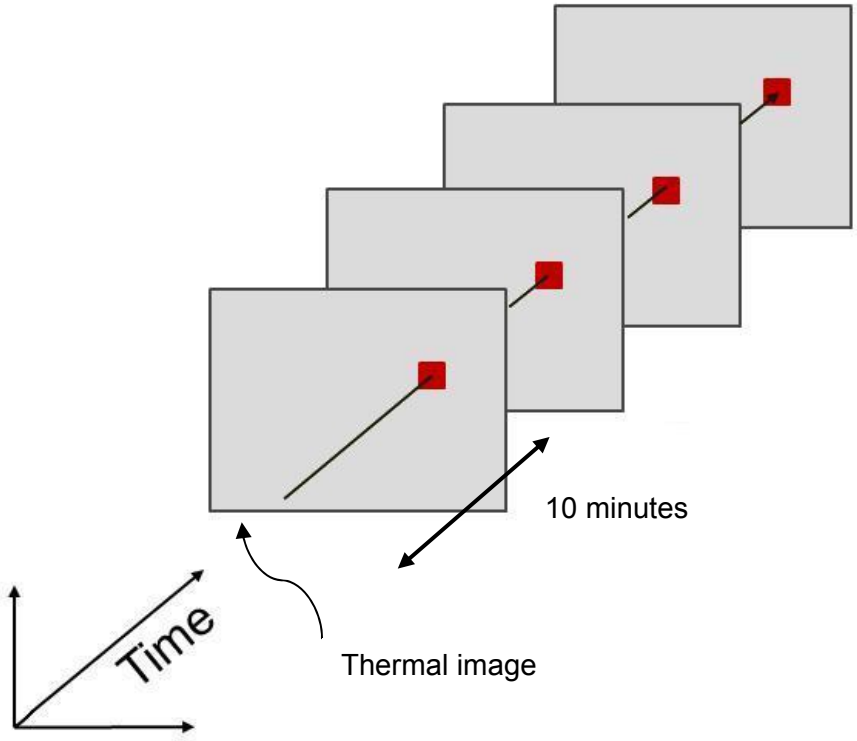

Figure 3.9 : Thermal contrast taken from image pixel every 10 minutes.

The results of this data processing are shown in Figure 3.10, which shows the thermal contrast for each of the four targets on the south side of the test block. The figure also shows the solar loading (radiant heating of the sun) for that day. The thermal contrast values correspond to the left vertical axis and the solar loading is on the right vertical axis. The horizontal axis is Time over a 24 hour period. As can be observed in this figure, the thermal contrast for each of the targets develops at different times of the day, with deeper targets developing thermal contrast later in the day. Additionally, the magnitude of the thermal contrast, that is the peak contrast value, is reduced as the target depth increases. This is the behavior anticipated based on fundamental heat transfer theories.

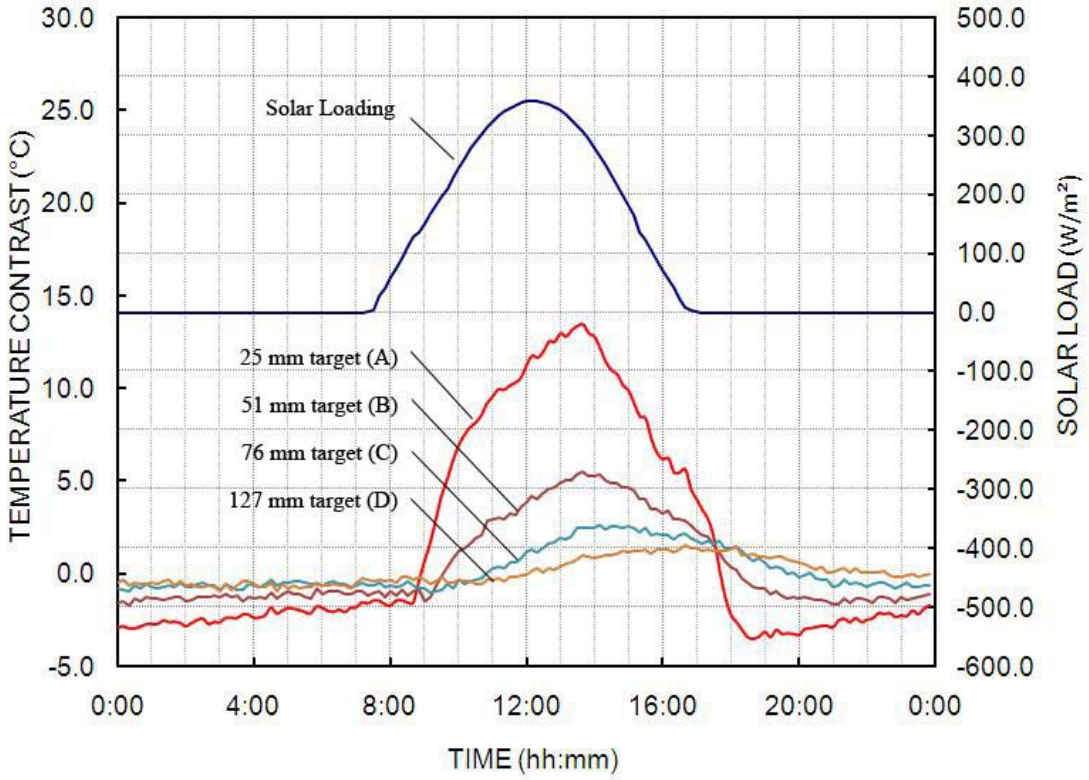

Figure 3.10 : Thermal contrast developed in the test block for each of the targets, and the solar loading.

Figure 3.11 shows an image of the north side of the test block captured during the day (Figure 3.11A) and an image of taken at night (Figure 3.11B). During the day a warming trend exists such that the targets have positive thermal contrasts, which mean that the delaminated regions are at a temperature higher than the sound concrete. During the night (Figure 3.11B) a cooling trend exists (ambient temperature falling after sunset) resulting in the targets having a negative thermal contrast, which mean that the delaminated regions are at a temperature lower than that of sound concrete.

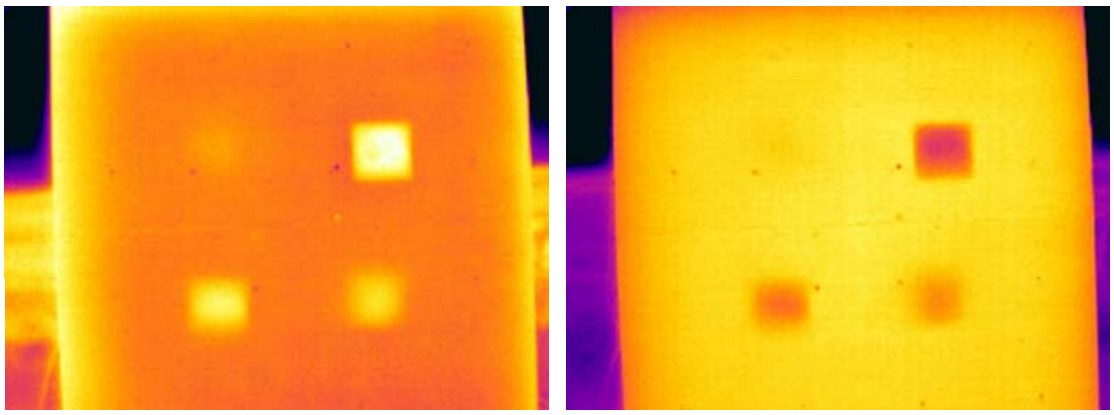

A B

Figure 3.11 : Thermographic images of test block (north side) taken A) during the day and B) during the night.

3.3.3 Preliminary Data Reduction

This section of the report explains the data reduction done for both the north and south sides of the block. First the basic analysis common to both faces of the block is explained. This is followed by a description of data reduction that was unique to the north or south sides of the block.

Data was collected at the test site for a total of 89 days on the south side of the block (November 1, 2007 to January 29, 2008) and for 92 days on the north side of the block (May 1, 2008 to July 31, 2008). All the data from various sources like thermal data from IR images, thermocouple data and environmental data from the weather station were reduced to provide measurements on a 10 minute time interval. Consequently, each day of data is comprised of 144 data points for each of the environmental parameters, thermocouple measurements and thermal contrast values.

For much of the analysis, this data collected at 10 minute intervals was analyzed to determine single values that would represent behavior of specific parameters on a given day, to be compared with the thermal contrast achieved on that day. For example, one might wish to compare the maximum thermal contrast achieved on a particular day with the maximum ambient temperature on that day. As such, the parameter of temperature is reduced to a single

value, maximum temperature, and compared with a single value for the thermal contrast for that day. Such reduction of data led to the simplification of 89 days of data for the south face and 92 days of data for north side into single values for each parameter that could represent the entire day. The data points were then used to correlate various parameters with the thermal contrast produced on the same day.

4 ANALYSIS

4.1 Quantitative Data Analysis

This section describes the methods of data analysis utilized to evaluate the data for both the north and south sides of the test block. The data analysis and processing methods were used to develop quantitative data on the thermographic results from observation of the test block. In some cases, these methods differed for analysis of the north and south side of the test block. These differences are described here. Section 4.2 describes how thermal contrast values representing the behavior of the subsurface targets was calculated. Section 4.3 describes the thresholds used to define "good" thermal contrast. Sections 4.4 – 4.6 describes the analysis of the environmental parameters measured in the study. Sections 4.7 and 4.8 describe the analysis of inspection periods and rate of change (ROC) analysis, respectively. Finally, section 4.9 describes the analysis of data by division into "bins."

4.2 Thermal Contrast Analysis

Methods for analysis, of the thermal contrast for the north side and south side differed somewhat due to different behavior that was observed during the testing. Figure 4.1 shows the thermal contrast behavior for a typical day on the south side of the block (top) and a typical day on the north side of the block (bottom). Thermal contrast on the south side of the block during the day typically developed in a sinusoidal shape that mirrored to some extent the solar loading on the surface of the block. The shape of the thermal contrast curve was predictable and consistent, such that selecting a maximum value on the curve to represent the overall behavior was representative, especially with respect to the targets at depths of 51, 76 and 127 mm (2,3 and 5 in.). The shape of the contrast curve for the 25 mm (1 in.) deep target was more sensitive to short term effects, such as periodic cloud cover, and as a result was typically more varied than the deeper targets. This can be observed in Figure 4.1, when cloud cover occurs in the

afternoon, the contrast for the 25 mm (1 in.) deep target is reduced almost immediately. This cloud cover has some effect on the 51 mm (2 in.) deep target, but the effect is much smaller. Analysis generally focused on the 51 mm (2 in.) and 76 mm (3 in.) deep targets, which are at more realistic depths for defects in real concrete bridges and structures. Thermal contrast behavior for a single day could be characterized by the maximum thermal contrast that was observed for that day on the south side of the block.

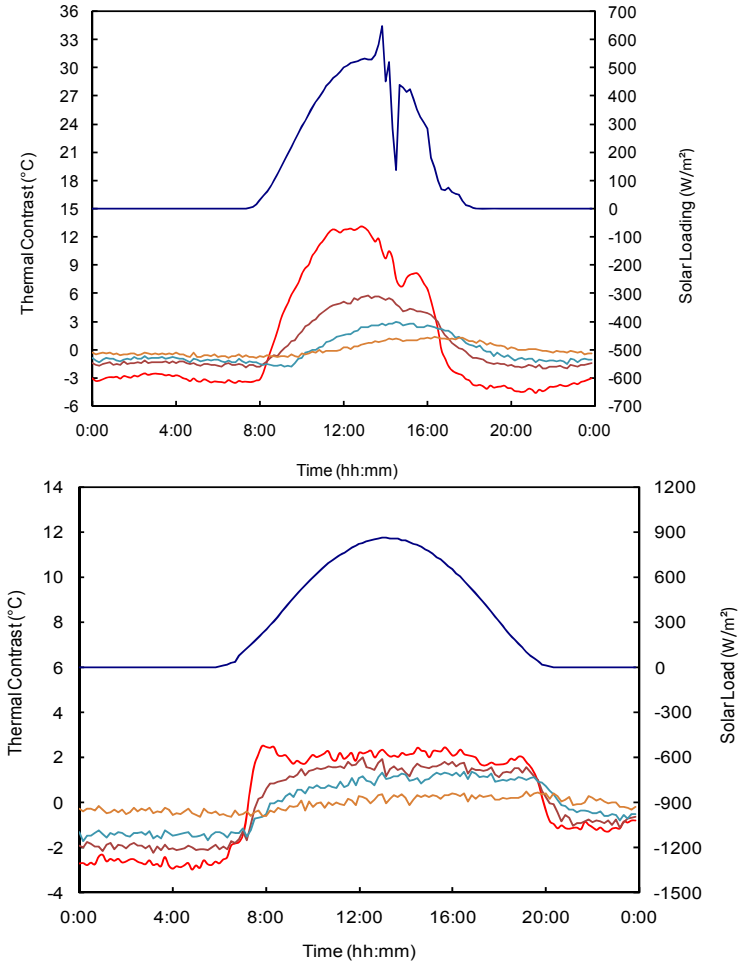

Figure 4.1 : Thermal contrast for a typical day on the south side (top) and the north side (bottom).

However, for the north side of the block, the shape of the thermal contrast curve typically displayed a long period of sustained contrast, though at a much lower level than the south side. This sustained period of thermal contrast had some variation over time, such that selecting the

maximum contrast value might not be representative of the overall behavior. In other words, selecting a single maximum value for thermal contrast might characterize a peak value that occurred over a very short time period, and this may not effectively represent the overall behavior. The maximum thermal contrast was determined by its maximum (or minimum for the case of nighttime) average value over a specific period of time. A study was conducted to determine the effects of averaging the thermal contrast over various time periods ranging from 0.5 to 3 hours. It was found that averaging the thermal contrast over 1 hr was effective in eliminating the effects of minor, short-term contrast variations while still providing a meaningful measure of the overall block behavior.

4.3 Thresholds

Threshold values for the thermal contrasts developed in the test block were utilized as a data analysis tool to characterize the quality of thermal images produced during the experiments. These threshold values were arbitrarily selected to provide a means of characterizing the level of thermal contrast observed during particular days, such that days could be grouped into categories of “good” days vs. “bad” days. Because the targets in the concrete block provide an ideal model of a subsurface defect, thermal contrast in the test block would be expected to be much greater than for a real, naturally occurring delamination at a similar depth in concrete. Therefore, the fact that thermal contrast exists in the block for a particular set of environmental parameters would not indicate that a real delaminations would necessarily be observable in the field. For naturally occurring delaminations, the thermal contrast would be lower than in the idealized model for the same environmental conditions (and the same depth). Ideally, there would exist a transfer function that could be used to relate the magnitude of thermal contrast for the test block to the magnitude of a real delamination. However, “real” delaminations do not have well-defined characteristics; they vary in depth in the concrete, surface texture, size and shape etc., all of which could be expected to effect the

thermal contrast produced. Consequently, there is not a defined transfer function that relates the behavior of an idealized model such as the foam target in concrete and a real defect. Therefore, it was necessary to select a threshold value for the thermal contrast in the test block that could indicate when a real delamination was likely to be detectable in the field. The values of 1°C (1.8°F) and 2°C (3.6°F) were selected for two primary reasons:

- 1°C (1.8°F) at least an order of magnitude higher that the sensitivity of the camera (0.08°C, 0.14°F), such that much smaller variations in surface temperature were easily detectable by the equipment. This value is 20 times the sensitivity of the cameras used by States during field testing (0.05°C, 0.09°F)
- The ASTM specification indicates that 0.5°C (0.9°F) is the necessary contrast between sound concrete and a defect. 1°C (1.8°F) is twice, and 2°C (3.6°F) is four times the requirement.

Under field conditions, there will be "noise" in the thermal images caused by material property variation on the surface of the concrete, such as stains, patches, lane striping etc. that will contribute to making an image more difficult to analyze. This is a consideration in the threshold of the 0.5°C (0.9°F) contrast requirement in the ASTM specification. The threshold value selected was intended to be sufficiently high to generally consider this effect to provide representative values for conditions when thermographic inspection was likely to be effective in the field. As mentioned previously, there is no direct transfer function that relates contrast development for an ideal target such as used here and an actual defect. The values selected were thought to provide conservative estimates for dry, relatively uniform delaminations. This may be a suitable area for research in the future.

4.4 Changes in Ambient Temperature

The effect of ambient temperature changes is an important factor for the thermographic inspection of concrete, particularly for inspecting portions of a structure not exposed to solar

loading. To evaluate the effect of ambient temperature changes on the thermal contrast observed in the test block, it was necessary to separate positive ambient temperature variations that occur during the day from negative ambient temperature variations that occur at night.

Positive changes in the ambient temperature typically occur between the morning and the afternoon, when the day is warming as shown in Figure 4.2A. To determine the positive change in ambient temperature for a given day, it is necessary to determine the maximum and minimum ambient temperature over a time period of 12:00 am to 12:00 am as shown in the Figure 4.2A. This positive ambient temperature change results in positive thermal contrast at the targets as shown in the Figure 4.2A.

Negative ambient temperature changes occur in the overnight time period, when temperatures are dropping. To determine the negative ambient temperature change for a given overnight period, it is necessary to evaluate a time period between 12:00 pm on the previous day and 12:00 pm on the day being evaluated. This time period is shown in Figure 4.2B. As shown in the figure, this negative ambient temperature change results in negative thermal contrast at the test block. This adjustment in the data is necessary to ensure that change in ambient temperature for negative trend analysis includes the heat of the previous day and the cooling that is maximum the following morning (the next calendar day).

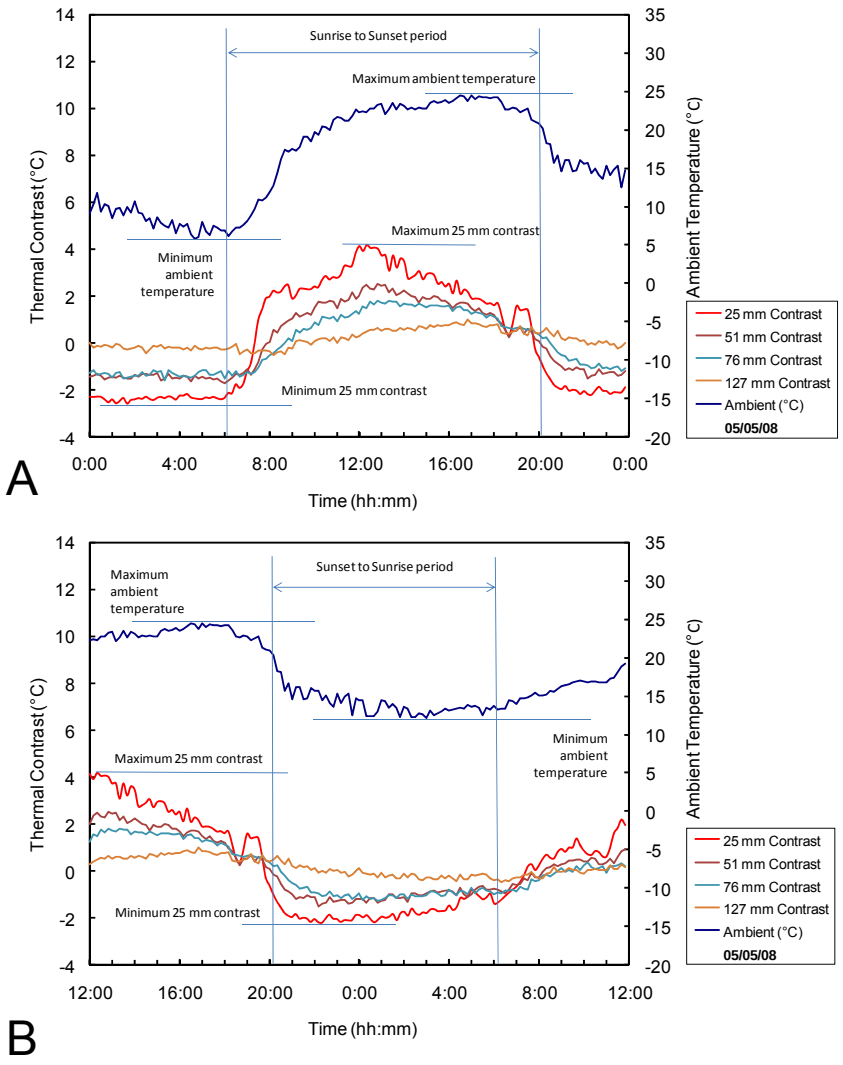

Figure 4.2 : Example of positive contrast time period (A) from midnight to midnight, negative contrast time period from noon till noon (B), showing ambient temperature vs. thermal contrasts over 24 hour period.

4.5 Wind Speed Analysis

Initial assessment of the wind speed data collected on the south side of the block indicated that although wind speeds varied over the course of a typical day, sudden changes in wind speed (over minutes) did not have a strong effect on the thermal contrast developed in the test block, particularly for targets at depths of 51, 76 and 127 mm (2, 3, and 5 in.). It was also observed that isolated high wind speeds did not typically occur; the winds were generally high on some days, and generally low on others. To characterize the effects of wind, it was

necessary to determine time periods over which wind speeds could be characterized in a meaningful way, such that wind speeds could be evaluated by an inspector in the field to guide inspections. Figure 4.3 shows wind speed data for a typical day. The wind speed values shown in the figure are wind speeds sampled every 10 minutes at the on-site weather station. The figure shows that wind speeds vary over the course of the day, but there are time periods of a day that may be "windy" and time periods that are "calm." In general, night times have lower wind speeds than daytimes due to the lack of radiant heating from the sun.

In was determined that an effective way to characterize wind speeds was to break down each 24-hour period into four quarters of 12:00 midnight to 6 AM, 6 AM till 12:00 noon, 12:00 noon till 6:00 PM, and 6:00 PM till 12:00 midnight as shown in Figure 4.3. These time periods were selected for two reasons. First, they provide a general measure of the wind speed during times of high ambient temperature change that is separate from time of more sustained thermal conditions. For example, the morning was separated from the afternoon. In this manner, the influence of wind speed during the development of thermal contrast at the targets could be evaluated separately from the influence of the wind speed at the time maximum (south side) or sustained (north side) thermal contrast were occurring. Second, it was assumed that inspections would typically be conducted during the normal business day when possible. As such, it could be useful to understand the effect of morning wind conditions vs. afternoon wind conditions in terms of determining if a particular day was a "good day" for thermography or "bad day." For example, if it was determined that high winds in the morning reduced the thermal contrast observed in the afternoon, this may be useful in decision-making regarding use of a thermal camera.

Other forms of wind speed, such as daily average, maximum, and average from sunrise to sunset were also assessed during the course of the research. Overall, it was decided that the 2nd and 3rd quarter wind speeds were most critical to thermal contrast development, in particular 2nd quarter (2nd quarter wind speed for positive analysis takes place between 6:00 AM

and 12:00 noon, while 2nd quarter wind speed for negative analysis takes place between 6:00 PM and 12:00 midnight). The second quarter wind speeds are important because these are the time periods when thermal contrast is being developed, and the rate of heat transfer from the environment to the concrete was thought to be most significant in terms of the resulting thermal contrast.

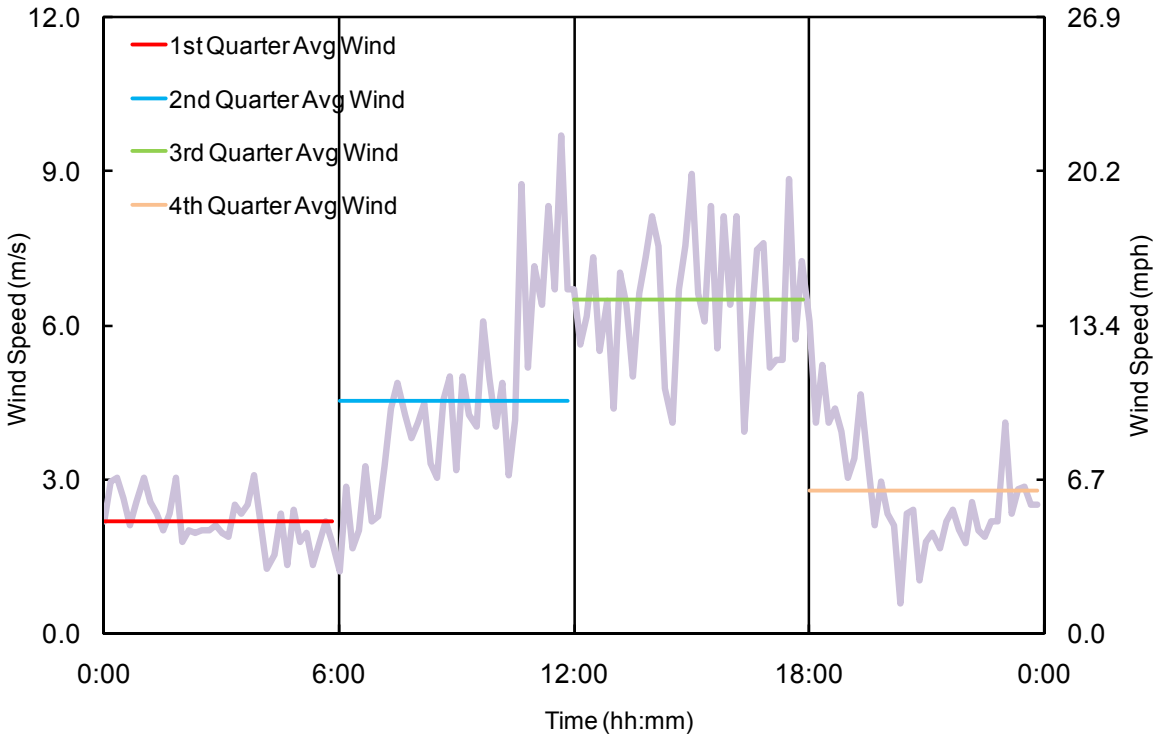

Figure 4.3 : Wind speed quarter averages for 24 hours (June 7th, 2008).

4.6 Relative Humidity Analysis

The values utilized to represent humidity in the analysis included average values acquired between sunrise and sunset for the positive analysis, and between sunset and sunrise for the negative analysis. Figure 4.4 shows the period that is used for positive analysis. It is typical for relative humidity values to be low during the day, and high during the night based on common weather patterns.

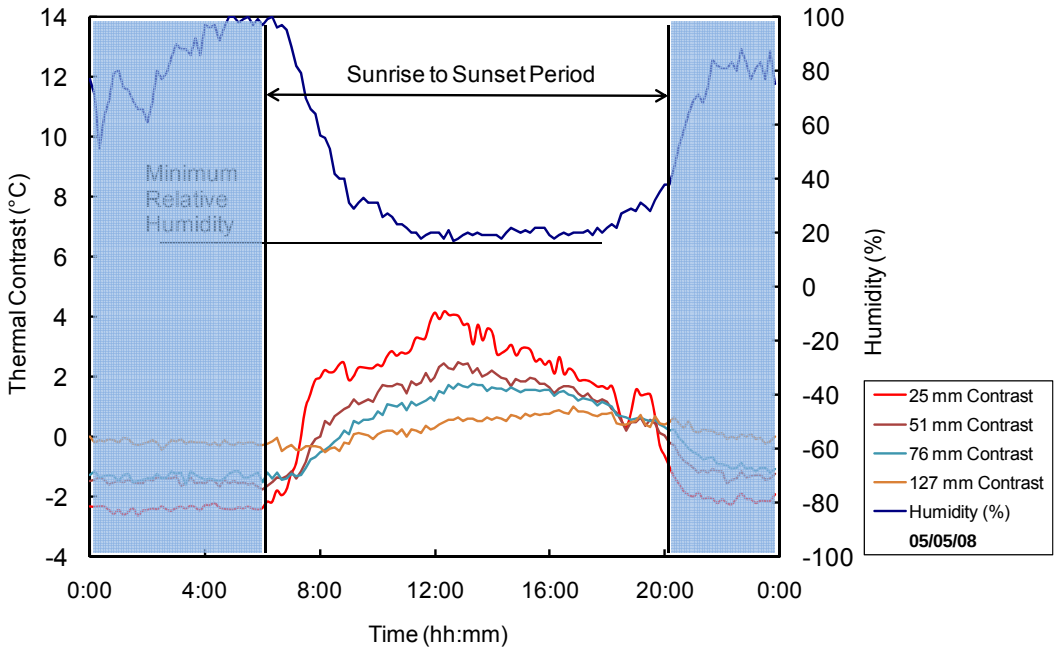

Figure 4.4 : Example of data used in humidity positive analysis (May 5th, 2008).

Another factor that was used for evaluating the effects of humidity was the change in relative humidity. Because humidity is typically high at night and low during the day, the change in relative humidity, that is the difference between the maximum relative humidity in the overnight period and the minimum relative humidity during the daytime period, was assessed to determine correlations with the thermal contrast development.

4.7 Analysis of Inspection Periods

A practical consideration for the implementation of thermography for bridge inspection is the time of day (or night) during which inspection should be conducted to provide the greatest likelihood that subsurface defects could be detected. Data analysis was conducted for the purpose of determining a useful “inspection period” for both the day and night. Time periods were identified using the threshold values for the thermal contrast developed at the subsurface targets.

The results gained from threshold analysis included the time it took for contrasts to become useful, the time the contrast remains useful and the time the target ceases to be of useful contrast, based on the threshold values selected. The time of day (based on 24:00 hrs) was normalized to the sunrise and sunset of each day to account for variations in day length over the course of time. Figure 4.5 shows the inspection period based on the 1°C (1.8°F) threshold. As can be seen in the figure, the threshold is achieved at different times for each target, depending on the target depth. The time period over which a particular target's contrast value exceeds the threshold also varies depending on target depth. The time at which the contrast exceeds the selected threshold was defined as the "inspection period" during which thermoghraphy is most likely to be useful for bridge inspection. The results of this analysis are included in section 5.4.

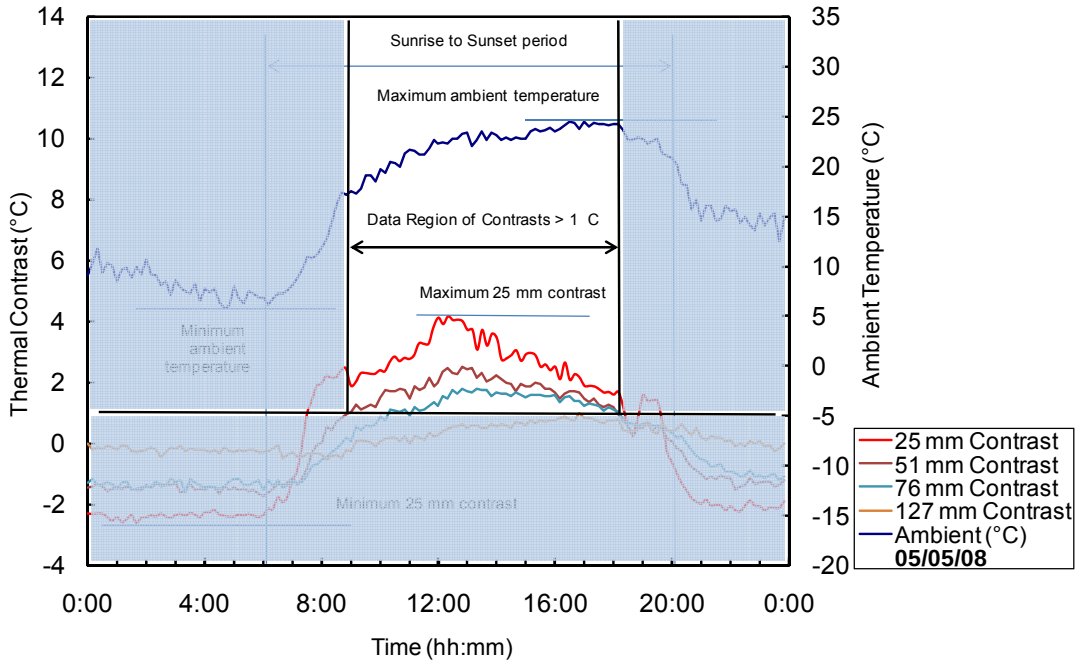

Figure 4.5 : The selection of 51 mm target positive thermal contrasts greater than 1 °C for May 5th, 2008 as compared to thresholds of sunrise and sunset, north side.

4.8 Rate of Change Analysis

Figure 4.6 shows ambient temperature and thermal contrast for a typical day. When analyzing the initial data from the north side of the block, it was observed that the rate of change (ROC) of the ambient environment had an effect on the thermal contrast for the 25 and 51 mm (1 and 2 in.) deep targets. It was observed that frequently, when the ROC of the ambient temperature was close to 0, that is, ambient temperatures were constant, contrast in the block began to diminish.

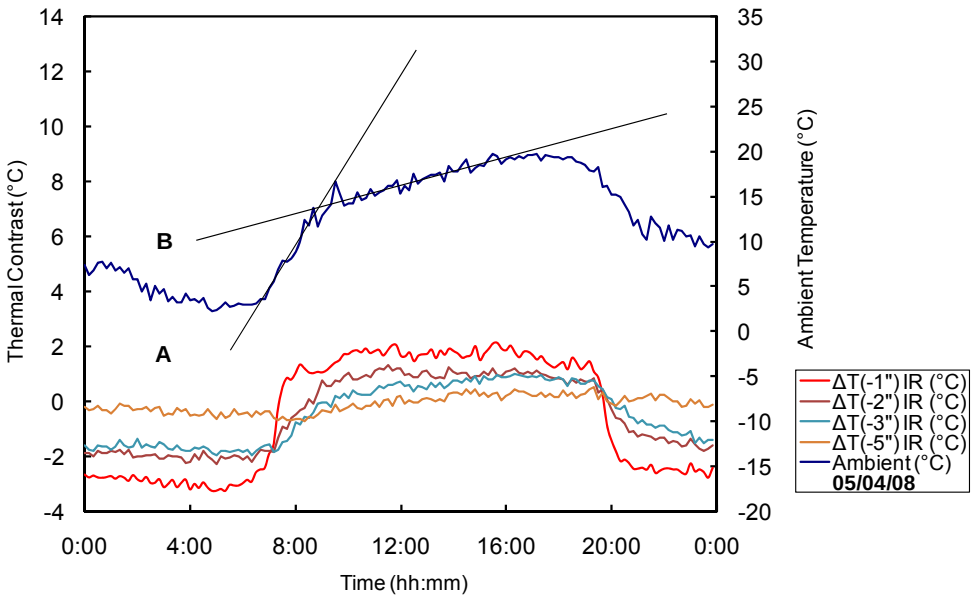

Figure 4.6 : May 4th, 2008 during daytime, with thermal contrast and ambient temperature, and includes two distinct rates of change.

Analysis of the data showed that a typical day had two distinct ROCs during the warming trend. Slope A shown in Figure 4.6 illustrates the rapid change in temperature (high ROC) that is caused by warming at sunrise. It is associated with the initial development of contrast in the test block. Slope B is the more gentle increase in temperature which occurs until the late afternoon and this rate of change is associated to the relatively constant thermal contrast which exists throughout the day. Following slope B, the slope of the ambient temperature goes to 0 before changing signs and becoming a negative slope (cooling). At the point of 0 slope, it can

be observed that the 25, 51 and 76 mm (1, 2 and 3 in.) deep target contrasts are beginning to diminish slightly.

The importance of this in terms of bridge inspection is that when ambient temperatures are constant or declining, the effectiveness of the thermal camera as an inspection tool may also be diminishing. As such, if a clear relationship could be found, an inspector could evaluate the quality of environmental conditions in terms of the ROC of the environment, and use this data in decision-making processes.

To explore these relationships, the ROC of the ambient environment was related to thermal contrast development and the ROC of thermal contrast development. A time interval of 3 hrs was found through analysis to provide a useful measure of the ambient temperature ROC. For the results reported here, this three-hour interval was used. Analysis of other time intervals was conducted and is reported in a thesis by Fenwick (Fenwick, 2009, in revision).

4.9 Bin Analysis

Division of data into separate “Bins” was used in some cases to provide analysis of typical average values for one parameter within a selected range of a second parameter. Most commonly the range parameter was thermal contrast, and the average parameter was an environmental variable. For example, thermal contrast value might be in separate “bins” or ranges such as 0 to 1°C (0 to 1.8°F), 1 to 2°C (1.8 to 3.6°F), 2 to 3°C (3.6 to 5.4°F) etc. The average value for an environmental parameter, for example wind speed, for each of the defined bins was calculate along with the standard deviation for the parameter (within the particular bin). This analysis provided for assessment of characteristic values for the environmental parameters at different levels of thermal contrast, to determine what values were typically measured (and their variation) for each bin.

5 RESULTS

5.1 Environmental Relationships with Thermal Contrast – South Side

This section examines the relationship between thermal contrast on the south side of the block, which is exposed to direct sunlight. Because of the radiant heating of the sun, the thermal contrasts for this side of the block are typically significantly higher than those observed on the north side of the block. Data analysis focused primarily on the behavior of the test block during the daytime, since the radiant heating of the sun was available and consequently this would be the time that inspections would be conducted. With the exception of some data analyzed to determine optimum inspection times, the environmental variables were all assessed during the daytime period. A series of scatter plots were developed and analyzed to assess the relationship between the environmental parameters and the contrast developed in the test block. The contrast for the 51 mm (2 in.) deep target was typically used in the analysis, because this target is at a realistic depth in terms of naturally occurring delaminations.

5.1.1 Ambient Temperature Change

Figure 5.1 shows the scatter plot of ambient temperature change versus the thermal contrast for the 51 mm (2 in.) deep target. The vertical axis indicates the thermal contrast in units of °C. A best-fit line was calculated for the data points and the equation of the trend line is in the graph along with coefficient of determination (R^2 value), which shows the degree of correlation of the data, on a range of 0 to 1. The data in this figure was derived by taking the range of ambient temperature changes for a given day, and plotting that against the maximum thermal contrast for that day. As shown in the figure and by the relatively low R^2 value (0.22), there was relatively poor correlation between the ambient temperature change and the resulting thermal contrast in the test block. However, the trend line does have a positive slope, which indicates that higher ambient temperature changes correlate somewhat with increased thermal

contrast that developed for the 51 mm (2 in.) deep target. However, it can be observed that on certain days, even though there was a high ambient temperature change, significant thermal contrasts were not developed.

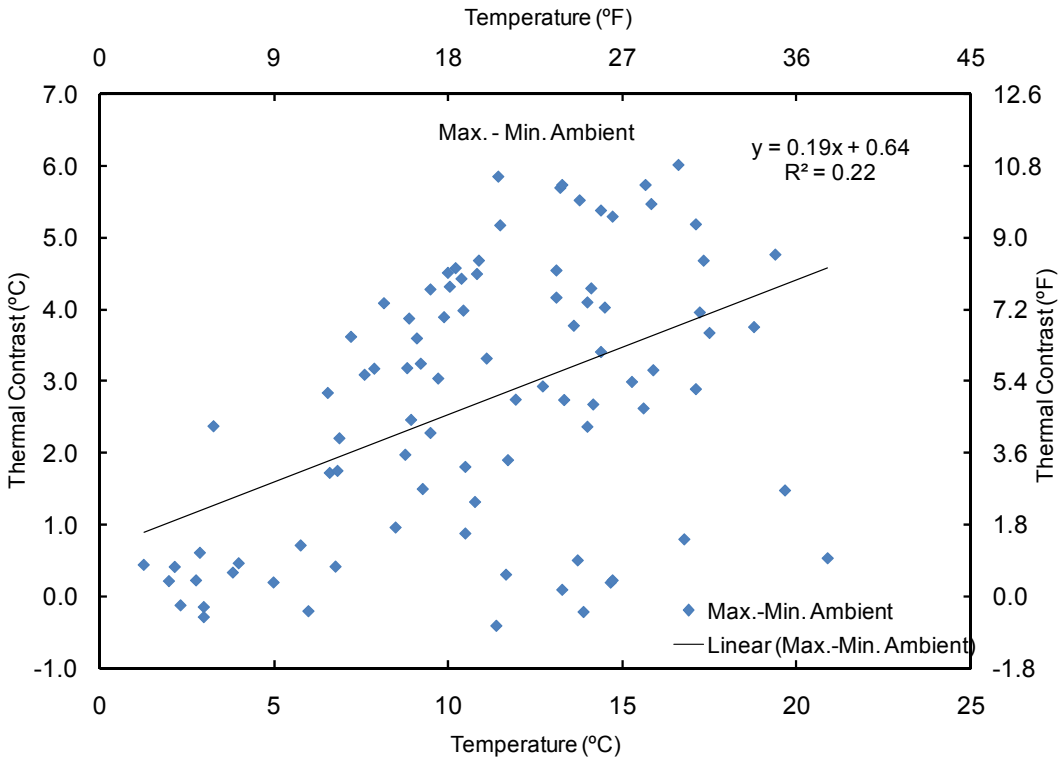

Figure 5.1 : Scatter plot with trend line for ambient temperature change versus thermal contrast.

5.1.2 Solar Loading

Solar radiation was measured at the on-site weather station. Because the south side of the block is exposed to direct sunlight, measurement of the solar radiation provides a quantitive description of the intensity of sunlight for a given time period. Figure 5.2 shows the correlation between the Solar loading (radiation) vs. the thermal contrast for 51 mm (2 in.) deep target. The maximum solar loading represents the most intense sun period of the day. This may occur for only a short period if there are periodic clouds that block the sun. As the figure indicates, there was a correlation between the maximum solar loading and the thermal contrast developed. However, the R^2 value for this correlation is relatively low, only 0.55. It can be observed in the data that the days with the most intense sunlight, over 700 watt/m^2, did not correspond to the

highest thermal contrast values. This indicates the maximum solar load may not be the most effective measure when characterizing the quality of a day for thermographic inspection. Other factors such as periodic cloud cover, which interrupts the solar loading, need to be considered.

Data was analyzed to consider the solar loading imparted into the concrete over the course of the entire day. To calculate this value, the area under the solar loading curve was calculated for each day, and this value was then correlated with the observed maximum thermal contrast.

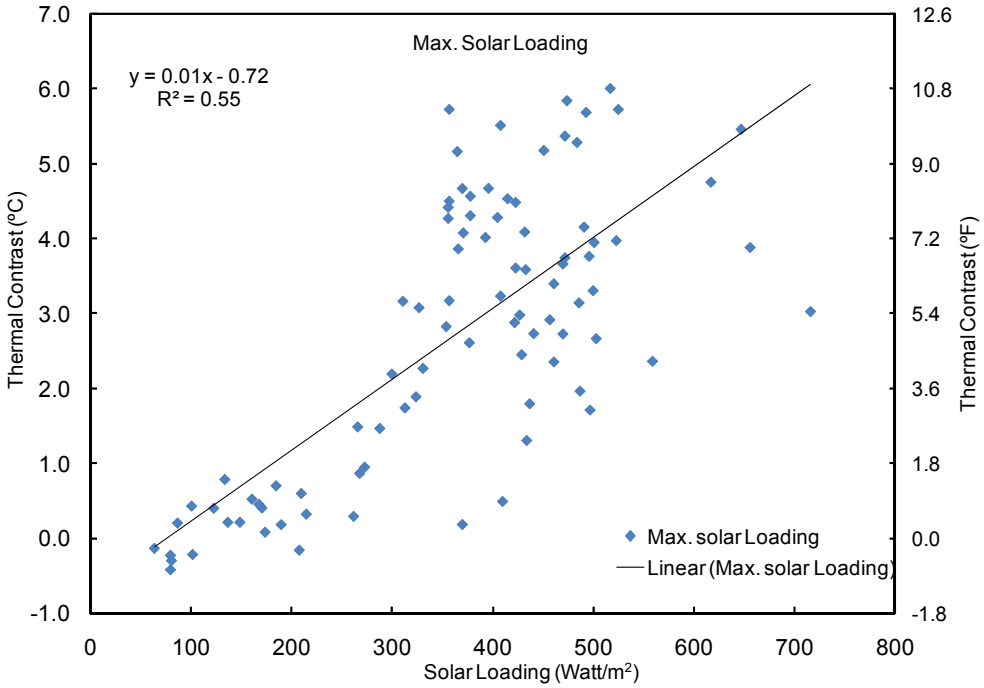

Figure 5.2 : Scatter plot with trend line for maximum solar loading versus thermal contrast.

Figure 5.3 shows the results of this analysis, which showed a strong, linear correlation between the level of developed contrast and the amount of solar loading for a given day. This implies that a strong linear relationship exists between the development of thermal contrast and solar loading. The high R^2 value (0.75) suggests the area of solar loading has a very good correlation with the development of thermal contrasts. Applying a minimum threshold or 1°C for usable thermal contrast, it was found that for 90% of the days with at least 0.7 kW-hr/m^2 there was at least 1°C (1.8°F) of contrast. This was calculated by determining the intercept of a

horizontal line, drawn at 1°C (1.8°F), with the trend line in the figure, and calculating the percentage of days remaining above 0.7 kW-hr/m^2 and 1°C (1.8°F) of contrast as a portion of all days with solar loading of at least 0.7 kW-hr/m^2. The significance of this in terms of inspection is that periodic cloud cover that reduces the intensity of sunlight for short periods has a negative impact on the thermal contrast developed, and that the solar loading over the course of the day may be more important than the intensity of sunlight at any particular time. This is consistent with the importance of the radiant heating from the sun to develop thermal contrast in a concrete structure. Additionally, because the relationship between the area of solar loading and the thermal contrast was found to be linear, longer periods of intense sunlight are proportionally better than shorter time periods. In other words, inspection conducted during longer days (summer) will provide improved results over inspections conducted on shorter days (winter).

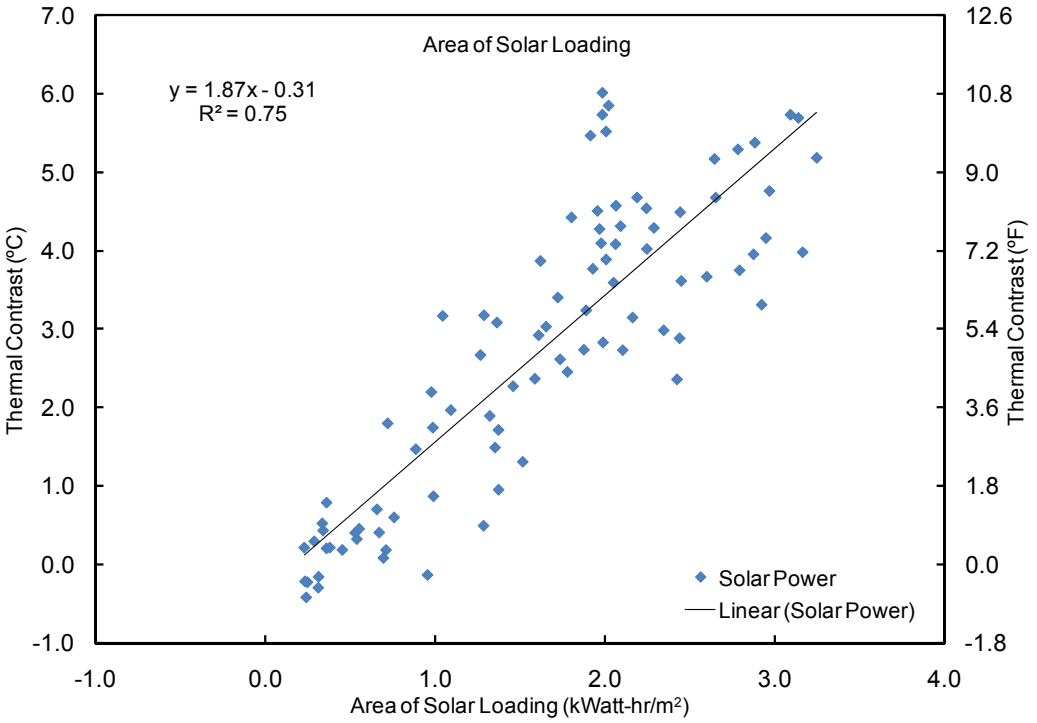

Figure 5.3 : Scatter plot with trend line for area of solar loading versus thermal contrast.

5.1.3 Wind Speed – South Side

Analysis was conducted of the effect of wind speed on the thermal contrast for the south side of the block. To assess the relationship between the thermal contrast developed at the 51 mm (2 in.) deep target and the wind speed, each 24 hour period was broken into six-hour quarters. Using the average wind values from each quarter and the bins analysis method, the effect of wind speed on thermal contrast was explored. Two graphs are shown using the 51 mm (2 in.) deep target thermal contrast bins and the second and third quarter wind speeds. Figure 5.4 shows the graph with error bars (standard deviations) for second quarter wind speeds and Figure 5.5 shows the graph with error bars for third quarter wind speeds for the different bins.

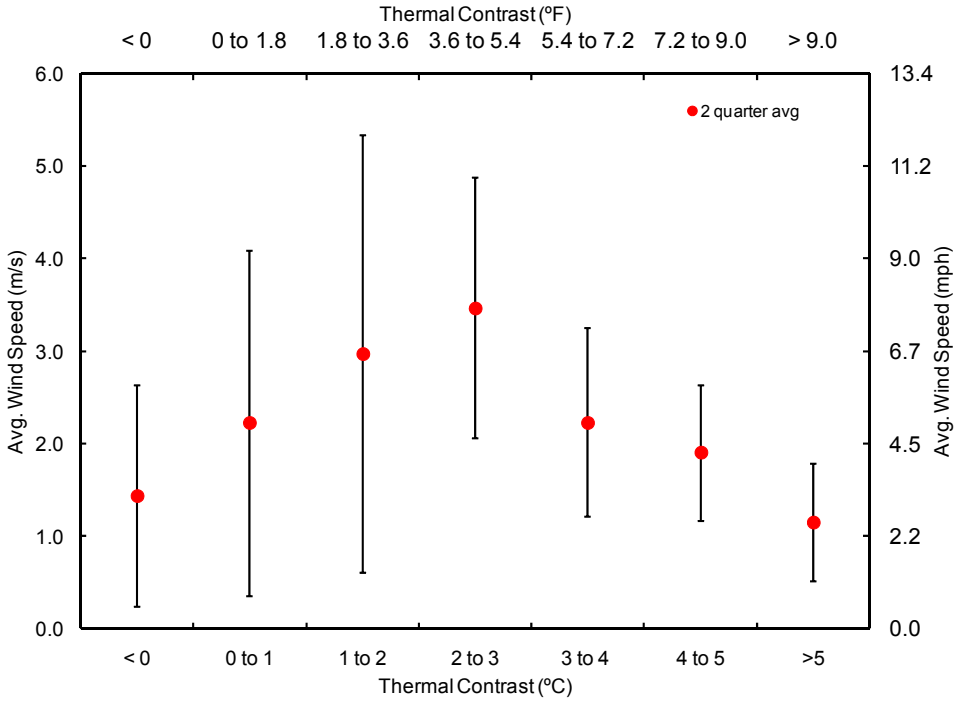

Figure 5.4 : Graph of second quarter wind speed versus thermal contrast for 51 mm (2 in.) deep target with error bars.

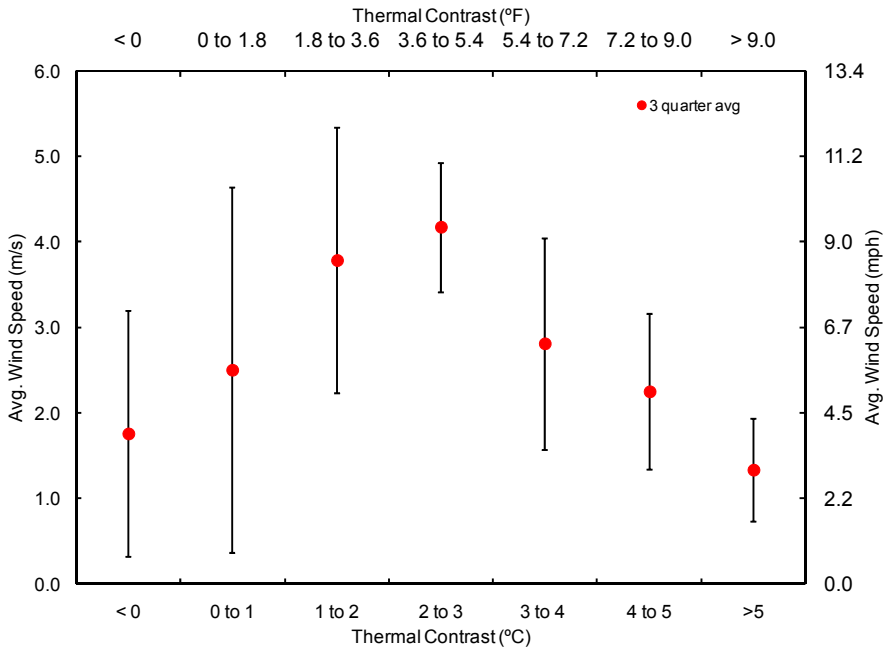

Figure 5.5 : Graph of third quarter wind speed versus thermal contrast for 51 mm (2 in.) deep target with error bars.

If the Figures 5.4 and 5.5 are studied you can see the average wind speed and standard deviation are reduced for the higher contrast relative to lower contrast. It is also shown that the average values for very poor thermal contrasts have low average wind speeds. This corresponds to days in which the solar loading is not adequate to develop thermal contrast, but may be calm conditions in terms of wind. This finding suggests that days with optimum conditions for thermographic inspection may have low wind speeds, as would be expected. It is difficult to define specifically a limiting value for wind speed, but the figures show that days with the best thermal contrast, say greater the 3°C (5.7°F) typically were characterized by winds of less than ~ 3 m/s (7 mph) to ~ 4 m/s (9 mph) based on 2nd and 3rd quarter analysis, respectively. These values consider +1 standard deviation of the data.

This data was further analyzed by examining the characteristic thermal contrasts for three groupings of wind speed, 0 to 4 mph (low wind speed), 4 to 8 mph (moderate wind) and >8 mph (high wind speeds). Analysis of this data using a scatter plot of the solar loading and the maximum thermal contrast showed that the trend for thermal contrast was lower for days

with high winds (>8 mph) relative to the trend for all days combined, and much lower than the trend when winds were low. Figure 5.6 shows the scatter plot for maximum thermal contrast vs. the solar loading area (kW-hr/m^2), with the three wind categories, low, moderate and high shown as different markers. Also shown on the plot is the trend line for high winds (long dash lines), low winds (short dashed lines), and all of the data as one group (solid line). As can be seen, the trend of the correlation for days with low wind speeds is much higher than days with high winds. Figure 5.7 shows the same relationships for the 3rd quarter wind speeds. The third quarter is from the hours of 12:00 noon to 6:00 pm., which is envisioned as the primary time for inspections, due to the time delay for the concrete to warm over the course of the day.

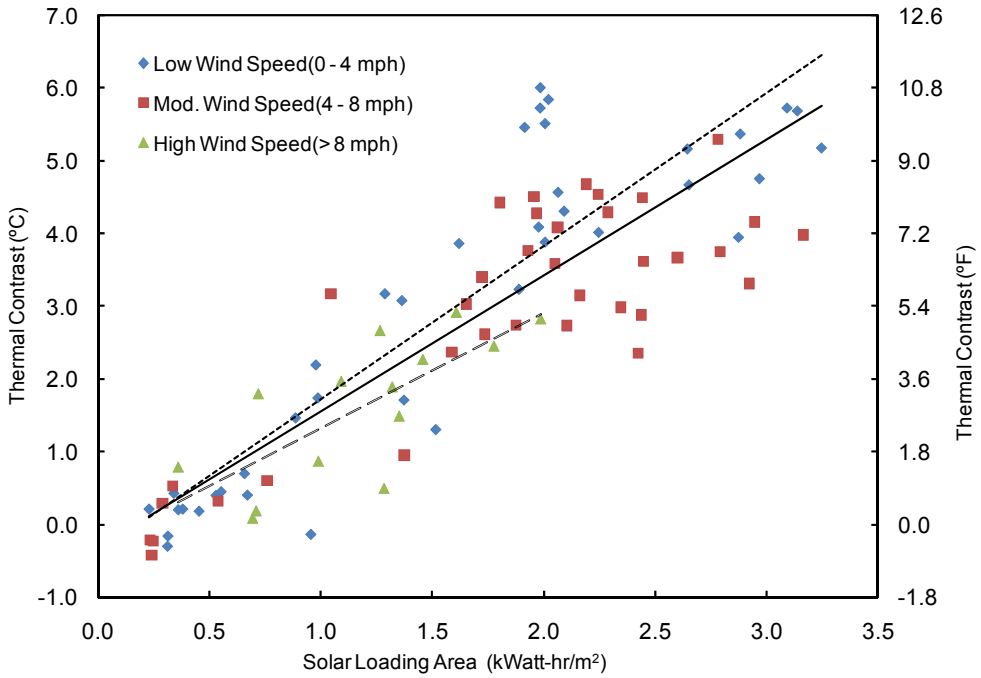

Figure 5.6 : Scatter plot of solar loading vs thermal contrast, with low, moderate and high wind speeds, 2nd quarter.

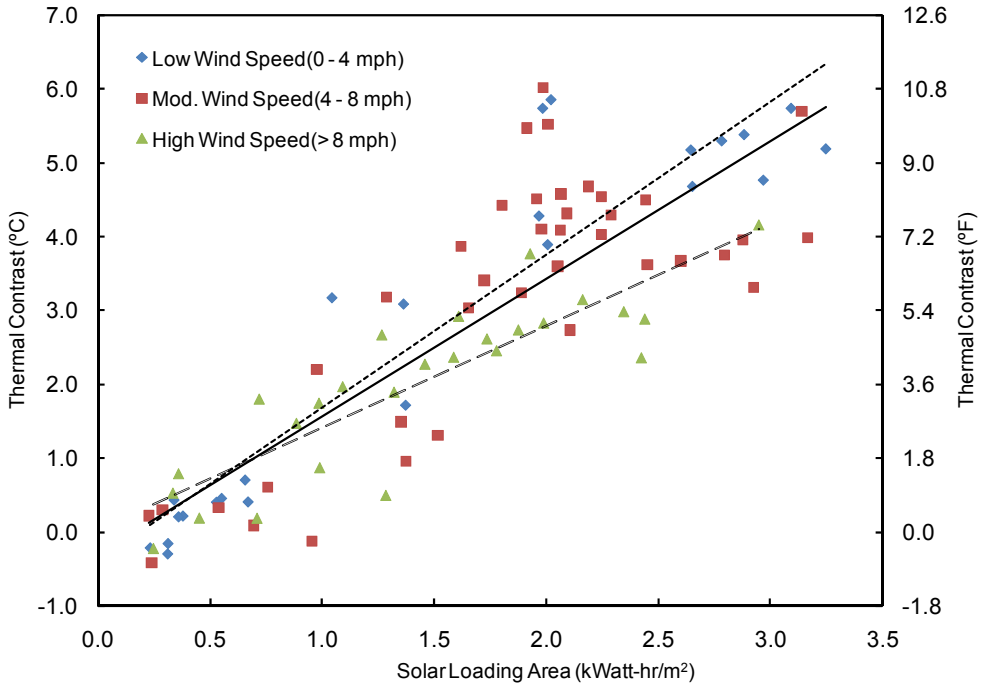

Figure 5.7 : Scatter plot of solar loading vs thermal contrast, with low, moderate and high wind speeds, 3rd quarter.

5.1.4 Discussion

The analysis of the effects of wind speed on the south side of the test block showed that average wind speeds had an effect on the thermal contrast for two reasons. First, the trend of the correlation plots for low wind speeds was much higher than trends for high wind speeds. In other words, for the same amount of solar loading, days with lower wind speed developed higher thermal contrast than days with high wind speeds. Table 5.1 shows the regression parameters from the analysis of wind speeds. This data indicates that the rate of change for days with low wind speeds is much greater than days with high wind speeds. Additionally, the R^2 values are much lower for high wind speeds, indicating that this data is more scattered. Second, it was observed that days with higher solar loadings had the characteristic of being days with low to moderate winds. Therefore, applying a threshold of 8 mph for the maximum average wind speed will result in improved conditions for detection of subsurface features, based on the fact that trends were higher and the observation that the highest solar loading was

observed on days with low to moderate wind speeds. This "threshold" is not a fixed limit value for wind speed, but is suggested by the data as a useful general guideline based on the results of the study.

Table 5.1 : Regression parameter data from analysis of 2nd and 3rd quarter wind speeds.

Regression Parameters	Slope		Intercept		R^2	
Wind Category	2nd Quarter.	3rd Quarter	2nd Quarter	3rd Quarter	2nd Quarter	3rd Quarter
Low Wind	3.79	3.74	-0.69	-0.71	0.81	0.88
High Wind	1.59	1.38	-0.27	0.04	0.55	0.75
All Data	1.87	1.87	-0.31	-0.31	0.75	0.75

It should also be noted that this wind speed is calculated as a 6-hr average wind speed, to characterize an overall condition for a particular time period of six hours. Most data reported by various weather stations is over a much smaller time interval. Therefore, when applying this threshold consideration of the overall wind condition is necessary. Such data can be determined from the web site developed under this research, though this feature has not yet been implemented. Such improvements to the weather web site are suggested as part of the implementation recommendations contained in Section 7.3.

5.2 North Side Data Results

This section provides an overview of results from monitoring the north side of the test block. The north side of the test block is never exposed to ambient sunlight, and therefore provides a model of a shaded area of a bridge, such as the soffit area. This analysis was conducted from 92 days of collected data. The analysis was conducted considering both the positive thermal contrast developed during the day, when conditions are warming, and in the overnight period, when conditions are cooling. It was found through the research that the average contrast developed was the same for the nighttime as it was for the daytime, 1.4°C (2.5°F), with the contrast being positive during warming and negative during cooling. Overall,

there were 83 days that developed a positive contrast of at least 1°C (1.8°F) and 72 nights that develop negative contrast of at least 1°C (1.8°F).

5.3 Environmental Relationships with Thermal Contrast – North Side

This section will focus on the relationship between thermal contrast and ambient temperature, ambient temperature change, wind speed, and relative humidity to provide quantitative results for the different environmental conditions for the North side of the test block. The majority of the data included in this section will be based upon the analysis of the environmental conditions during the 92 days of observation of the North side of the test block. Some will be based on a reduced set of data, which excludes certain rain conditions, and this is indicated in the text.

5.3.1 Ambient Temperature

This section discusses the effect of ambient temperature changes on the thermal contrast developed in the north side of the block. Ambient temperature changes that occur during the course of the day results in thermal gradients in the concrete, and provides the driving force for the development of thermal contrast at a subsurface defect. The change in ambient temperature is the key environmental parameter for the detection of subsurface defects in concrete when radiant heating from the sun is not available to induce thermal gradients in the concrete.

To evaluate the effect of ambient temperature, the maximum thermal contrast for the 51 mm (2 in.) deep target was correlated with the changes in ambient temperature. As noted previously, this maximum value is based on a 1-hr, running average value. Figure 5.8 shows the results of this analysis for both positive (daytime) and negative (nighttime) contrast on a single plot. The figure shows the thermal contrast for all 92 days of data collected on the north side of the test block. The vertical axis is the change in ambient temperature and the horizontal axis is the thermal contrast observed for the 51 mm (2 in.) deep target.

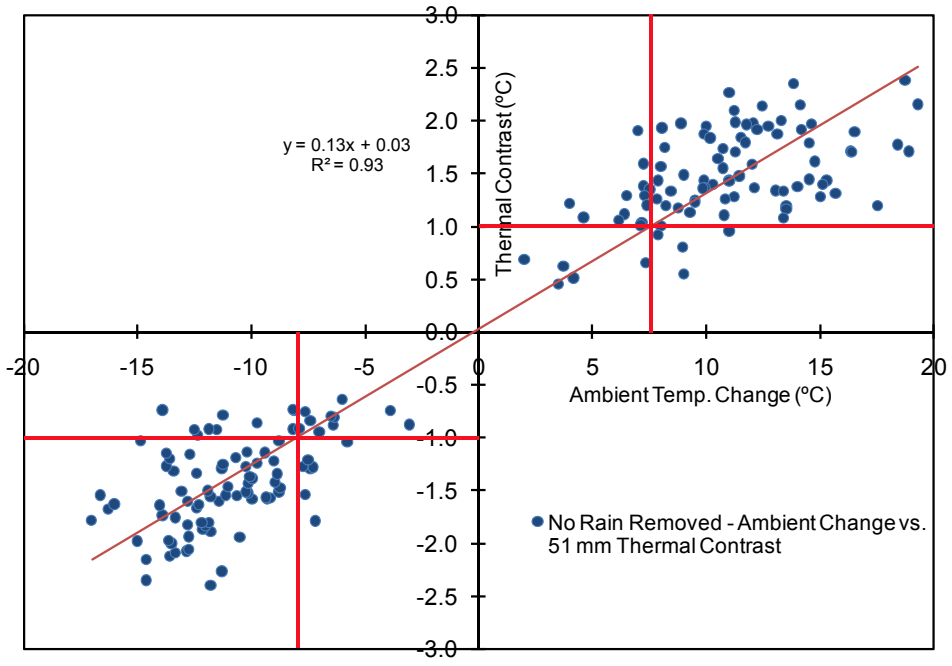

Figure 5.8 : Thermal contrast in north side of test block compared with ambient temperature changes.

As the figure shows, there is a strong relationship between the changes in ambient temperature and the thermal contrast in the test block. The coefficient of determination (R^2) value for the data was found to be 0.93 when the entire group of measurements (both positive and negative) were considered.

This data was analyzed to determine if there could be a threshold ambient temperature change determined to guide the inspection of bridges. A vertical line was placed on the graph at the 1°C (1.8°F) point for the positive and negative thermal contrast. This threshold was used to estimate adequate thermal contrast at the targets to represent a useful contrast in practical applications for real delaminations, as discussed previously. The intersection point of this threshold with the best-fit line was used to draw the horizontal lines shown at approximately +7.5°C (12.6°F) and -7.9°C (13.5°F). It was found that for the positive contrast, 95% of the days with at least 7.5°C (12.6°F) of ambient temperature change had positive contrasts that were at

least 1°C (1.8°F). Applying this threshold to the negative contrast, it was found that 86 % of the days had at least -1°C (1.8°F).

To evaluate the effects of rain on the thermal contrast developed, the days in which rain was measured at the on-site weather station were grouped according to the extent of rainfall for a specific day. This was done because it was found that rain may occur over part of a day, but if the ambient temperature changes were adequate, thermal contrast would still develop (assuming that the surface being observed is not wet).

The following criteria were used to characterize the extent of rainfall on a particular day:

- Rainfall (mm) – greater than 7.5 mm (0.3 in.)?
- Duration of rainfall (hh:mm) – greater than 2 hours?
- Significance of rainfall (does it occur during period of useful thermal contrast?)

The complete 92 days of data were refined by the removal of days in which all of these questions were answered yes. For this condition, from 92 days of data, this method of rainy day removal left 80 days for positive contrast analysis and 83 days for negative contrast analysis. Data was refined by the removal of days to which any of the questions in were answered yes. Far more days were removed from the summarized set using this method in which the rain may or may not be affecting the contrast observation, but ensured the removal of data that might bias the results. The conservative method left 62 days of data for both positive and negative analysis in which all days that met any of the rainfall criteria were met.

Figure 5.9 shows the correlation between the thermal contrast and the ambient temperature changes when all of the criteria are met (80 days positive, 83 days negative). As the figure shows, this method of rain removal had little effect on the correlation between the ambient temperature variations and thermal contrast.

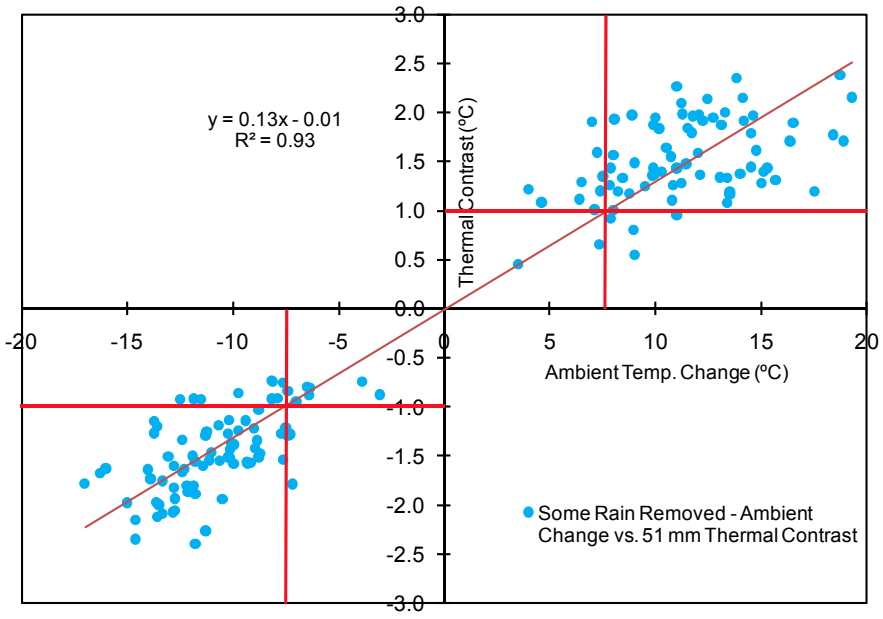

Figure 5.9 : Thermal contrast in north side of test block compared with ambient temperature changes, with days including rain removed.

The results of analyzing the data to determine the ambient temperature variations required to develop 1°C (1.8°F) at the 51 mm (2 in.) deep target are shown in Table 5.2. The data in this table includes the best fit line intercepts for each of the three rain criteria, and the resulting percentage of days that met the criteria of having at least 1°C (1.8°F) of contrast for the calculated intercept value.

Table 5.2 : Percentage of thermal contrast meeting threshold criteria.

Condition	Type	Threshold (°C) (Intercept value)	% of data above threshold and greater than +/- 1°C
No rain removed	Positive	7.5	95
	Negative	-7.9	86
Moderate Removed	Positive	7.8	94
	Negative	- 7.6	88
All rain removed	Positive	8.2	96
	Negative	- 7.2	90

This analysis showed that there was slight improvement in the percentage of the population with at least 1°C (1.8°F) if days that included rain were removed from the analysis,

though this improvement is small and does not change the overall results. Applying a threshold environmental condition of +/- 8°C (~15°F) ambient temperature change will result in a high likelihood that thermal contrast will exist for subsurface defects at a depth in concrete of 51 mm (2 in.). Applying this threshold (+/- 8°C (~15°F)) to the data collected during the study, using only days in which there was no measured rain, resulted in 96% of the positive contrasts and 91% of the negative contrast exceeding the 1°C (1.8°F) threshold. If all 92 days were assessed, the results were 96 % and 87% for the positive and negative thermal contrasts, respectively.

The data set was further partitioned into separate bins according to the magnitude of the thermal contrast for the 51 mm (2 in.) target. This analysis was done to determine the characteristic ambient temperature changes for thermal contrast of greater than 1°C (1.8°F) and greater than 2°C (3.6°F). The result of this analysis show the average ambient temperature changes that occurred for days with thermal contrast in separate bins. For example, the data in Table 5.3 shows that for days in which the thermal contrast was in the range of 1 to 1.5°C, the change in ambient temperatures were on average greater than 10°C (16°F) both positive and negative thermal contrast. For the range of 1.5 to 2 °C, the average ambient change was ~12°C, and for more than 2°C of contrast that average ambient change was ~14 and ~13°C for the positive and negative thermal contrasts, respectively. Data for each of the rain conditions analyzed is shown in the table, although the removal of days with rain had little effect on the ambient temperature changes that were observed to develop the necessary thermal contrast.

Table 5.3 : Average ambient temperature changes for thermal contrast bins ranging from 0 to 3°C.

	Positive Contrast (°C)				Negative Contrast (°C)			
Contrast Range	0 to 1	1 to 1.5	1.5 to 2	2 to 3	0 to -1	-1 to -1.5	-1.5 to -2	-2 to -3
All Data	6.4	10.2	12.1	14.2	-8.5	-10.3	-12.1	-13.1
Some Rain Rem.	7.9	10.6	12.3	14.2	-7.9	-10.1	-11.9	-13.1
All Rain Rem.	7.9	11.4	12.6	14.9	-8.1	-9.8	-11.8	-13.1

5.3.2 Wind Speed Analysis – North Side

The relationship between thermal contrast and wind conditions is quite a complicated one for shaded structures, in comparison to sun exposed structures. If high winds exist on a sun exposed surface then the wind will drive away the heat which has built up in the surface due to solar loading. The issue with shaded structures is the fact that the concrete relies upon convection alone to transport heat to the structure and to the delaminated regions. High wind speeds provide additional heat transfer from the environment to the concrete, which would presumably result in increased thermal gradients and increased sensitivity to subsurface defects.

The results were analyzed to determine the average wind speeds for the various ranges of thermal contrast. Analysis revealed that the second quarter of a 24 hour period had the most significant effect on the thermal contrast. For positive thermal contrast, the time period was between 6:00 am and 12:00 pm, and for negative thermal contrast this time period is between 6:00 pm and 12:00 am. These time periods were determined to be significant because it is within these time periods, which encompassed sunrise and sunset, that the thermal contrast is actually developed; it is then maintained for some period of time, as discussed earlier.

Figure 5.10 is the scatter plot that relates the ambient temperature change to the thermal contrast developed for the 51 mm (2 in.) deep target. Wind speed categories are shown as different markers on this plot. Wind speeds are broken down into 3 categories; high winds being > 3.6 m/s (>8 mph), moderate between 1.8 and 3.6 m/s (4 and 8 mph), and low between 0 and 1.8 m/s (0 and 4 mph), as with the south side analysis. Also shown on the plot is the trend line for high winds (long dash lines), low winds (short dashed lines), and all of the data as one group (solid line). The trend lines indicate that the slope of the trend line for the high wind category is higher than that for the low wind category, the opposite of what was found on the south side, and the low wind trend line actually has a slightly lower slope that the trend line for the overall population. This may indicate that because the north side relies on convection only

for the heating of the block, the high wind speeds may actually assist in the development of thermal contrast by increasing convective heat transfer. However, the scatter of the data is so substantial that it is difficult to determine if this is a real effect or just a statistical anomaly for this particular data set.

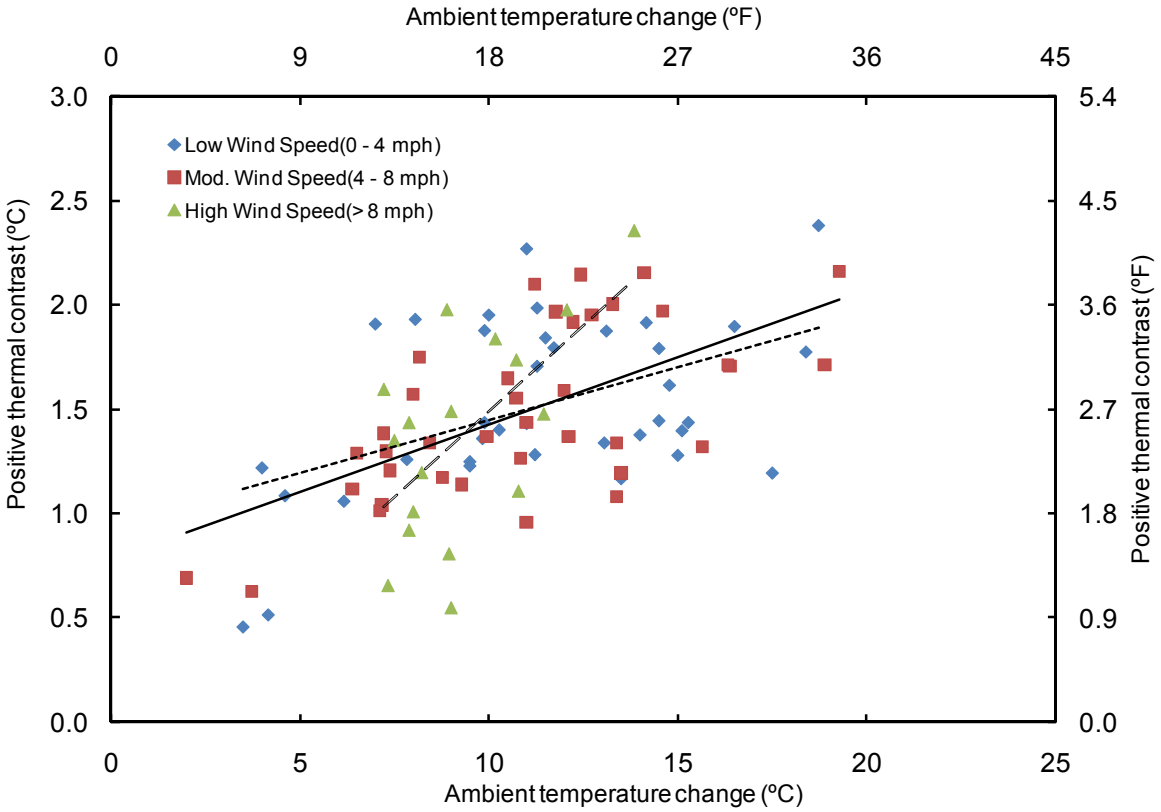

Figure 5.10 : Scatter plot showing positive thermal contrast developed vs. ambient temperature change, with wind speed categories of high, moderate and low. North side, 2nd quarter.

The wind effects during the night showed that low wind speeds correlated with the highest thermal contrast for the same ambient temperature change. The data is shown in Figure 5.11, showing the negative thermal contrast developed in relation to negative ambient temperature changes in the overnight hours. Again trend lines are for high winds (long dash lines), low winds (short dashed lines), and all of the data as one group (solid line). These trends show that low wind speeds result in a higher negative trend than high wind speeds. However, few conclusions could be drawn from this data, because it is typical for overnight periods to be

calm, such that the majority of wind speed data from the overnight period can be categorized as "low". For further analysis of the overnight period, the reader is referred to the thesis associated with this work (Fenwick, 2009). It can be stated that the highest thermal contrasts were observed to have low wind conditions.

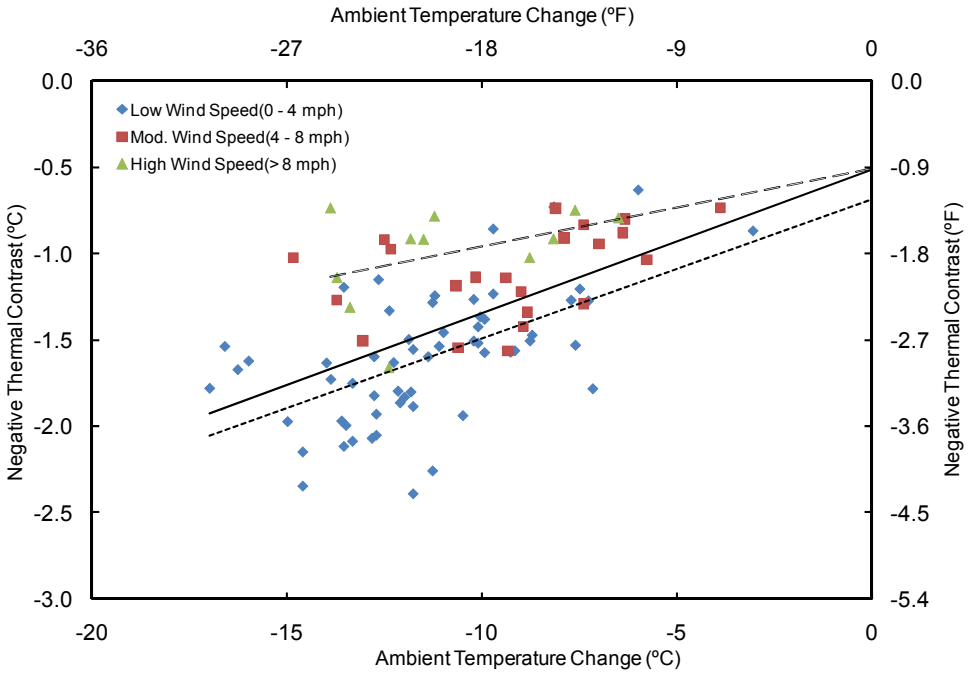

Figure 5.11 : Scatter plot showing negative thermal contrast developed vs. ambient temperature change, with wind speed categories of high, moderate and low. North side, 2nd quarter (night time).

5.3.3 Discussion on Wind Speeds

The results for wind speed on the north side of the block were inconclusive, showing opposite trends for day and night, which one would not expect. There may be several reasons for the lack of consistency in the data. One possibility is that the direction of the wind speed plays a role in the convective heat transfer, and since this was not analyzed in this research, there appears to be a great deal of unexplained scatter in the data. The wind direction was not analyzed because it was not thought to be a practical way to characterize the wind under field conditions at a bridge. Since the bridge has surfaces oriented in many different directions, it is unlikely that a bridge inspection could be effectively executed within wind direction limits.

Additionally, the actual wind directions affecting a bridge may be complex due to the aerodynamic properties of the structure. As such, the goal of the wind analysis was to characterize the wind conditions overall, regardless of the direction. For the south side analysis, this is likely adequate, due to the dependence of the methods on radiant heating from the sun. For shady conditions, the wind direction may play a much larger role, and this should be considered for future research in this area.

5.3.4 The Effects of Humidity on Thermal Contrasts

This section discusses the analysis of the effects of humidity on the thermal contrast developed on the north side of the test block. During the day, between the hours of 8 am and 8 pm, there was an average minimum relative humidity of 32% for the 92 days from May to July with an overall average of 49%. During the night, the relative humidity typically tends toward 100%, but averaged 94% maximum and 82% average between the hours of 8 pm and 8 am. Attempts were made to find patterns between relative humidity data and thermal contrasts.

Figure 5.12 shows the ambient change versus positive thermal contrast for 92 days, this time with the specific relative humidity conditions highlighted. Relative humidity was characterized as “high” (>60%), “moderate”, (30 – 60%) and “low” (0 to 30%). Trend lines for high humidity (long dash lines), low humidity (short dashed lines), and all of the data as one group (solid line) are shown. The data shows that the trend line for high humidity has a higher slope than for low humidity, which may support the theory that increased humidity assists with convective heat transfer. However, there are very few days with high humidity that have high ambient temperature change; high humidity days typically have low ambient temperature changes due to overall weather patterns. The trend line for moderate humidity also has a higher slope than the overall trend line (this is shown as a long dash-dot line). Qualitative observation of the data in the figure shows that high and moderate relative humidity days were typically above the overall trend line, low humidity below, as would be expected based on the

regression parameters. This would suggest that the convective heat transfer properties are improved for days with moderate to high humidity. For the south side, analysis of the effects of relative humidity indicated that low relative humidity typically occurred on days with long, sustained solar exposure and as such days with high thermal contrast in the block. Based on the data from both the north and south side of the block, it appears likely that low humidity is a characteristic of days with high solar loading, due to the generally clear skies, and that these days also have high ambient temperature changes due to the effect of the sun. Essentially, low relative humidity occurs on good days for thermographic inspection. Conclusive data was not found to show that the low humidity itself was the source of variation in the thermal contrast observed in the test block. For the north side of the block presented here, the data seems to show improved thermal contrast for moderate humidity relative to low humidity, for the warming trend of the daytime. During the night time, relative humidity values are typically very high due to overall weather trends. The analysis of the data showed that high humidity was a characteristic of days with high negative temperature changes, and as such improved thermal contrast. But data on moderate and low humidity was limited due to the weather trends (night times have high relative humidity). A more detailed study of the effects of humidity is likely required to fully define the effects.

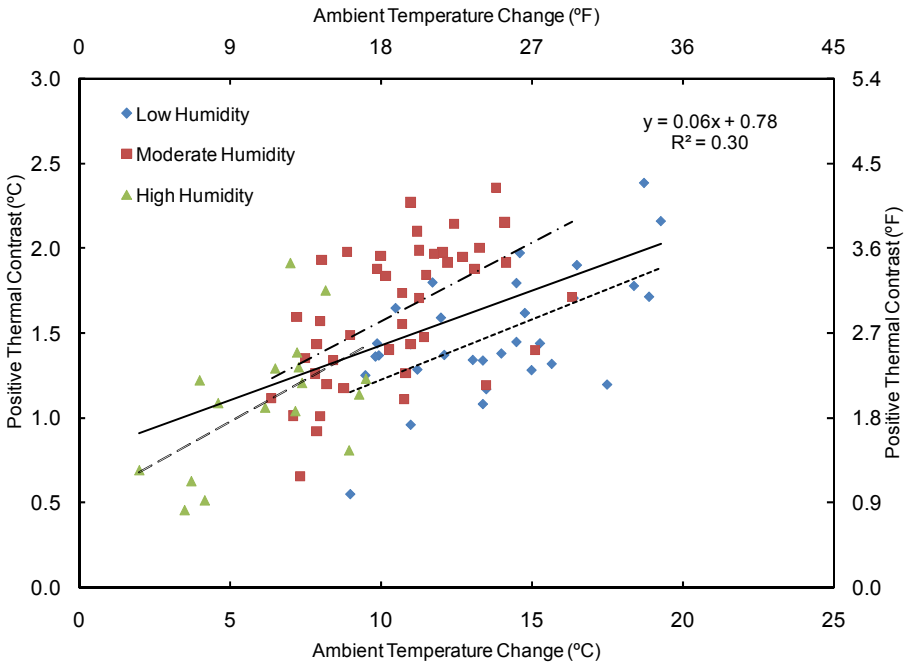

Figure 5.12 : Thermal contrast vs. ambient temperature changes with markers indicating high, moderate and low humidity.

5.4 Inspection Time

The determination of appropriate inspection times is of significant importance for applying thermography to bridge inspection. Determining the appropriate time of day for inspection to be conducted was one of the primary goals of the research, to enable the development of specific guidelines for applying thermography in typical inspection scenarios. This section will describe the determination of "inspection periods" based on the application of the thresholds of 1 and 2°C (1.8 and 3.6°F).

5.5 North Side Inspection Times

Data from observation of the north side of the test block was analyzed to determine the times of day when an inspection would most likely be able to detect subsurface defects in concrete structures. This analysis focused on the 62 days that had no rain measured by the on-site weather station. It was necessary to remove days that included rain from this data set, because the timing of the rainfall could influence the timing of development of thermal contrast.

For example, if it were rainy in the morning, then stoped raining and warmed up in the afternoon, the development of thermal contrast might occur very late in the day. However, this is a very specific effect due to the rainfall, and not generally representative of the overall behavior of the test block. Therefore, this data was removed from the analysis. When applied to actual inspections, the effect of rainy conditions on the appropriate inspection times would need to be considered.

Table 5.4 shows the results of analysis for the observation times and sunrise differential for both warming and cooling trends for the north side of the block. In the table, the average time of day when contrasts of 1 and 2°C (1.8 and 3.6°F) were reached are shown for each of the targets. This is the average time of day over the 62 days that were evaluated and the time values have been rounded to the nearest ½ hour. This data was normalized to the sunrise time for each specific day, to provide data that was not dependant on the time of year, but rather the initiation of the warming of the ambient environment. For example, considering the 51 mm (2 in.) deep target, the average time that the thermal contrast reached 1°C (1.8°F) was 9:30 am. Normalized to the sunrise time, the target reached the threshold value at an average time of 3:30 hrs after sunrise, and the contrast remained above this threshold for a period of 8:30 hrs. To reach a contrast of 2°C (3.6°F) took until 12:30 pm, or 7:00 hrs after sunrise, and remained above that threshold for only 1:00 hr on average. For the 76 mm (3 in.) deep target, the useful inspection time began at 7:00 hrs after sunrise and remained above the 1°C (1.8°F) for 4:30 hrs. For a contrast threshold of 2°C (3.6°F), there was not adequate data to assess inspection times for the 76 mm (3 in.) target, although there were some days when this occurred for a short time period, but the thermal contrasts for the 76 mm (3 in.) deep target were typically less than 2°C (3.6°F).

Table 5.4 : Observation times, sunrise differentials and inspection periods for 1, 2, and 3, targets for the warming trend and cooling trend with contrast limits of 1 and 2°C (1.8 and 3.6°F), North side of test block.

Warming Trend (Day Time)									
Target Depth	1 in. Deep Target			2 in. Deep Target			3 in. Deep Target		
Contrast Threshold	Time (hh:mm)	Sunrise Diff.	Inspection Period	Time (hh:mm)	Sunrise Diff.	Inspection Period	Time (hh:mm)	Sunrise Diff.	Inspection Period
Contrast > 1 °C (1.8 °F)	8:00	2:00	11:00	9:30	3:30	8:30	13:00	7:00	4:30
Contrast >2 °C (3.6 °F)	9:00	3:00	7:30	12:30	7:00	1:00	X	x	x
Cooling Trend (Night Time)									
Contrast Threshold	Time (hh:mm)	Sunset Diff.	Inspection Period	Time (hh:mm)	Sunset Diff.	Inspection Period	Time (hh:mm)	Sunset Diff.	Inspection Period
Contrast < -1 °C (-1.8 °F)	20:30	0:00	10:00	20:30	0:30	9:30	23:00	2:30	7:30
Contrast < -2 °C (-3.6 °F)	21:00	1:00	7:30	23:00	2:30	5:00	X	x	x

It can be observed from the data the contrast develops very rapidly after sunset, as the daytime temperature drop suddenly with the setting of the sun. For example, for the 51 mm (2 in.) deep target, the thermal contrast of -1°C (1.8°F) develop just 30 minutes after sunset, and this contrast remains for 9:30 hours. It can also be considered that the length of time for which the 51 mm (2 in.) target has at least -2°C (3.6°F) of contrast is 5:00 hrs, much longer than was observed during the warming trend, when this contrast was only maintained for 1:00 hr (on average).

This tabular form of data is represented quite clearly and practically in Figure 5.13 to give a very useful overall picture of the inspection periods which can be applied in the field based upon sunrise and sunset times. The important stipulation to this data is that this is effected by the time of year that the measurements were made. In this case, the measurements were made during the summer months, when days are longer than nights, and ambient temperature changes at sunset are rapid due to the loss of radiant heating from the sun.

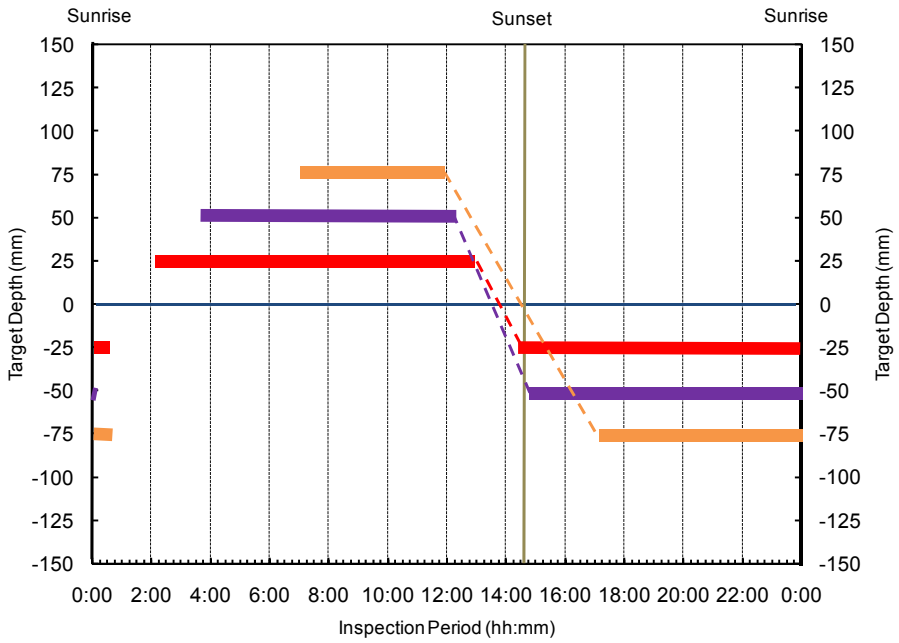

Figure 5.13 : Indicates the suggested times of observation relative to sunrise and sunset. Separated by the y-axis centerline, the time and duration of positive and negative contrasts greater than +/- 1 °C can be taken directly from this guide.

5.6 South Side Inspection Times

Data from the south side of the block was evaluated to determine the useful inspection times for surfaces expose to direct sunlight. In this analysis, 10 days out of the 89 days in which data was collected on the block were omitted, due to the potential influence of rainfall on the timing of thermal contrast development. The results for the warming trend (day time) and cooling trend (night time) periods are shown in Table 5.5. The table presents the time of day at which the threshold contrasts of 1°C and 2°C (1.8°F and 3.6°F) were reached, the average differential between this time and sunrise (based on the sunrise for each day), and the period of time in which contrast was maintained above that threshold. As indicated in the table, for the deep 51 mm (2 in.) deep target, the contrast exceeded the 1°C (1.8°F) threshold at 3:30 hrs after sunrise, and this contrast was maintained on average for 6:00 hrs. To exceed the threshold of 2°C (3.6°F), the sunrise differential was 4:00 hrs, and contrast was maintained above the threshold level for 5:00 hrs. Again, this data is rounded to the nearest ½ hour. In

general, due to the solar loading from the sun, the thermal contrasts were much higher during the inspection intervals than indicated by the threshold values selected, such that the optimum times of day were reached at a later time as discussed in section 5.6.

The useful inspection intervals were also calculated for the night time, when thermal contrast were negative. This data may be somewhat less relevant, since surfaces exposed to sunlight would likely be inspected during the day, since the contrasts observed for a given defect would be much greater. However, it was also considered for cases where a nighttime inspection was necessary for some reason, such as access could not be gained during the day, or that an inspector may want to inspect both solar-exposed surfaces and surfaces not exposed to sunlight. It can be noted from Table 5.5, in comparison with the north side of the test block, it takes much longer for negative thermal contrast to develop at the targets. This is due to the carry-over of heat developed at the targets during the day. It should also be noted that in contrast to the north side of the test block, the 127 mm (5 in.) deep targets reach the threshold level of 1°C (1.8°F) for both the daytime and the nighttime. For the case of the daytime, this is not unexpected, as the radiant heating from the sun provides a significant driving force for the development of thermal gradients in the block that leads to thermal contrast, even as deep as 127 mm (5. in.). For the nighttime, the increased thermal contrast for the deepest target is the result of the thermal mass of the block reducing the change in surface temperature relative to the target area. Above the target area there is very little concrete between the target and the surface that needs to be cooled, and hence this area cools much faster than the intact areas of the block, leading to increased thermal contrast. This phenomena also occurs on the north side of the block, but because the overall variations in temperature of the block are small, it’s simply not observable.

Table 5.5 : Observation times, sunrise differentials and useful inspection times for targets for the daytime and nighttime, with contrast limits of 1 and 2°C (1.8 and 3.6°F), South side of test block.

Warming Trend (Day Time)												
Target Depth	1 in. Deep Target			2 in. Deep Target			3 in. Deep Target			5 in. Deep Target		
Contrast Threshold	Time (hh:mm)	Sunrise Diff. (hh:mm)	Inspection Period (hh:mm)	Time (hh:mm)	Sunrise Diff. (hh:mm)	Inspection Period (hh:mm)	Time (hh:mm)	Sunrise Diff. (hh:mm)	Inspection Period (hh:mm)	Time (hh:mm)	Sunrise Diff. (hh:mm)	Inspection Period (hh:mm)
Contrast > 1°C (1.8°F)	10:00	2:30	6:30	11:00	3:30	6:00	12:30	5:00	5:00	15:00	8:00	3:00
Contrast >2°C (3.6°F)	10:00	3:00	6:30	11:30	4:00	5:00	13:30	6:30	3:00	x	x	X
Cooling Trend (Night Time)												
Contrast Threshold	Time (hh:mm)	Sunset Diff. (hh:mm)	Inspection Period (hh:mm)	Time (hh:mm)	Sunrise Diff. (hh:mm)	Inspection Period (hh:mm)	Time (hh:mm)	Sunset Diff. (hh:mm)	Inspection Period (hh:mm)	Time (hh:mm)	Sunset Diff. (hh:mm)	Inspection Period (hh:mm)
Contrast < -1°C (-1.8°F)	18:00	1:30	13:30	20:00	3:30	12:00	23:30	6:30	8:30	2:30	10:00	5:00
Contrast < -2°C (-3.6°F)	19:30	2:30	10:00	20:30	4:00	8:00	x	x	x	x	x	x

A graphical representation of the suitable inspection periods for the south side of the test block was also developed. This is shown in Figure 5.14, which shows graphically the inspection times for each of the targets. In addition to the 25, 51 and 76 mm (1, 2, and 3 in.) deep targets, data for the 127 mm (5 in.) deep targets is shown (1 °C (1.8 °F) threshold).

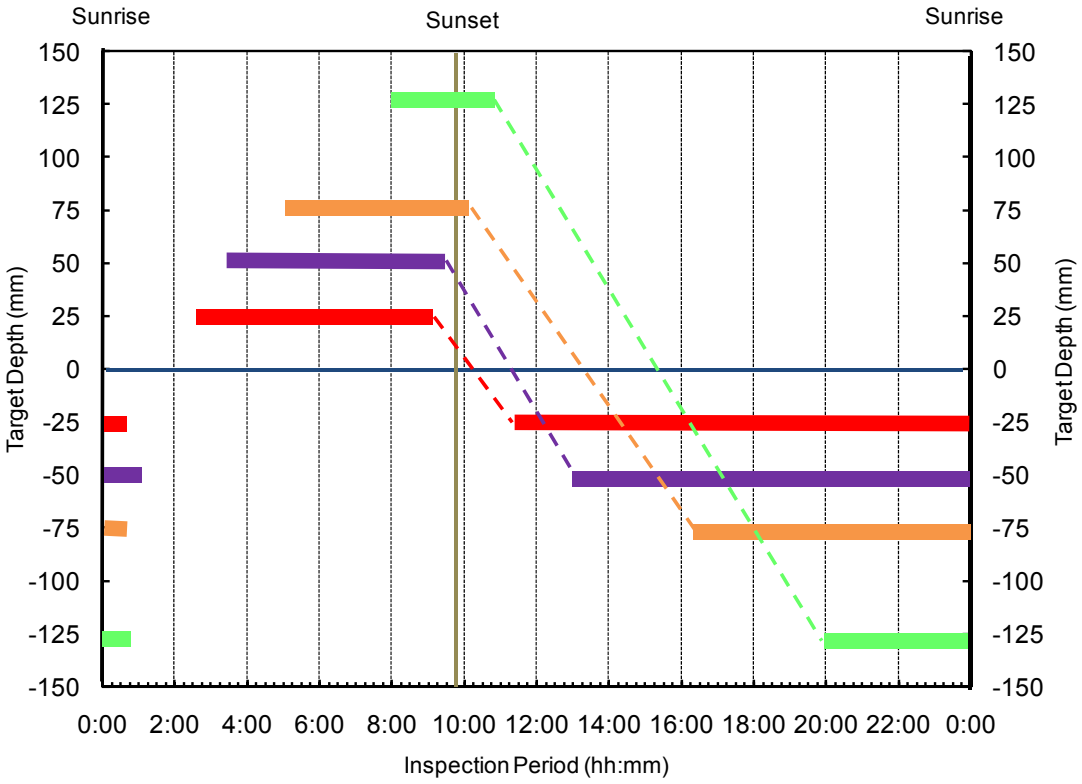

Figure 5.14 : Inspection periods for different target depths of 25, 51, 76 and 127 mm on the south side of the block.

5.7 Optimum Inspection Time – South Side

Thermal contrast for the subsurface targets in the test block on the south side of the block varied over the course of a day in a sinusoidal manner, meaning that thermal contrast had a specific peak value during the day that could be identified consistently. This maximum contrast value was evaluated to determine the optimum time of day for an inspection. It was found that the optimum time of day to conduct inspections varied as a function of the depth of the target, as would be expected, with deeper target developing their maximum contrast very late in the day, after sustained solar loading. Figure 5.15 shows a scatter plot for the development of the

optimum contrast for targets at 51, 76 and 127 mm depths (2, 3 and 5 in.). The vertical axis displays the level of maximum contrast, and the horizontal axis shows the time relative to sunrise that the maximum contrast occurred. As the figure shows, the shallower targets develop a much higher contrast over the course of the day, greater than 5°C (9°F) in some cases, and this typically occurs at 6 hours or more after sunrise. To develop a relationship between the depth of the target and the timing of an optimum inspection, this data was analyzed using only those days when the thermal contrast for the 2 in. (51 mm) target developed at least 2°C (3.6°F) of thermal contrast, to omit "bad" days when conditions are otherwise poor for the use of thermography.

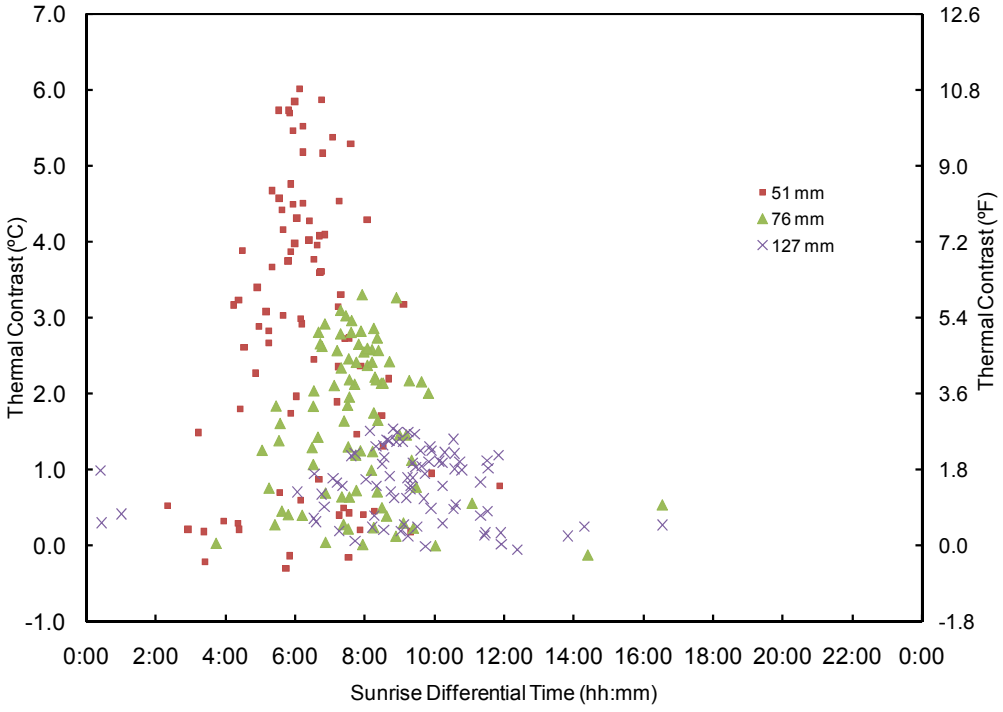

Figure 5.15 : Scatter plot of sunrise differentials against maximum contrast for 51, 76 and 127 mm (2, 3 and 5 in.) targets.

The results of this analysis are shown in Figure 5.16. This figure shows the relationship between the target depth and the optimum inspection times. The optimum inspection time for the 51, 76, and 127 mm (2, 3 and 5 in.) deep targets were found to be 6:17, 7:44 and 9:09 hrs, respectively. These values differed on the order of a few minutes if all days with at least 1°C

(1.8°F) were included in the analysis. The standard deviations for this measure were on the order of 1 hr.

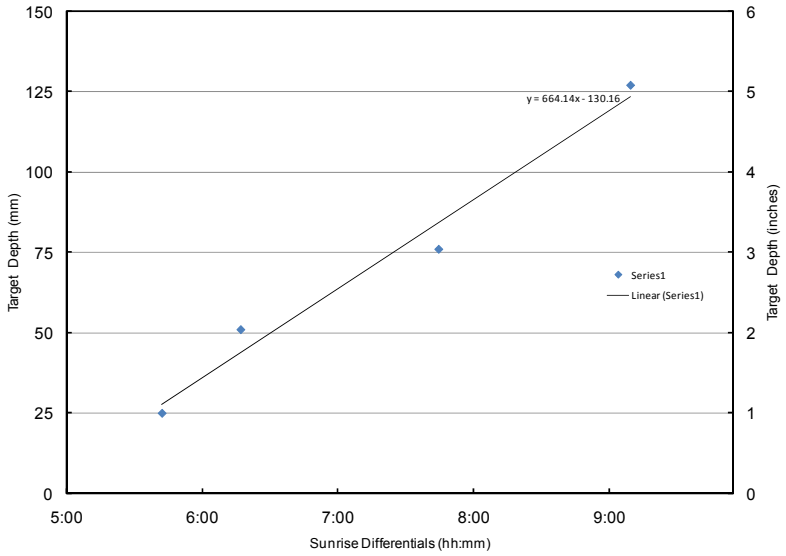

Figure 5.16 : Sunrise differential as a function of target depth for optimum inspection conditions, south side of test block.

The significance of this finding in terms of application of thermography for bridge inspection is twofold: first, there is a significant delay between sunrise and the optimum time for conducting inspections, and second, that knowledge of the expected depth of the defect can help guide an inspector to the appropriate time to conduct an inspection. For example, if the suspected area of delaminations is between an 51 mm (2 in.) overlay and the concrete deck, then waiting 5 or 7 hrs after sunrise would likely provide the optimum conditions. If the suspected area of delamination is at the level of rebar and the cover is 76 mm (3 in.), than waiting until 7 or 8 hrs after sunrise would provide the optimum conditions.

5.8 Rate of Change

It was observed during the course of the research that thermal contrasts for the targets diminished when the ambient temperature stopped increasing and began decreasing, such as in the late afternoon. This was also noticed for the negative contrast that developed overnight; when the ambient cooling stopped decreasing, there was a reduction in the thermal contrasts at

the targets. This is important in terms of practical inspections, because it indicates that the optimum time to conduct inspections would be before the rate of change in the ambient environment changed from, for example, cooling to warming. To quantify this effect, and determine if useful guidance to be provided, an analysis of the rate of change of the environment compared with the rate of change of thermal contrasts for the targets was conducted.

Analysis was conducted of the rate of change (ROC) for both the thermal contrast developed at the 2 in. (51 mm) target and the ambient temperature. Figure 5.17 shows the relationship between ambient temperature and the *rate of change* of the ambient temperature, for a typical week of observation for the north side of the test block. The rate of change for the ambient environment is calculated based on a 3 hour time differential. As can be seen in the figure, during the early part of the day, when the air temperature is increasing, the rate of change is positive; when the ambient temperature is not changing, that is, when temperature is maintained at a given level, the rate of change is near zero. If temperatures are cooling, the rate of change is negative.

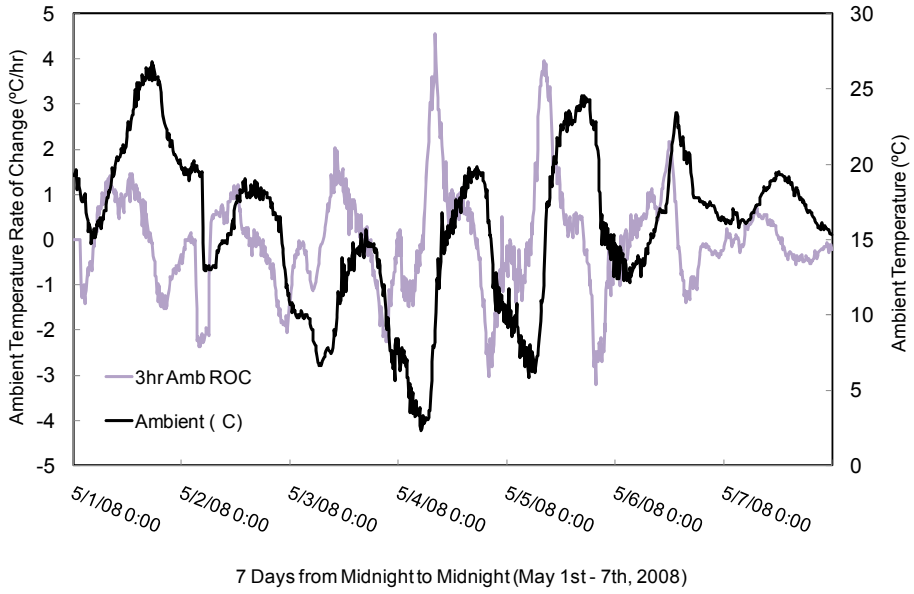

Figure 5.17 : Ambient temperature variations and the ROC for the variations for 1 week.

To quantify the effect of ROC of the ambient temperature, data was divided into sub groups of 0.5 °C/hour (0.9 °F/hour) ranges using the bins methodology. For example, the data sets for positive ambient rate of change 0 to 0.5 °C/hour were all grouped together to compare the averages to those of the thermal contrast ROCs for the 51 mm (2 in.) deep target. Figure 5.18 shows the results of this analysis. In the figure, the ROC data for the ambient environment over 3 hrs is shown, along with the ROC for the thermal contrast. It can be observed in the figure that there is a strong correlation between the ambient ROC and the contrast ROC, such that contrast is developing at a high rate during times of rapidly increasing or rapidly decreasing temperature in the ambient environment. The data also indicates that when the ROC for the ambient environment is in the range of -0.5°C/hour to 0.5°C/hour, the contrast ROC is at or very close to zero for that same range. In fact, the standard deviations for the data extend into the negative region, that is, the contrast ROC is of the opposite sign from the ambient ROC, and as such the contrast is diminishing. The importance of this to bridge inspection is three-fold:

1. Performing inspection during times of rapidly increasing or decreasing temperatures provides the highest increases in positive and negative contrast, respectively, for that same time period.
2. Thermal contrast will be greatest following times of high ambient ROC, because the ROC of contrast will have been high for that same time period,
3. As the ROC for the ambient environment begins to decrease, so does the ROC for the thermal constrast.

This is significant in that it indicates that for performing inspections, knowledge of the ROC for the ambient environment can provide guidance on whether the optimum conditions exist. When conducting inspections during the warming cycle (daytime), once the temperature begin to cool (negative ROC) the optimum time for inspection has passed, and the thermal contrast begins to diminish. For nighttime inspections, when the ambient temperature ROC

changes from negative to positive, i.e. the day begins to warm, the negative contrast is diminishing. In areas where the ROC for the ambient temperature is close to zero, the contrast ROC may be of the opposite sign, indicating that contrast has begun to diminish. This data is based on the 51 mm (2 in.) deep target; for a deeper target, effects are delayed as would be expected.

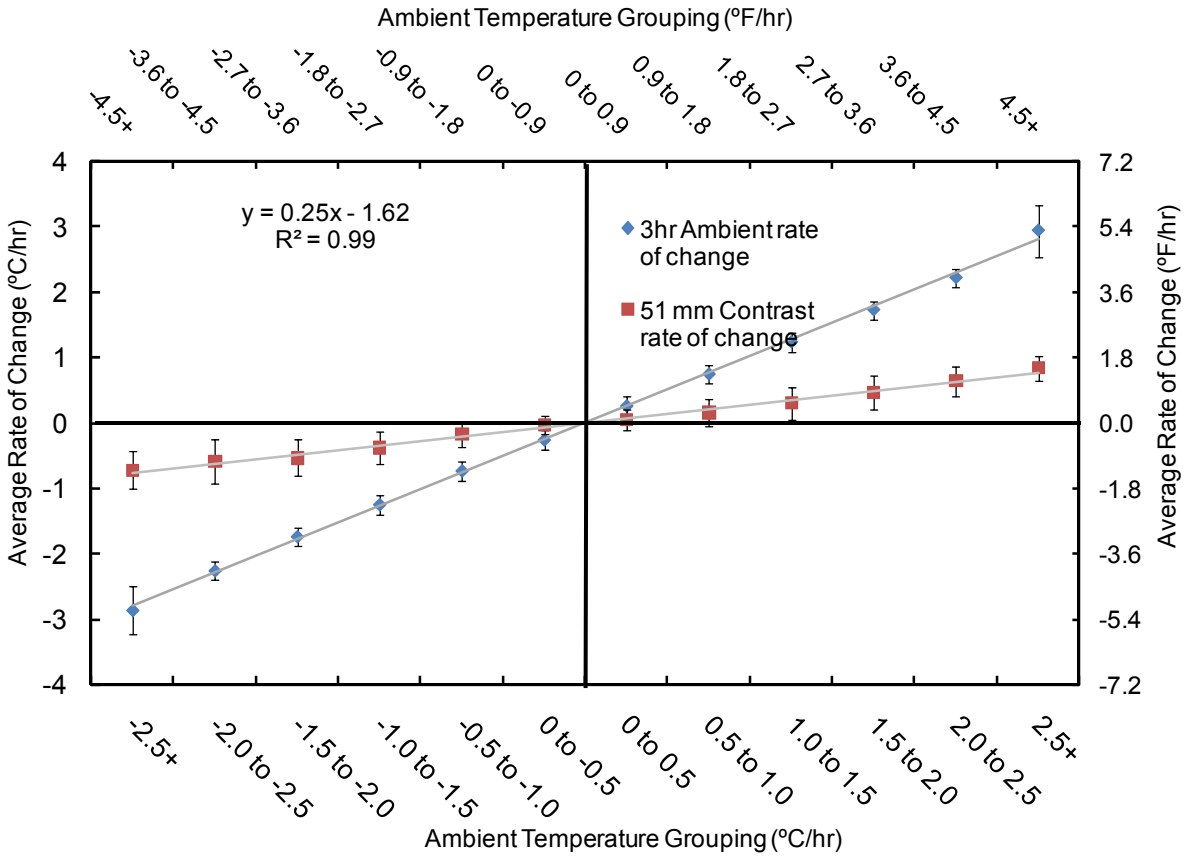

Figure 5.18 : Relationship between ambient temperature rate of change (x-axis) and thermal contrast rate of change (y-axis).

Data was analyzed to determine if there is a correlation between the ROC for the ambient environment and the magnitude of the thermal contrast that developed. These results are shown in Figure 5.19, which shows the correlation between maximum 3 hr. ROC for the ambient environment and the magnitude of the thermal contrast that developed that particular day. As shown in the figure, there is a strong relationship between these two variables. This is very significant in terms of developing guidelines for inspection; as the figure shows, this is valid

for both the positive contrast developed during the day and the negative contrast developed during the night. The strong correlation (R^2 = 0.9) provides clear evidence that inspections conducted following periods of high ambient environment ROC will be more likely to result in developing thermal contrast for subsurface defects than days with lower ROC for the ambient environment. Again applying a 1°C (1.8°F) threshold to represent a "good" condition for the detection of subsurface defects, the corresponding limit for ambient ROC was applied for both the positive and negative thermal contrasts. For positive contrast, the intersection was located at 1.5°C/hr (2.7 °F/hr). Applying this threshold to the data, it was found that 96% of the days with maximum ambient ROC of at least 1.5°C/hr (2.7 °F/hr) had a contrast develop of at least 1°C (`1.8°F). For the negative thermal contrast, the intersection was located at -1.7°C/hr (- 3.1°F/hr). Applying this threshold to the data, it was found that 91% of the days with maximum ambient ROC of at least -1.7°C/hr (- 3.1°F/hr) had a contrast develop of at least 1°C (1.8°F).

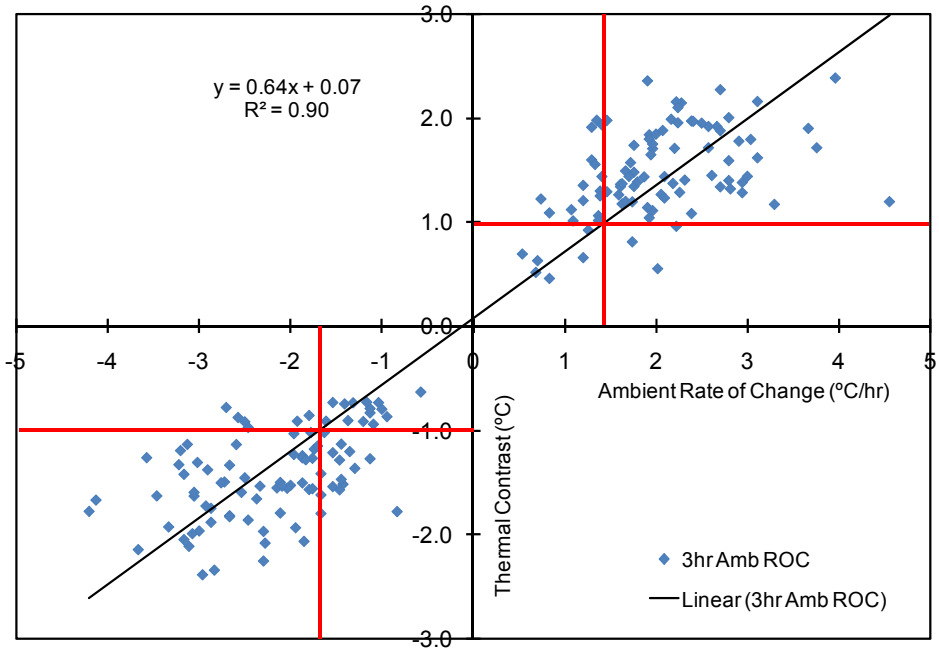

Figure 5.19 : Maximum 3-hour ambient rate of change vs. 51 mm contrast with equation.

5.8.1 Discussion

The ROC analysis showed that the rate of change for the 2 in. deep target was related to the ROC for the ambient environment, and that high thermal contrast that resulted from a high ROC. This is consistent with the finding that days with largest ambient temperature changes had the largest thermal contrast, since a large variation in ambient temperatures would typically have high ROC based on the overall characteristics of diurnal temperature variations. However, because it was found that when the ambient ROC is close to zero, the contrast may be diminishing, it suggests that the quality of thermal images, i.e. the detectability of subsurface features, begins to diminish once temperatures stabilize in the late afternoon (ROC ~0) and are diminishing once the ROC becomes negative.

It is important to note that this analysis is focused on the 51 mm (2 in.) deep target. It would be expected that for deeper targets, the effects would be delayed in time. As such, the observed thermal contrast for a defect at 76 mm (3 in.) would not begin to diminish until sometime after the ambient ROC has become negative. For very shallow delaminations, the effect would be more pronounced, such that image quality would be reduce once the ambient ROC dropped below 0.5°C/hr.

6 EXPERIENCES OF STATE DEPARTMENTS OF TRANSPORTATION

An important aspect of the research was to evaluate the operational characteristics of infrared thermograpy by providing cameras to inspection personnel in the three participating states and allowing those states to utilize the cameras in general day-to-day operations to the extent they could, during the research. This chapter briefly describes that portion of the research.

6.1 Cameras

Participating states were provided with FLIR B400 hand-held infrared cameras. These cameras are designed for field operation, specifically for the inspection of buildings. The cameras have a variety of features to make them suitable for use in the field. The cameras are hardened to survive in the field, have an intuitive menu structure that can be quickly learned, and have ergonomic features (such as an articulating lens) that make them suitable for application in the field. Thermal images are stored in .jpg format so that they are easily transferrable between computers and integrate well with other programs. Reporting software provided with the cameras allows for thermal contrast in the images to be adjusted post-inspection for further analysis of images in the office. A photograph of the camera is shown in Figure 6.1.

Figure 6.1 : Photograph of student holding B400 camera.

Thermal images are observed on a 3.5 in. LCD display. A sunscreen is typically required to view images in sunlight, as is typical with computer screens. The cost of the cameras at the time they were purchased for the research was $19,950. At the time of purchase, the camera was the latest development from the manufacturer, such that lower costs would be anticipated with time. The thermal resolution for the camera is 0.05°C, which is slightly better than the research camera used to observe the test block. In addition to the cameras, a wide angle lens was purchased (cost = $3,500). The wide angle lens was provided to enable the inspection of a larger area, say a larger area of the deck, from a standing position along the side of the deck.

6.2 Training

Training modules were developed to assist state DOTs with implementation of the technology. Typical training involved a ½ day of classroom instruction and ½ day of field testing with the camera. The classroom portion of the training covered topics including an introduction to infrared radiation, the basics of heat transfer, discussion of how to make a good image, initial results of the research, and a brief overview of the operation of the camera. Training was delivered in the states of Texas, New York and Missouri.

6.3 State Experiences

In general, utilization of the technology by participating states was somewhat limited. The reasons for this are believed to include limited resources, in terms of manpower, for testing "new" technologies in the course of normal operations, typical resistance to new technologies, and the fact that the application of the technology for routine inspection tasks is as yet unproven. One state utilized the technology selectively as part of their routine inspection at the district level, and the following were reported"

- Cameras are relatively easy to use after one understands the theory behind what the camera does.
    - Training was worthwhile

- Wind did not really negatively affect images
- Rain, fog or high humidity gave poor images
- Top of deck and bottom of deck images were most useful
    - Stay in place forms precluded the use of the camera
- Adjacent box girders provide another good candidate for the technology
- Sunny days with rapid temperature change seemed to help with all kinds of bridges
- The fact that the camera captures a digital image at the same time it captures the thermal image is a huge advantage
    - It appears that the thermal image is “closer up” than the digital image

A second state that utilized the technology in the field reported that they found the technology useful for inspection of composite overwraps to look for subsurface delaminations. Experiences utilizing the technology for deck inspection did not show the technology to be an advantage over chain drag in two exploratory tests that they conducted. These tests were conducted in December on a day with high ambient temperature change. In a third test utilizing the technology on a deck overlay, delaminations were observed in the bridge deck. Examples of these are given in the following section.

6.4 Example Field Test Data

This section of the report provides exemplar data from field application of thermography. This data is experiential in nature, showing several applications where thermography was useful in defining subsurface defects in concrete.

6.4.1 Detection of Delaminations in Concrete Deck with Overlay

Figure 6.2 shows defects in a concrete bridge deck as imaged in the field in Texas using the B400 thermographic camera. The bridge deck consists of a 191 mm (7.25 in.) slab with a 32 mm (1.25 in.) concrete overlay. The image on the left shows the digital photograph (optical image) capture by the digital camera, the image on the right is the thermal image showing two

defective areas. The thermal image captures a smaller area relative to the digital image (the digital camera and the thermal camera do not have the same optical path). In this image, the radiant heating from the sun has resulted in a strong thermal contrast in the image where the delaminations have developed in the bridge deck. Note that the span for the thermal image is 8.5°F (~5°C). The depth of the defect was not measured in the field, but based on high thermal contrast apparent in the figure, it is likely a debonded section of overlay. The depth of rebar, designed to have 51 mm (2 in.) of clear cover in the slab, is 83 mm (3.25 in.) from the surface of the deck. A delamination at the depth of the rebar would likely not have sharp contrast at the edges of the defect due to heat diffusion in the concrete.

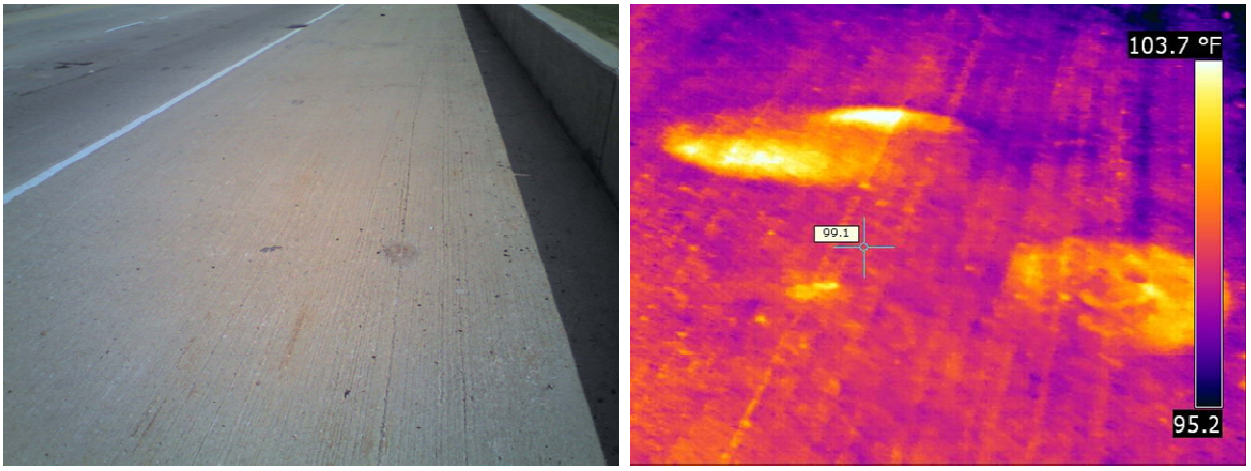

Figure 6.2 : Digital photograph and thermal image of concrete overlay with delaminations/debonding.

6.4.2 Bridge Soffit – Missouri

Figure 6.3B shows a thermal image of a patched section of concrete on the soffit of a bridge in Missouri. In this case, the patch is pulling away from the underlying concrete, and as a result is heating at a much higher rate that the other areas of the soffit, and other areas of the patch itself. Again, the image on the left (Figure 6.3A) is the optical image captured by the digital camera, the image on the right (Figure 6.3B) is the thermal image. Note the span for the image is 5.3 °F (~3°C). Also shown in the thermal image is the thermal signature from sonatubes within the concrete.

Figures 6.3C and 6.3D show the soffit of a different bridge in Missouri, and also shows an area of delamination in the concrete. In this case, some of the area of the delaminated concrete appears to be a patch, while the other area appears to be original concrete. As shown in the image, there is a clear contrast for this defective area relative to the other areas of the soffit. A column can be seen in the image. This image was collected on a day when the ambient temperature change was ~20°C (35°F). This provided an optimum day for thermal inspection.

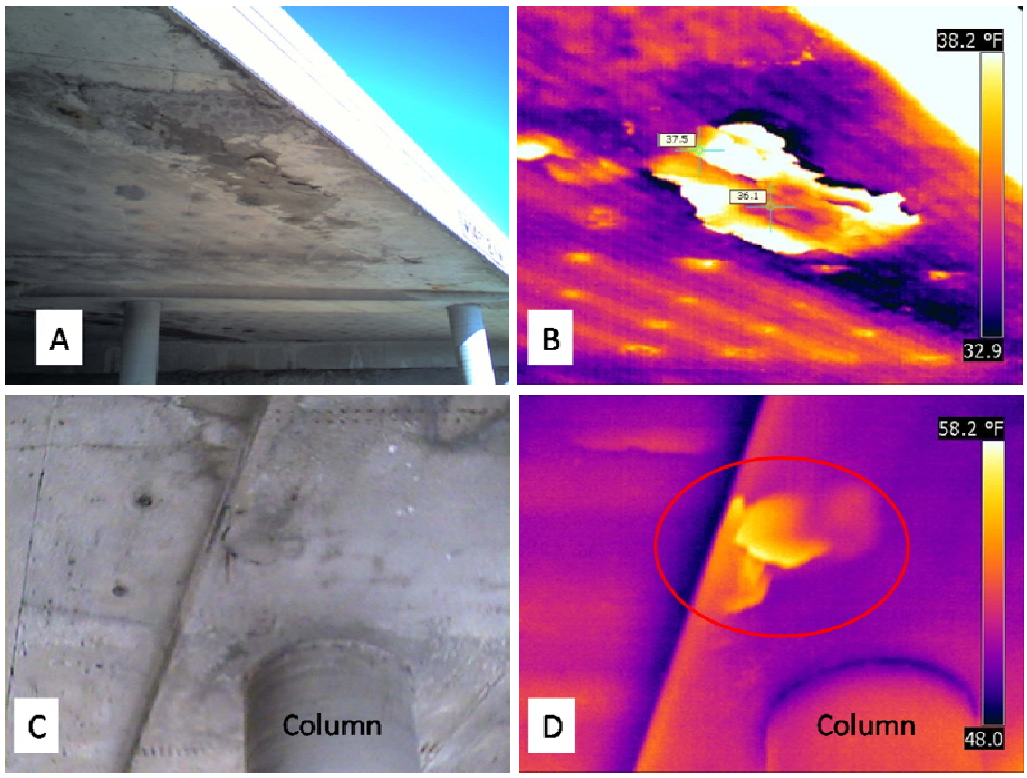

Figure 6.3 : Photographs and thermal images for delamination in the soffit of a bridge.

6.4.3 Pier Cap – Texas

Figure 6.4 A-D show thermal images of a pier cap in Texas. For this bridge, the anchor rods that hold the bridge bearing are being stressed by the thermal expansion and contraction of the members carried by the bearing. The anchor rods are not adequately confined to carry these stresses, and as a result a spall is developing in the concrete. The thermal image in Figure 6.4B shows clear contrast for the area that is about to break free from the surrounding

concrete. As seen in Figure 6.4A, the boundaries of the developing spall are apparent through a visual inspection. The thermal image in Figure 6.4D shows boundaries of a delamination (different location on the same structure as 6.4A and B) In this case, the boundaries of the delaminations are not apparent through a visual inspection; the concrete appears intact as shown in Figure 6.4C, the optical image of the pier cap. These images were captured during the field testing portion of the training associated with the overall project. Although exact weather conditions for this day were not recorded, it was a windy day by observation. Note the span for these thermal images is 5.1°F (~3°C).

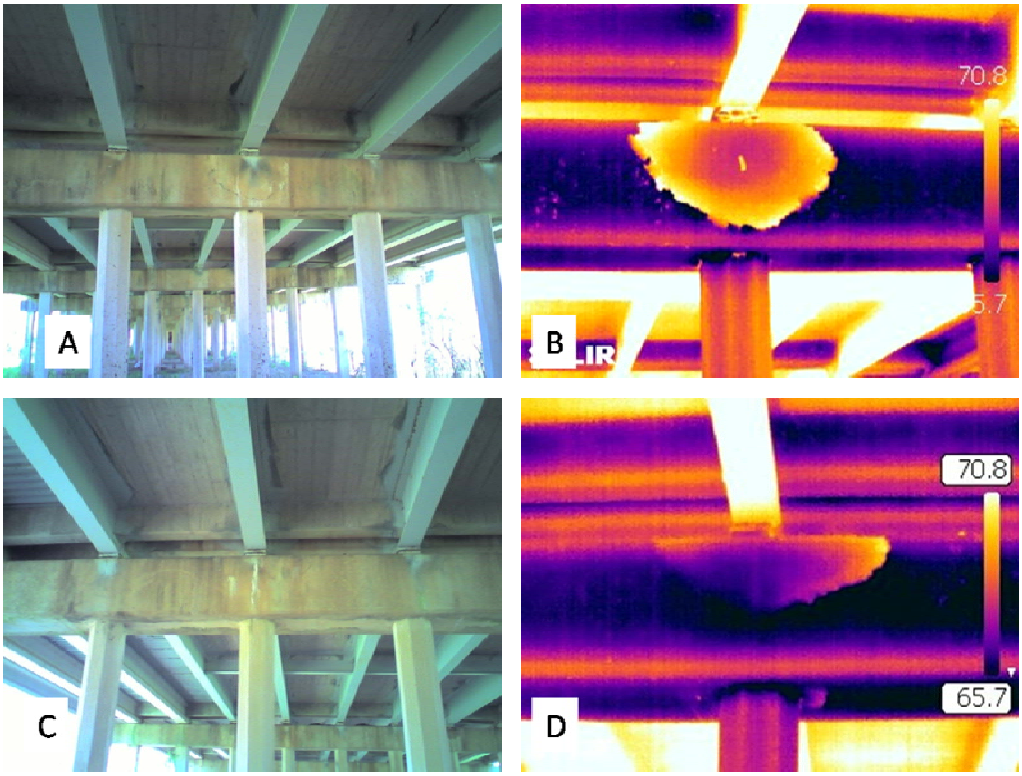

Figure 6.4 : Optical and thermal images of a pier cap in Texas showing delaminations in the bearing areas resulting from thermal expansion and contraction of the bridge.

6.4.4 Composite Overwraps - Texas

The next image shows delaminations in composite overwraps in Texas. In these images, the areas of delaminations appear as cold spots on the image. There are two reasons that that the delamination in the composite material would appear as a cold spot on the image

during the warming cycle of the day. First, moisture may have collected in the defective areas. Water has a higher thermal mass than concrete and composite materials, and as such would lag behind these other materials when warming during the day. As a consequence, the areas appear as cold spots because the areas are not heating as fast as the concrete. Second, if the images are taken very early in the warming cycle, such that the negative contrast developed during the overnight cooling cycle remains. Figures 6.5A and B are a photograph and thermal image of a composite overwrapped column, while Figures 6.5C and D are from a composite overwrapped pier cap. These images were all collected in the shaded portion of the bridge, indicating the usability of thermography even though radiant heating from the sun is not available. The images were collected very early in the day, just after sunrise, such that the cold spots that show delaminations are likely negative contrast from the overnight period.

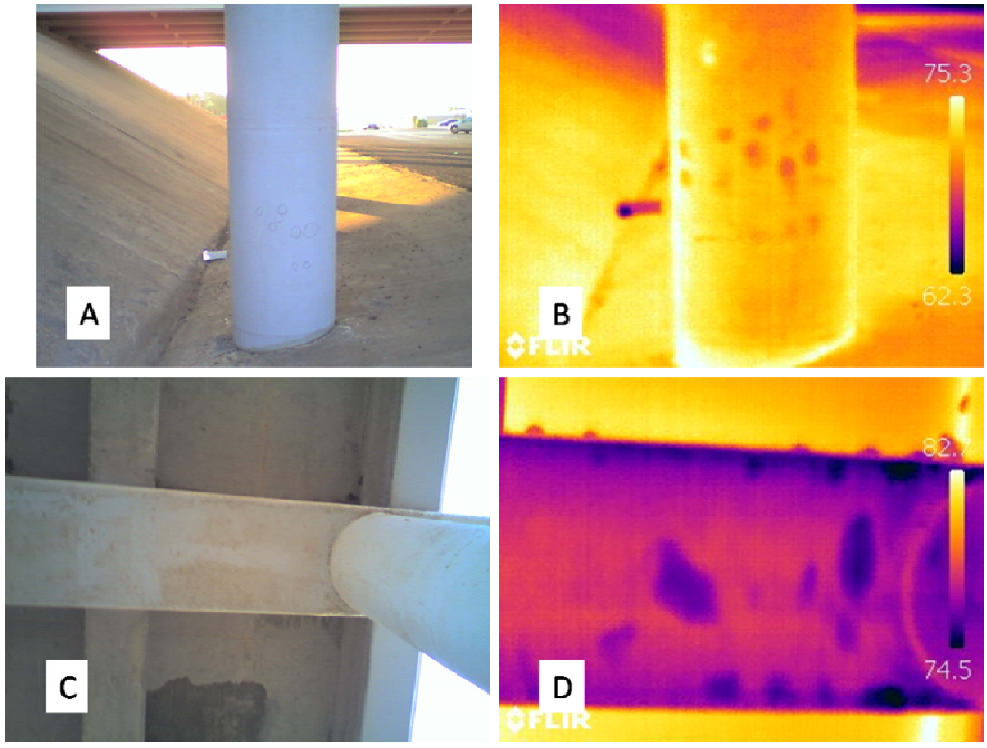

Figure 6.5 : Optical and thermal images of composite overwraps showing subsurface delaminations as cold spots in the image.

6.4.5 New York: Concrete Saturation and Adjacent Box Girders

The state of New York has probably utilized the technology most frequently during the course of routine inspection conducted within their district. Experiences for the bridge inspector are described above. Figure 6.6 A-D show two example applications from New York. Figure 6.6A and 6.6B show the optical image and thermal image of a deck soffit, respectively. The image is of the bottom side of a deteriorated concrete bridge deck. Efflorescence is apparent in Figure 6.6A. The thermal image shows the area surrounding this efflorescence to be cold relative to the surrounding areas of concrete. This is likely an area of concrete that is saturated with water. Because it takes more energy to heat and cool water than it does concrete, this area appears cold relative to the other areas of the block. Evaporative cooling may also play a role, as well as variations in the emissivity if moisture is on the surface. Regardless, this area appears as a region in which there is anomalous thermal behavior. This example suggests the application of thermography to better describe the conditions at the bridge during an inspection and to document the extent to which the deck is saturated.

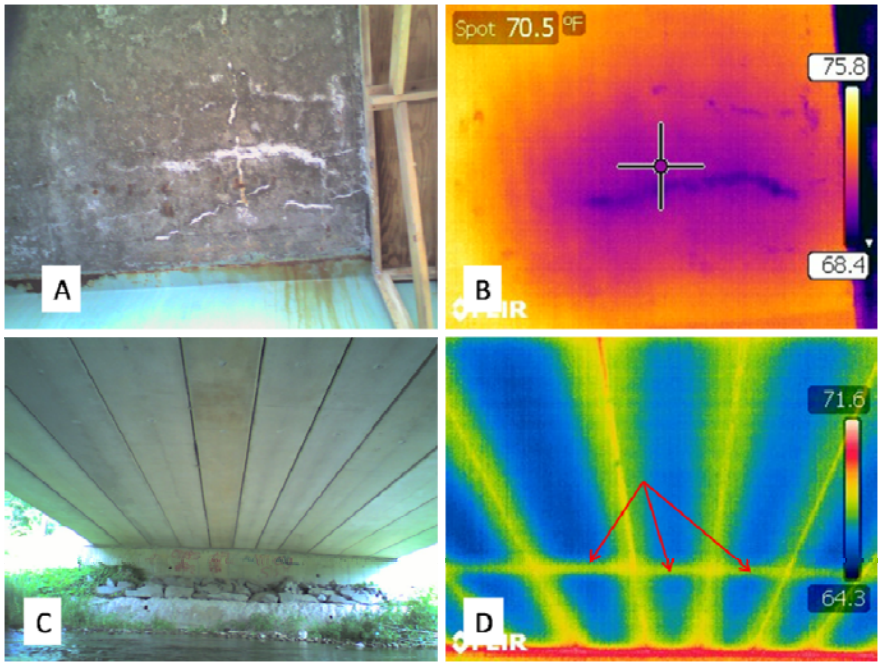

Figure 6.6 : Optical and thermal images of bridges in New York, A and B show the soffit of a bridge deck with saturation, C and D show the soffit of an adjacent box girder bridge.

Figures 6.6C and 6.6D show a thermal image of the soffit of an adjacent box girder bridge. There are no delaminations shown in this image; the soffit appears intact. In can be noted in the image that the internal diaphragms of the box girder result in thermal signatures when observing the soffit area with a thermal camera. The appearance of these subsurface features in the image illustrates that a thermal gradient exist through the depth of the concrete. The diaphragms are creating a perturbation in the heat transfer into the concrete because of their thermal mass. Figures 6.6C and 6.6D are significant because they illustrate the ability of thermography to confirm the inspection finding that there is not significant delaminations in the box girder, confirming the visual inspection result. This provides the inspector with additional information regarding the adequacy of his visual assessment. It also shows how internal features in the concrete, such as diaphragms, can provide a soft “calibration” of the technique. The appearance of these subsurface features confirms that there is a thermal gradient established in the concrete as a result of ambient temperature variations. However, in this case, the soffit area of the bridge is cool relative to the latent heat in the diaphragms, which are out of phase with the overall environment. This is likely latent heat from the previous day. This suggests that the negative thermal gradient from the overnight time period has not yet been overcome by ambient temperature increases. For this case, waiting for a positive thermal gradient to develop, when the diaphragms will appear as cold rather than warm, would provide a more optimal condition for thermographic inspection. This effect was not discussed in the training modules provided, because at the time they were developed its utility was not known. This should be added to future training regimes. It has been observed in other bridges that at times of strong, positive thermal gradient in the concrete, internal diaphragms appear cold, as shown in Figure 6.7, indicating a positive thermal gradient in the concrete. This is an example of the usefulness of practical testing in the field to help develop effective procedures for infrared thermography. Such an effect is extremely valuable for practical application of the technology, but is unlikely to arise through laboratory testing.

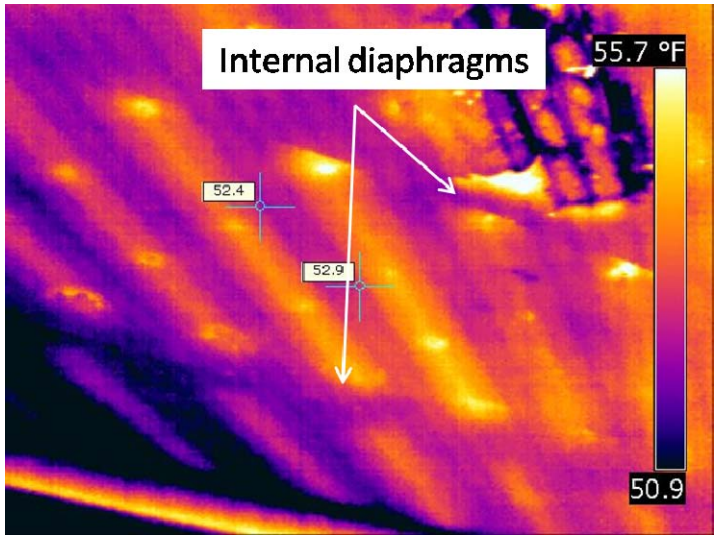

Figure 6.7 : Thermal image of the soffit of a bridge deck showing thermal signature of internal sonatubes and diaphragms.

6.5 Weather Web Site

A web site was developed during the course of the research that enables current and previous weather conditions to be obtained in the field. The site can be accessed over the internet from any location. The data is collected from the Meteorological Assimilation Data Ingest System (MADIS) server. This data would be helpful for the inspectors to understand the weather trends in the field, such as the changes in ambient temperature for the day. The web site works by inputting your current location in GPS coordinates. An algorithm is used that determines the weather station in the MADIS database that is closest to your reported location. Data for that location for the most recent 14 day period, ending on the previous hour, is collected from the database. Figures are presented as shown in Figure 6.8 that show the ambient hourly temperatures, wind speed measurements and relative humidity. This web site, though not widely used in the current research, may be a key tool for implementation of the suggested guidelines contained in appendix A. Using the web site, inspectors could learn the ambient temperature changes and average wind speeds required to know if the current time meets the requirements of the guidelines for the specific location of the bridge to be inspected.

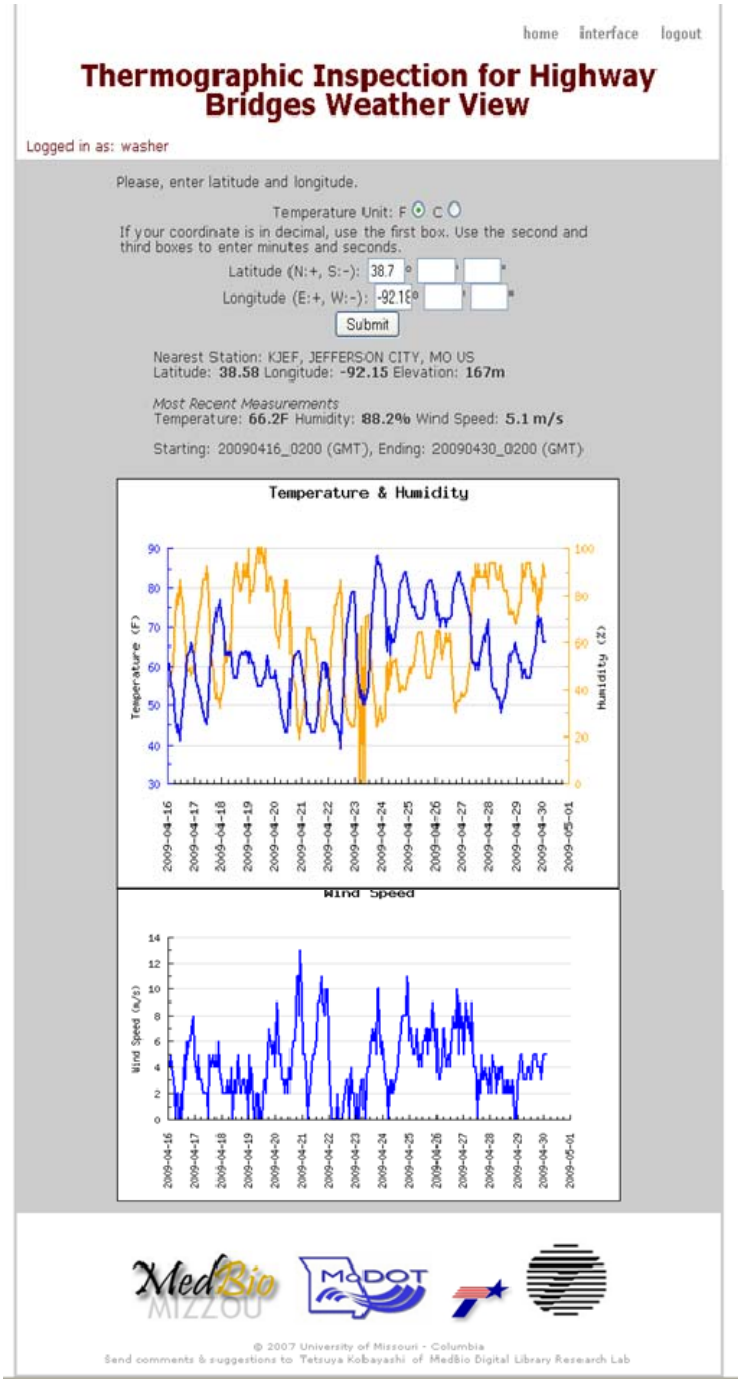

Figure 6.8.: Page view of the thermographic inspection weather web site.

7 CONCLUSIONS

The objectives of this research were to:

1. Develop guidelines for the use of IR thermography for the condition assessment of highway bridges by characterizing the environmental conditions necessary for thermography to be effective; evaluate the effects of environmental parameters including solar loading, diurnal temperature variations, wind speed and relative humidity on the detectability of subsurface defects in concrete; and explore the application of thermography for imaging defects with and without radiant heating from the sun
2. Investigate the operational constraints to implementation by providing thermographic cameras and training to participating states.

This section of the report indicates the results of the research. Conclusions are separated into south side (solar exposed), north side (no solar exposure), inspection timing and state results. Concise guidelines have been developed based on the conclusions of the study and the work conducted. These guidelines are included in Appendix A.

7.1 Solar Loading – South Side

The results from the south side of the test block, which is exposed to direct solar loading, are as follows:

1. There is a linear relationship between the total solar loading area and the thermal contrast developed for subsurface targets in concrete.
    a. Direct, uninterrupted radiant heating from the sun provides the strongest thermal contrast.
    b. Clear skies throughout the day will provide stronger thermal contrast relative to days with periodic cloud cover.
    c. Longer days (summer) will provide higher thermal contrast than shorter days (winter).

2. High wind speeds were associated with lower thermal contrasts for targets in the test block.
    a. Days with the highest solar loading area tended to have low to moderate wind speeds.
    b. The trend of results for high winds speeds was found to be lower than the trend for low wind speeds.
3. A practical guideline for maximum average wind speeds during thermographic inspections is 3.6 m/s (8 mph), based on a 6 hour average.
4. Optimum times for inspection under solar loading varied linearly as a function of depth of the target in the test block, ranging from a little greater than 6 hrs after sunrise for the 51 mm deep (2 in.) target to more than 9 hrs for the 127 mm (5 in.) deep target.
5. Inspection periods were calculated based on the thresholds of 1 and 2°C (1.8 and 3.6°F) for each of the targets in the test block. For daytime inspections of targets at 51 mm, the inspection periods based on 1 and 2°C (1.8 and 3.6°F) were 6:00 hrs and 5:00 hrs, respectively.
6. The effects of humidity on the thermal contrast developed under solar loading was not found to be significant, because days with strong solar loading were typically characterized as having low relative humidity

7.2 Shaded - North Side

Based on the result for the north side of the test block, the following conclusions are made:

1. On average, the magnitude of positive thermal contrast during the day was the same as that developed at night for the 51 mm (2 in.) deep target.

2. There is a strong relationship between ambient temperature changes and the magnitude of thermal contrast developed, both for positive temperature changes (daytime) and negative temperature changes (nighttime).
    a. Applying a threshold for ambient temperature change of at least 8°C (almost 15°F), it was found that thermal contrasts of at least 1°C (1.8°F) were developed for a significant majority of the days, for both positive and negative thermal contrast.
3. The occurrence of rain had only minimal effects on the development of thermal contrast in the test block. If the ambient temperature variations were sufficient to create thermal contrast, and the surface being observed was not wet, the effect of rain was minimal. However, rainy days sometimes do not have the requisite ambient temperature change to develop thermal contrasts.
4. High wind appeared to improve the trend of thermal contrast for a given positive ambient temperature change, but results were highly scattered.
    a. At night, low wind speeds are typical and were a characteristic of the days with the best thermal contrast (with high ambient temperature change).
5. High humidity is a characteristic for daytimes with low ambient temperature change due to typical weather patterns.
    a. Moderate humidity appeared to improve the trend between ambient temperature change and thermal contrast during the warming trend (daytime).
    b. High humidity is a characteristic of the nighttime (cooling trend), with high humidity corresponding to large cooling trends.
6. With an ambient temperature rate of change (ROC) greater than 0.5°C/hr thermal contrast is either increasing or stable for positive and negative thermal contrasts for a 51 mm (2 in.) deep target.

a. With an ambient temperature rate of change below 0.5°C/hr, thermal contrast may be diminishing for a 51 mm (2 in.) deep target.
b. Maximum ambient temperature ROCs of >1.5°C/hr were found to correlate with thermal contrast development of >1°C.

7. Inspection periods were calculated based on the thresholds of 1 and 2°C (1.8 and 3.6°F) for each of the targets in the test block. For daytime inspections of targets at 51 mm (2 in.), the inspection periods based on 1 and 2°C (1.8 and 3.6°F) were 8:30 hrs and 1:00 hrs, respectively.

7.3 Implementation Recommendations

Guidelines for the inspection of concrete bridges using infrared thermography have been developed. These guidelines should be validated through field testing and experience. The following implementation recommendations are suggested:

1. A concise guideline for the application of infrared thermography for the condition assessment of concrete bridges has been developed and is attached in Appendix A, *Guidelines for Thermographic Inspection Of Concrete Bridges*. This guideline was developed based on the results of this study, and provides detailed guidance on the necessary environmental conditions for effective application of this technology in the field. This guideline should be used for implementation of the technology in the field.
2. A focused study of the application of the guidelines included in Appendix A is needed to validate the guidelines and assess necessary improvements. The study should collect and categorize results and experience of the participating States as a means of validating the utility of the technology and the guidelines. This study should include a number of collaborative inspections between researchers and State personnel to assess necessary improvement to the developed guidelines (Appendix

A), identify training needs, improve technology transfer, and provide a focal point for utilizing the technology. This study would identify specific applications in the field where the technology has been most useful and define limitations of the technology under field conditions. The study should document successful (and unsuccessful) applications where the technology has demonstrated utility when applied by State forces to actual condition assessment challenges in the field. Such data is critical for use by other States in decision making regarding adopting the technology, as well as being important for the participating States assessing increased utilization within their respective organizations. The study should also assess the barriers to application of the technology in the field, both technical barriers and sociological barriers that constrict the widespread application of the technology. Without such a focused task for further study, the results of the current study may not be fully utilized to the benefit of the participating States.

7.3.1 Future Research

In addition to the implementation recommendations included above, the following suggestions for future research are made:

1. A validation study on a test bridge with known delaminations could be conducted to validate the guidelines. This study would consist of frequent or continuous assessment of the thermal contrast developed for known defects for comparison with the research results and to demonstrate how to utilize the technology under real world conditions.
2. Additional states have expressed interest in participating in validation testing of the guidelines to improve bridge inspection practices within their states. The study could be expanded to include these states to provide support for validation testing.

3. The web site developed under this research should be further developed and tailored to guideline recommendations, such that inspectors could use this website to assess environmental parameters from field locations. This could have a significantly positive effect on the implementation of the research results. Such an activity requires only modest support, since the website is already developed and the most difficult technology challenges have already been overcome.

References

Arnold, R. H., Furr, H.L., Rouse, J.W. (1969). "Infrared Detection of Concrete Deterioration." Texas A&M University Remote Sensing Center, College Station, TX.

ASTM. (2007). "Standard Test Method for Detecting Delaminations in Bridge Decks Using Infrared Thermography." Standard ASTM D4788 - 03(2007), ASTM International, West Conshohocken, PA, United States.

Clark, M. R., McCann, D. M., and Forde, M. C. (2003). "Application of infrared thermography to the non-destructive testing of concrete and masonry bridges." *NDT and E International*, 36(4), 265-275.

Clemena, G. G., McKeel, W. T. (1978). "Detection of Delamination in Bridge Decks with Infrard Thermography." *Transportation Research Record*, 664, 180-182.

Huston, D., Fuhr, P., Maser, K., and Weedon, W. (2002). "Nondestructive testing of reinforced concrete bridges using radar imaging techniques." *Final Research Report NETC*, 94-2.

Love, B. (1986). "The Detection of Delamination in Reinforced Bridge Decks Using Infrared Thermography." Indiana Departement of Highways, West Lafayette, IN.

Manning, D. G., and Holt, F.B. (1980). "Detecting Delaminations in Concrete Bridge Decks." Concrete International, 34, 41.

Manning, D. G., and Holt, F.B. (1983). "Detecting Deterioration in Asphalt-Covered Bridge Decks." *Transportation Research Record*, 899.

Maser, K. (2008). "Integration of Ground Penetrating Radar and Infrared Thermography for Bridge Deck Condition Testing." *Materials Evaluation* 66(11), 1130-1136.

Maser, K. R., and Roddis, W. M. K. (1990). "Principles of Thermography and Radar for Bridge Deck Assessment." *Journal of Transportation Engineering*, 116(5), 583-601.

Masliwec, T. (1988). "An experimental and theoretical evaluation of IR thermography for surveying the condition of bridge decks." Thermosense X, SPIE.

Yehia, S., Abudayyeh, O., Nabulsi, S., and Abdelqader, I. (2007). "Detection of Common Defects in Concrete Bridge Decks Using Nondestructive Evaluation Techniques." *Journal of Bridge Engineering*, 12, 215.

Zhang, J., Gupta, A., and Baker, J. (2007). "Effect of Relative Humidity on the Prediction of Natural Convection Heat Transfer Coefficients." *Heat Transfer Engineering*, 28(4), 335-342.

Appendix A Guidelines for Thermographic Inspection Of Concrete Bridges

Development of Hand-held Thermographic Inspection Technologies, RI06-038

August, 2009

The following are suggested guidelines for the thermographic inspection of highway bridges, based on the results of the research.

1.0 Surfaces exposed to Direct Solar Loading

1.1 Solar loading

1.1.1 Conduct inspections on days when there is direct, uninterrupted solar loading. Cloud cover should be minimal.

1.1.2 Due to the more intense and longer solar exposure, summer days are preferred over winter days.

1.2 Wind Conditions

1.2.1 In general, wind reduces the effect of radiant heating from the sun and reduces the thermal contrast resulting from subsurface defects. Lower wind speeds will result in improved thermal contrast for surfaces exposed to solar loading.

1.2.2 Average wind speeds should be less than 8 mph prior to and during the inspection period. The average wind speed should be calculated based on a 6 hour average.

1.3 Inspection Period

1.3.1 Inspections should be conducted starting no sooner than 4 hours after sunrise to allow for thermal contrast to develop when anticipated depth of the delamination is approximately 2 in. from the surface of the concrete. The useful inspection period is expected to last approximately 6 hours. If the anticipated depth is 3 inches, inspection should be conducted starting 5 to 6 hours after sunrise. The useful inspection period will last approximately 5 hours. See note 1.

2.0 . Shaded Surfaces – Daytime inspection

2.1 Ambient Temperature Changes:

2.1.1 Inspection should be conducted on days when the ambient temperature differential is expected to be at least 15°F.

2.1.2 The measured ambient temperature differential should be at least 10°F within the first 6 hours after sunrise.

2.1.3 In general, more rapid increases in ambient temperature will result in improved thermal contrast.

2.1.4 When ambient temperatures begin to decrease, thermal contrasts will also begin to decrease for a 2 in. deep delamination.

2.1.5 Local environment: The indicated ambient temperature differentials must be applied at the surface to be inspected. If the location and geometry of the bridge results in reduced ambient temperature changes at the surface to be inspected, this should be considered in determining if adequate conditions exist for detection of subsurface defects. A simple temperature monitoring device that stores hourly temperatures can be used to assess the local conditions at a bridge.

2.2 Wind Speed

2.2.1 High average wind speeds are not necessarily detrimental to the development of thermal contrast for shady conditions. A practical limit of 10 mph average wind speed is suggested, based on a 6 hour average.

2.3 Inspection Periods

2.3.1 Inspections should be conducted starting 4 to 5 hours after sunrise to allow for thermal contrast to develop when anticipated depth of the delamination is approximately 2 in. from the surface of the concrete. The useful inspection period is expected to last approximately 8 hours. If the anticipated depth is 3 in., inspection should be conducted starting approximately 7 hours after sunrise. The useful inspection period is expected to last approximately 4 hours. See note 1.

3.0 Shaded Surfaces – Nighttime inspections

3.1 Ambient Temperature Changes:

3.1.1 Inspection should be conducted on nights when the ambient temperature differential is expected to be at least -15°F. This value is measured from the highest temperature in the afternoon to the coldest temperature in the overnight period.

3.1.2 The measured ambient temperature differential should be at least -10°F during the 6 hours preceding sunset for the previous day.

3.1.3 In general, more rapid decreases in ambient temperature will results in improved thermal contrast.

3.1.4 When ambient temperatures begin to increase, thermal contrasts will begin to decrease for a 2 in. deep delamination.

3.2 Local environment: The indicated ambient temperature differentials must be applied at the surface to be inspected. If the location and geometry of the bridge result in reduced ambient temperature changes at the surface to be inspected, this should be considered in determining if adequate conditions exist for detection of subsurface defects.

3.3 Wind Speed

3.3.1 High average wind speeds are not necessarily detrimental to the development of thermal contrast for shady conditions. However, low wind speeds are characteristic of the overnight period. A practical limit of 8 mph average wind speed is suggested, based on a six hour average.

3.4 Inspection Periods

3.4.1 Inspections should be conducted starting 1 hour after sunset when the anticipated depth of the delamination is approximately 2 in. from the surface of the concrete. The useful inspection period is expected to last approximately 9 hours. If the anticipated depth is 3 inches, inspection should be conducted starting approximately 3 hours. after sunset. The useful inspection period is expected to last approximately 7 hours. See note 1.

4.0 Camera Settings

4.1 Focus: To allow for small temperature contrasts at delaminations to be detected, cameras should be properly focused on the inspection surface. Placement of a regularly shaped object, such as a tool or a coin, on the surface to be inspected can be used to assist in focusing the camera properly. Well defined edges or an object on the structure surface, such as utility connections, can also be used.

4.2 Level and span: Level and span settings for the camera should be manually adjusted. Contrast levels for delaminations are typically small, ~1-2°F. As such, span

settings in the range of 4 to 8°F are recommended for applications where solar loading is not applied. For solar loaded areas, a span of up to ~15°F may be warranted, but consideration should be given to the associated loss in sensitivity to thermal contrast in the image. The level setting should be adjusted to allow for images to be properly interpreted based on the span. This may require frequent adjustment when temperatures vary across a structure.

4.3 Angle of Observation: Observing surfaces at a low angle can increase ambient reflections and frequently produces an apparent thermal gradient across the image. Inspections should be conducted as close to normal angles (90°) as practical. A practical guideline is to try to stay within +/- 45 degrees from normal. Angles of more than 60° from normal should be avoided. Utilization of a wide angle lens can assist in maintaining normal angles when deck inspections are being conducted. Figure A1 below shows the indicated angles for reference.

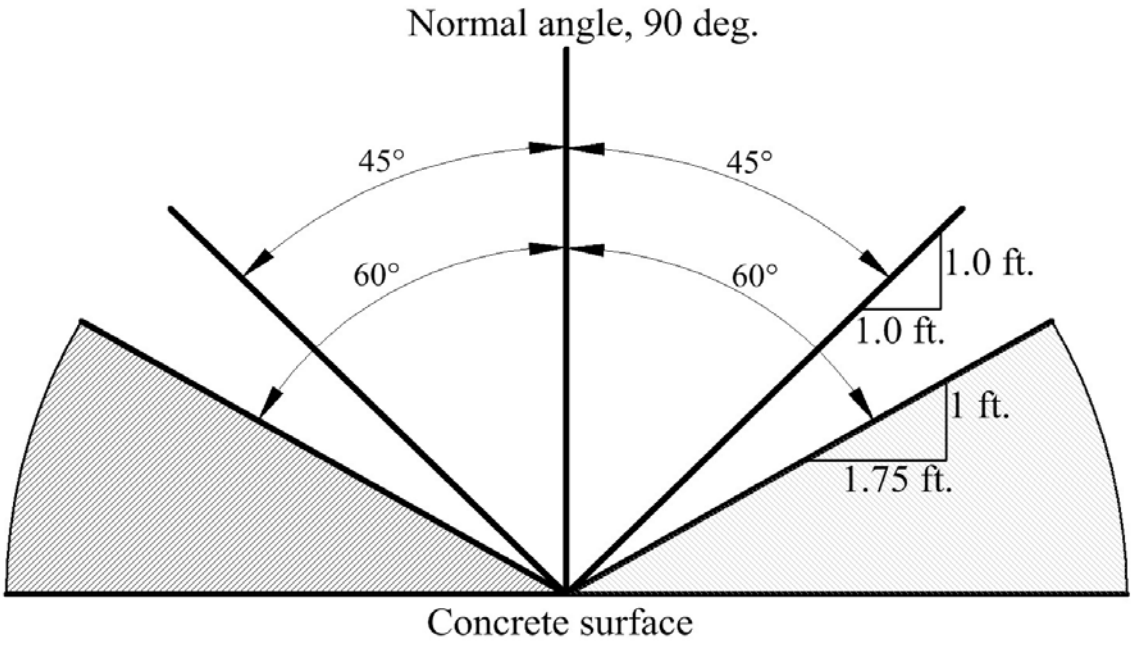

Figure A1. Schematic diagram of observation angles.

Note 1. Inspection time periods are based on observations in the research conducted. For solar exposed surface, measurements were made during the months of November, December and January, when there are fewer hours of sunlight than other times of the year. For shaded surfaces, measurements were made during the months of May, June and July, when there are more hours of sunlight than other times of the year. As a result, the inspection intervals suggested are for general guidance; the time of year in which the inspection is actually conducted should be considered in applying this guidance.